DOE/NV/0003590-05

Tonopah Test Range Air Monitoring: CY2016 Meteorological, Radiological, and Wind Transported Particulate Observations

Prepared by

Jenny Chapman, George Nikolich, Craig Shadel, Greg McCurdy,
Vicken Etyemezian, Julianne J. Miller, and Steve Mizell

Submitted to

U.S. Department of Energy
Environmental Management Nevada Program
Las Vegas, Nevada

October 2017

Publication No. 45279

Nevada System of Higher Education

DOE/NV/0003590-05

Tonopah Test Range Air Monitoring: CY2016 Meteorological, Radiological, and Wind Transported Particulate Observations

Prepared by

Jenny Chapman, George Nikolich, Craig Shadel, Greg McCurdy,
Vicken Etyemezian, Julianne J. Miller, and Steve Mizell

Desert Research Institute
Nevada System of Higher Education

Publication No. 45279

Submitted to

U.S. Department of Energy
Environmental Management Nevada Program
Las Vegas, Nevada

October 2017

The work upon which this report is based was supported by the U.S. Department of Energy under Contract #DE-NA0003590 and Contract #DE-NA0000939. Approved for public release; further dissemination unlimited.

THIS PAGE INTENTIONALLY LEFT BLANK

EXECUTIVE SUMMARY

In 1963, the U.S. Department of Energy (DOE) (formerly the Atomic Energy Commission [AEC]), implemented Operation Roller Coaster on the Tonopah Test Range (TTR) and an adjacent area of the Nevada Test and Training Range (NTTR) (formerly the Nellis Air Force Range). This operation resulted in radionuclide-contaminated soils at the Clean Slate I, II, and III sites. This report documents observations made during ongoing monitoring of radiological, meteorological, and dust conditions at stations installed adjacent to Clean Slate I and Clean Slate III, and at the TTR Sandia National Laboratories (SNL) Range Operations Control (ROC) center. The primary objective of the monitoring effort is to determine if wind blowing across the Clean Slate sites is transporting particles of radionuclide-contaminated soil beyond the physical and administrative boundaries of the sites.

Three monitoring stations are in operation as follows: Station 400 near the ROC, and Stations 401 and 402 along the northwest perimeter fence lines of the Clean Slate III and Clean Slate I sites, respectively. All stations, including the ROC at the local workforce center, are downwind of the contaminated area during south-southeast winds. Those winds are from one of the two predominant wind directions through the area, the other being from the north-northwest. The stations—similar in design to the Community Environmental Monitoring Program (CEMP) stations operating at locations surrounding the Nevada National Security Site and TTR—include meteorological instruments, continuous-flow low-volume air samplers, pressurized ionization chambers for measuring gamma energy, saltation sensors, and saltation traps. Detailed meteorological data are recorded on data loggers, with periodic uploads via a satellite system to the Western Regional Climate Center (WRCC) at Desert Research Institute (DRI) to monitor instrument and site conditions. Air filter samples are collected biweekly and material in the saltation traps is collected as a sufficient sample for analysis accumulates (generally an eight-month interval).

Soil transport by suspension and saltation is strongly dependent on wind speed. Concentrations of PM_{10} (particulate matter of aerodynamic diameter $\leq$10 micrometers [µm], an indicator of small particles that are suspended in the air and can be easily inhaled) remain low until winds exceed approximately 32 km/hr (20 mph). Saltation particle counts also increase above the same general threshold wind speed. Wind speeds in excess of 32 km/hr (20 mph) occur less than two percent of the time. High winds are associated with two predominant directions: north-northwest and south. In 2016, the highest winds were from the south, in contrast to 2015 when the highest winds were observed from the northwest.

Radionuclide assessment of suspended airborne particulate matter in 2016 found the gross alpha and gross beta values of dust collected from the filters at the monitoring stations to be consistent with background conditions as approximated by data from the surrounding CEMP stations. Gamma spectral analyses of the air filters identified only naturally occurring radionuclides. Ambient gamma radiation measurements indicate that the average annual gamma exposure rate is similar at all three monitoring stations, and periodic intervals of slightly increased gamma values appear to be associated with storm fronts passing through the area. In contrast, alpha spectroscopy of select filters identifies the presence of plutonium-239+240 ($^{239+240}Pu$) at concentrations above background in the environment

immediately adjacent to Clean Slate I and III. Concentrations measured at the ROC station are below detection, which is consistent with the background data from the TTR airport location.

Concentrations of plutonium in the material that entered the passive saltation traps in 2016 are above background levels, although below risk-based action levels. The absence of a consistent difference in concentration between samples that entered the traps from the upwind and downwind directions (relative to the contaminated areas) suggests that the baseline concentrations of contaminants are elevated in the area surrounding the traps, complicating the determination of an overall predominant migration direction. The presence of plutonium in the saltation traps does demonstrate that plutonium is moving by saltation in the environment near the sites.

The meteorological and particle monitoring indicate that conditions for wind-borne contaminant movement exist at the Clean Slate sites and that transport of radionuclide-contaminated soil by both suspension and saltation is occurring. The CAU closure strategy uses a risk-based approach, whereby acceptable contaminant concentrations are determined as a function of anticipated human exposure. As a result, the fence lines at the Clean Slate sites encircle areas of higher concentration and the presence of contamination outside the fences is expected, albeit at lower concentrations.

CONTENTS

LIST OF FIGURES

LIST OF TABLES

LIST OF ACRONYMS

AEC	Atomic Energy Commission
BSNE	Big Spring Number Eight
CAU	Corrective Action Unit
CEMP	Community Environmental Monitoring Program
CS I	Clean Slate I
CS II	Clean Slate II
CS III	Clean Slate III
CY	Calendar year
DOE	Department of Energy
DRI	Desert Research Institute
GOES	Geostationary Operational Environmental Satellite
GZ	Ground zero
MDC	Minimum detectable concentration
NNSA/NFO	National Nuclear Security Administration, Nevada Field Office
NTTR	Nevada Test and Training Range
PIC	Pressurized ionization chamber
PM	Particulate matter
ROC	Range Operations Center
RSL	Radiological Services Laboratory
SNL	Sandia National Laboratories
TDR	Time domain reflectometry
TTR	Tonopah Test Range
VWC	Volumetric water content
WRCC	Western Regional Climate Center

THIS PAGE INTENTIONALLY LEFT BLANK

INTRODUCTION

In May and June of 1963, the U.S. Department of Energy (DOE) (formerly the Atomic Energy Commission [AEC]) implemented Operation Roller Coaster to evaluate the dispersal of radionuclides when nuclear devices were subjected to chemical explosions while in storage or transit (Dick *et al.*, 1963; Johnson and Edwards, 1996). The operation consisted of four tests: Double Tracks conducted in Stonewall Flat on the Nevada Test and Training Range (NTTR) and Clean Slate I, II, and III conducted in Cactus Flat on the Tonopah Test Range (TTR). The Clean Slate sites are the focus of this report and are located southeast of Tonopah, Nevada, in Nye County (Figures 1 and 2).

The primary purpose of the Clean Slate tests were to study plutonium dispersion from nonnuclear explosions of plutonium weapons (U.S. Department of Energy, 1996). The Clean Slate tests involved one device containing plutonium and several simulated weapons containing uranium (Dick *et al.*, 1963; Johnson and Edwards, 1996). For each test, data collection was distributed along arcs within a quarter-circle, wedge-shaped area that emanated from the test ground zero (GZ) and centered on a radius that extended from GZ to the south or southeast (Dick *et al.*, 1963; Johnson and Edwards, 1996), which were the expected downwind directions. Data collection during the tests focused on plutonium and uranium because of their radiological toxicity (Dick *et al.*, 1963). Subsequent surveys to characterize radionuclide-contaminated soils focused on the detection of plutonium through the measurement of the plutonium daughter product, americium-241 (^{241}Am; Proctor and Hendricks, 1995). Americium-241 can be more readily measured than the alpha-emitting plutonium isotopes because ^{241}Am emits gamma rays.

Immediate post-shot cleanup at each test involved disposing contaminated debris in a pit at GZ, scraping the surface soil around GZ to a depth of several inches, and placing the soil in the disposal pit or mounding it over the contaminated debris. The mound of contaminated materials was covered with additional soil, compacted, and then watered down (Johnson and Edwards, 1996). Fences were constructed around the contamination at each site. Based on soil survey data collected during 1973, a second fence was constructed at the approximate limit of 40 picocurie per gram (pCi/g) of plutonium in soil (Duncan *et al.*, 2000).

Aerial surveys of Operation Roller Coaster contamination areas were conducted in 1977 (EG&G, 1979) and 1993 (Proctor and Hendricks, 1995). These surveys used gamma detectors to identify ^{241}Am. Based on the 1977 survey, the total area of diffuse plutonium for all Operation Roller Coaster sites was estimated to be approximately 4,900 acres (Sandia, 2014). The 1993 survey estimated the maximum concentration at the Clean Slate I GZ to be between 200 and 400 pCi/g. At Clean Slate II and III, the maximum concentrations at GZ were reported to be in excess of 2,000 pCi/g. Contamination was reported outside the outer perimeter fence at all three Clean Slate sites. At Clean Slate III, plutonium concentration outside of the fence did not exceed 200 pCi/g. However, the concentrations reported outside the fences at Clean Slate I and II were greater than 200 pCi/g but less than 400 pCi/g (Proctor and Hendricks, 1995). Soil contamination at Clean Slate I was remediated in 1997 so that the concentration of transuranics was $\leq$ 400 pCi/g (SNL, 2012). Clean Slate II and III were not remediated as of 2016.

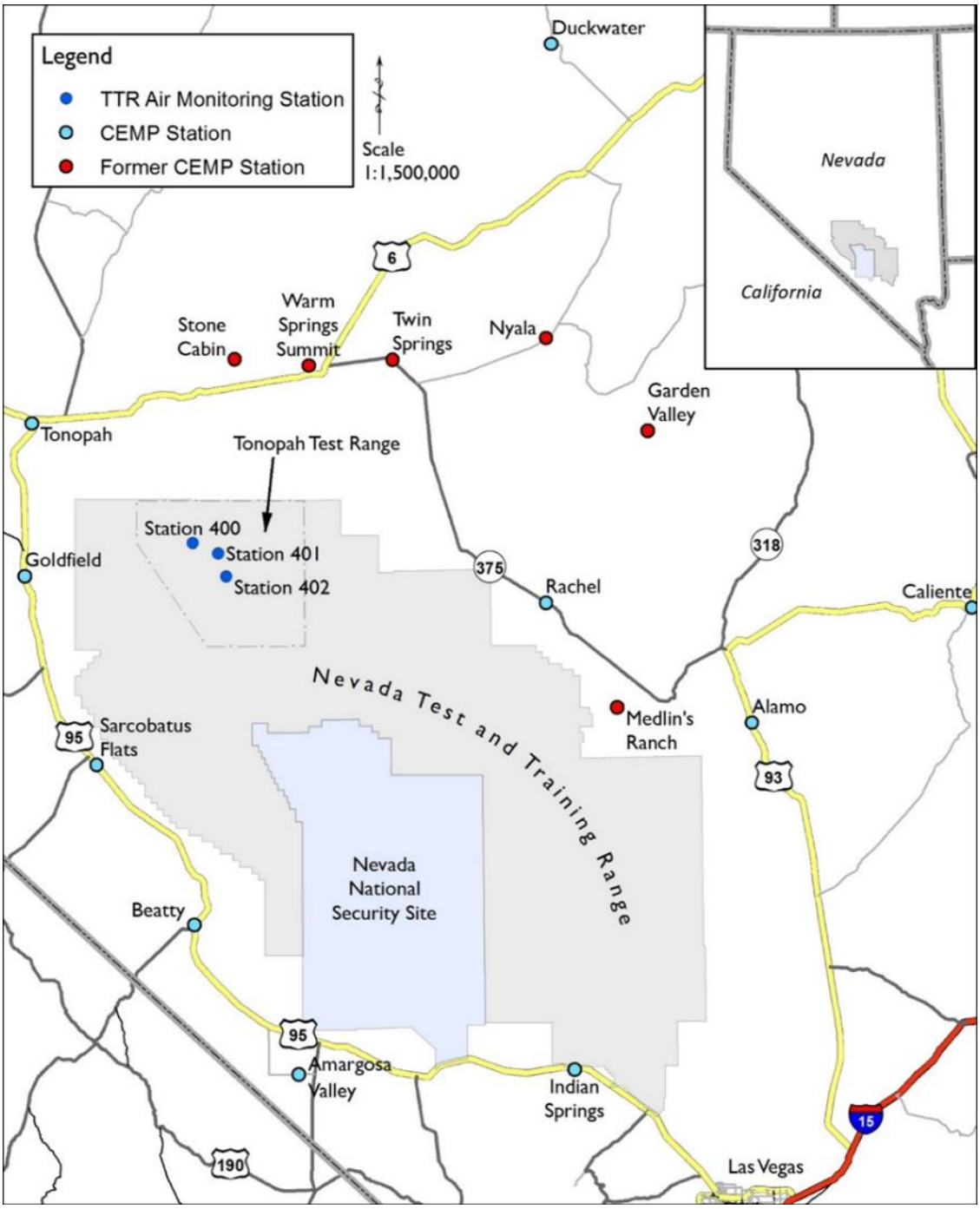

Figure 1. Location of monitoring stations at the Tonopah Test Range (TTR) in the north end of the Nevada Test and Training Range (NTTR) in southern Nevada. Also shown are current and former Community Environmental Monitoring stations (CEMP) for which monitoring data are available.

Figure 2. The TTR environmental monitoring stations are located on the south side of the Sandia National Laboratory compound (Station 400) and the north ends of the Clean Slate I (Station 402) and III (Station 401) contamination areas.

In 2008, at the request of the DOE National Nuclear Security Administration, Nevada Field Office (NNSA/NFO), the Desert Research Institute (DRI) constructed and deployed two portable environmental monitoring stations at the TTR as part of the Environmental Restoration Project, Soils Activity. A third station was deployed in 2011. Desert Research

Institute has operated these stations continuously since installation. The primary objective of the monitoring stations is to evaluate whether there is wind transport of radiological contaminants, specifically plutonium, from the Soils Corrective Action Units (CAUs) associated with Operation Roller Coaster and if so, under what conditions such transport occurs. Plutonium particles tend to attach to small soil particles so that wind-suspended dust and rainfall runoff are the likely mechanisms for transporting radiological contaminants. Inhalation of plutonium-contaminated dust particles is also the most likely mechanism for human exposure. The objective of this annual report is to document the operation of the TTR monitoring stations during calendar year (CY) 2016, present the data collected, interpret the results in the context of the monitoring objectives, and provide recommendations as needed.

MONITORING STATION LOCATIONS AND CAPABILIITIES

The TTR monitoring Stations 400 and 401 were installed in May and June 2008, respectively. Station 402 was installed in May 2011. Wind direction, access, and power availability were key considerations in selecting the specific monitoring station locations. Wind data for the Tonopah Airport (Engelbrecht *et al.*, 2008) indicate that the predominant wind directions in the area are from the northwest and south-southeast. Wind direction data collected from the TTR monitoring stations substantiate the assessment of Engelbrecht *et al.* (2008).

Station 400 is located at the Sandia National Laboratories (SNL) Range Operations Center (ROC). Station coordinates are given in Table 1. The ROC, adjacent TTR airfield, and surrounding work area are downwind of the Clean Slate contamination sites when winds are out of the south-southeast. At a distance of eight to nine kilometers (five to six miles), these facilities are the closest, regularly manned work locations to the Clean Slate contamination sites. Therefore, Station 400 facilitates the characterization of radiological conditions in the TTR work areas that may result from wind transport of radionuclide-contaminated soils at the Clean Slate sites and provides data to compare radiological conditions at the ROC with conditions at the Clean Slate sites. Station 400 was originally located just north of the center of the SNL compound, approximately 145 m (475 ft) west-northwest of the ROC. In the summer of 2012, the station was moved approximately 200 m (650 ft) to the southeast at the request of SNL. In the new location, Station 400 is approximately 90 m (300 ft) south of the ROC near the southeast corner of the SNL compound (Figure 2). Sandia National Laboratories provides line power to operate the equipment at Station 400, which consists of a meteorological tower and air sampling equipment installed on a 2.1 m x 4.3 m (7 ft x 14 ft) trailer (Figure 3). The wind instruments are located approximately 6 m (20 ft) above ground surface.

Table 1. Location coordinates for the TTR air monitoring stations.

Station	Latitude	Longitude
Station 400 – original	37° 47’ 15” N	116° 45’ 26” W
Station 400 – current	37° 47’ 10” N	116° 45’ 21” W
Station 401	37° 45’ 39” N	116° 40’ 58” W
Station 402	37° 42’ 33” N	116° 39’ 32” W

Figure 3. Station 400 is a trailer-mounted radiological and meteorological measurement system located near the Range Operations Center (ROC) in the Sandia National Laboratories (SNL) compound on the TTR.

Stations 401 and 402 are located at the demarcation fence on the northwest perimeter of the Clean Slate III and Clean Slate I sites, respectively (Figure 2). These locations were chosen because the monitoring instrumentation is placed in proximity to the contamination sites and on the downwind side of the sites during south-southeast winds, which is one of the two predominant wind directions through the area. The main workforce location in the area, at SNL-ROC, is also downwind of the Clean Slate sites during south-southeast winds. Both Stations 401 and 402 are solar powered with battery backup power and the batteries are recharged by solar panels. Table 1 gives the coordinates for these monitoring stations. At

Stations 401 and 402, the air samplers, solar panels, and the batteries used to power the samplers are on trailers. This arrangement requires that the meteorological towers be installed on free-standing tripods that are separate from the trailer (Figures 4 and 5). The wind instruments are approximately 3 m (10 ft) above ground surface.

Figure 4. The solar powered air sampler, saltation sensor, and meteorological tower (background, center, and foreground, respectively) at Station 401 are located along the north fence that bounds the Clean Slate III contamination area.

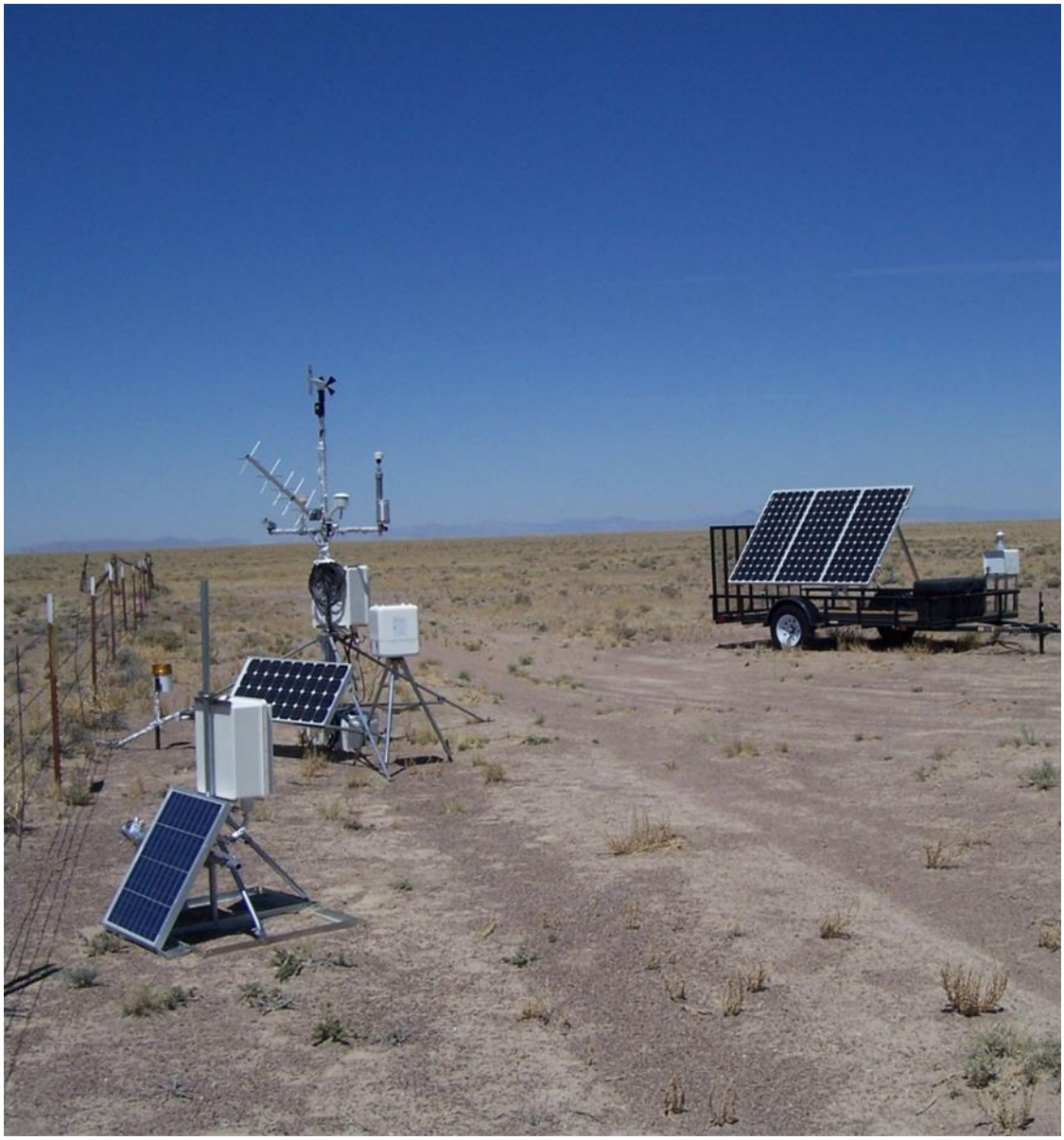

Figure 5. The solar powered air sampler, saltation sensor, and meteorological tower (center right, foreground left, and center left, respectively) at Station 402 are located along the north fence that bounds the Clean Slate I contamination area.

The fundamental design of these stations is similar to that used in the Community Environmental Monitoring Program (CEMP) (NSTec, 2013). The Quality Assurance Program is also patterned after that used by CEMP (Appendix A). The equipment deployed provides data on radiological, meteorological, and environmental conditions. Table 2 lists the parameters measured and the approximate date of the initial data collection at each of the three monitoring stations. Plutonium was the principal radionuclide released into the environment during the Clean Slate experiments. It attaches to small soil particles and may be suspended in the air and transported from the site along with windblown dust. Americium-241, a daughter product of plutonium-241 (^{241}Pu) that releases gamma energy

during decay, is much easier to detect than the alpha particles released during plutonium decay. Therefore, two radiological data collection systems are deployed at each of the monitoring stations. Gamma energy is measured using a pressurized ionization chamber (PIC) (Reuter Stokes, Youngstown, Ohio) and airborne particulate material is collected for radiological analysis. Continuous flow, low-volume (flow rate is approximately 0.05663 m^3 [2 ft^3] per minute) air samplers (Hi-Q Environmental Products, San Diego, CA) are used to collect airborne particulate material.

Glass-fiber filters with a pore size of 0.3 µm and diameter of 10 cm (4 in) are currently in use. Prior to CY2013, Stations 401 and 402 used cellulose-fiber filters with a pore size of 20 µm to 25 µm. The conversion to all glass-fiber filters was made to ensure that the smaller-sized particulate material to which plutonium might be attached is collected. Filters are retrieved every two weeks and are delivered to the Radiological Services Laboratory (RSL) at the University of Nevada, Las Vegas, for analyses.

Table 2. Radiological, meteorological, and environmental sensors deployed at the TTR air monitoring stations. The dates refer to the first occurrence of data collection for that parameter at the given station.

Instrument/Measurement	Station 400	Station 401	Station 402
Wind speed	5/27/2008	6/10/2008	5/18/2011
Wind direction	5/27/2008	12/22/2009	5/18/2011
Precipitation	5/27/2008	12/22/2009	5/18/2011
Temperature	5/27/2008	6/10/2008	5/18/2011
Relative humidity	5/27/2008	6/10/2008	5/18/2011
Solar radiation	5/27/2008	NA	5/18/2011
Barometric pressure	5/27/2008	NA	5/18/2011
Soil temperature	5/27/2008	12/22/2009	5/18/2011
Soil moisture content	5/27/2008	12/22/2009	5/18/2011
Airborne particle size profiler	5/27/2008	6/10/2008	5/18/2011
Airborne particle collector	5/27/2008	7/30/2008	8/23/2011
Saltation sensor	NA	8/9/2011	8/9/2011
Gamma radiation PIC	5/27/2008	12/22/2009	12/15/2011
MiniVol™ [1]	5/27/2008	NA	NA
Data logger	5/27/2008	6/10/2008	5/18/2011
GOES[2] transmitter	5/27/2008	12/22/2009	5/18/2011
BSNE[2] sand traps	NA	4/01/2014	4/01/2014

[1] Samples have never been collected from the MiniVol™ collectors.
[2] See text for acronym definition
NA = not available.

The total mass of collected dust is submitted for gross alpha, gross beta, and gamma spectroscopy analyses in an effort to assess the magnitude of radionuclides associated with the suspended dust. Gamma spectroscopy is performed to determine if ^{241}Am is present. If ^{241}Am is detected, then alpha spectroscopy is performed to confirm and determine the quantity of plutonium isotopes. Alpha spectroscopy was also used in 2016 on select air filters archived from 2015 and 2016 for comparison with alpha spectroscopy analyses on soil samples from saltation traps. Alpha spectroscopy is more sensitive than gamma spectroscopy because it can measure a narrower window of energy specific to plutonium isotopes because plutonium is chemically separated from the sample prior to analysis.

Suspension and transport of contaminated dust are controlled by local meteorological and other environmental conditions, such as wind speed and soil moisture content. Many meteorological parameters influence these conditions. Electronic sensors measure meteorological and other environmental conditions every three seconds. These measurements are averaged or totaled, as appropriate, and stored in the on-site data logger every 10 minutes. The maximum and minimum value of each parameter are also saved on the data logger. These values are used to evaluate data quality. The data loggers are downloaded during site visits every two weeks. To assess instrument performance and provide rapid updates of conditions, observations each hour are transmitted to the Western Regional Climate Center (WRCC) via the Geostationary Operational Environmental Satellite (GOES) system. At the WRCC, data are quality checked and archived for interpretation. A gap occurred in data collection at Station 402 from March 17 until March 29, 2016, which was caused by a problem with the telemetry system used for communication.

In addition to the automatic sensors, one MiniVol™ (Air Metrics, Springfield, Oregon) is deployed at Station 400. This sampler is intended to be run in the event of a nearby wildfire or during extreme dust storms because it is set up to facilitate analyses that distinguish organic and inorganic constituents. The MiniVol™ is a manually activated, low-volume air sampler equipped with Teflon™ filters. No events caused the MiniVol™ to be activated in 2016, so no data were collected from this instrument.

BSNE SAND TRAP INSTALLATION

On April 1, 2014, DRI installed Big Spring Number Eight (BSNE; Custom Products and Consulting LLC, Big Spring, Texas) samplers to monitor soil transported by saltation at Clean Slate I and III. The BSNEs are wind-aspirated samplers that collect sand that enters the opening (Figure 6). The inlet height is set at 15 cm (6 in) to collect the near-ground erodible soil material transported by saltation. Two collectors are installed at each mounting rod (Figure 7). One of the collectors is pointed toward the contaminated area at 160 degrees from north to collect material likely to have been transported from the Clean Slate site under the influence of south-southwesterly winds. The other collector is pointed in the opposite direction and is used to collect the material moving toward the Clean Slate sites. This physical setup and orientation allows the net movement of soil material from the Clean Slate sites to be determined.

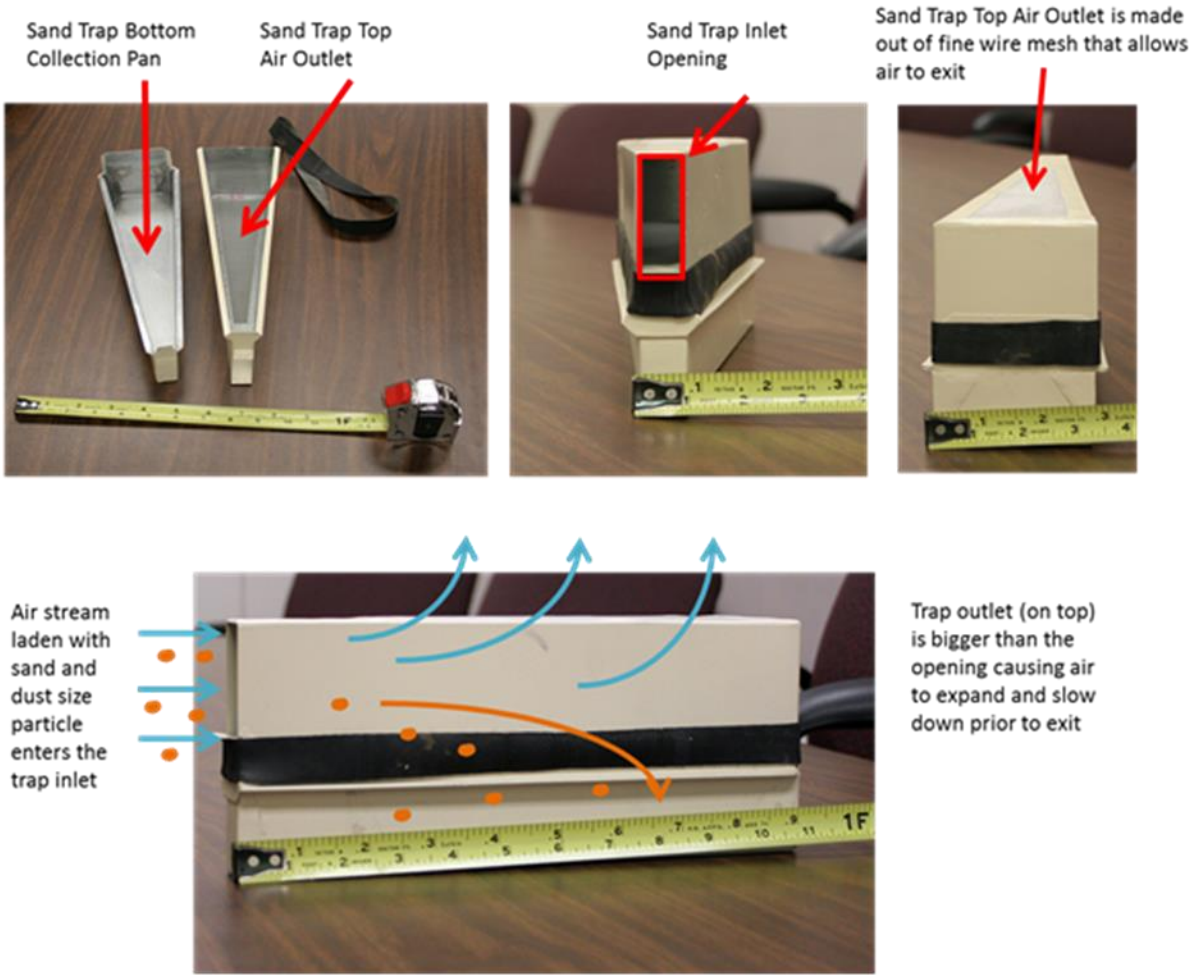

Figure 6. Sand particles are carried into the BSNE sand trap by fast-moving air. As the air slows down, momentum is lost and the particles settle on the bottom of the collection pan. Dust particles may be small enough to be carried out through the wire mesh at the top of the trap by air.

Figure 7. Northeast view at Station 401. In the foreground is one of three BSNE sand trap installations at TTR Clean Slate III. The Clean Slate III boundary fence is to the right. Behind the sand trap is the saltation sensor and meteorological station with additional sand traps located along the fence line.

Three replicate BSNE samplers with two collectors each were installed at both Clean Slate I and Clean Slate III (Figures 8 and 9) along the fence line. The information collected will help determine if contaminated material reaches the fence line and the amount of net soil migration over time. These samplers are passive and field operators check the sampler mass loading during the biweekly site visits. Desert Research Institute has developed a procedure in conjunction with other DOE contractors to collect and analyze the soil trapped in the BSNEs. The initial expectation was that a three- to four-month collection period would be used to better understand seasonal and geographic trends. However, it was nearly a year before there was enough material in the traps for laboratory analysis.

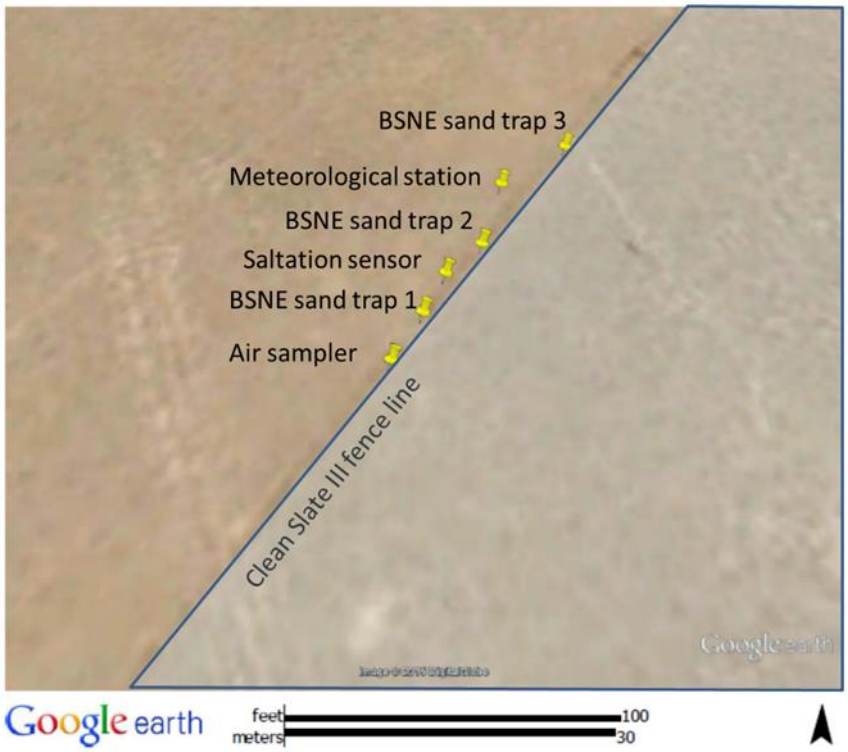

Figure 8. Equipment locations outside the fence line at TTR Clean Slate III, Station 401.

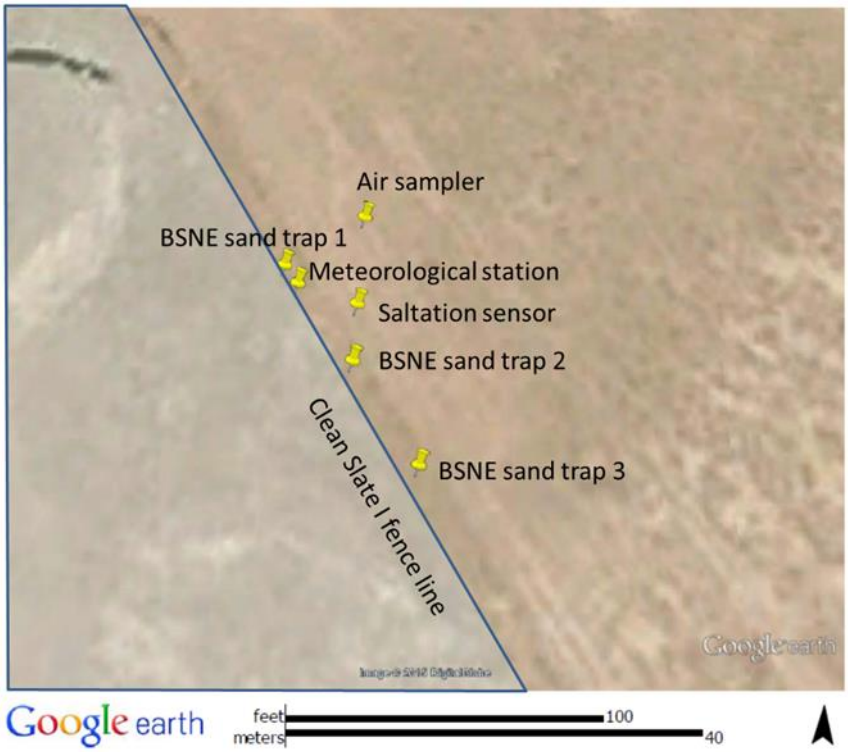

Figure 9. Equipment locations outside the fence line at TTR Clean Slate I, Station 402.

WEATHER CONDITIONS AND OTHER ENVIRONMENTAL PARAMETERS

Summary tables of the meteorological data recorded at the stations are presented in Appendix B and daily average meteorological and environmental data are plotted in Appendix C. These data are summarized and discussed below. Air temperature trends recorded during the year at Stations 400, 401, and 402 between January 1, 2016, and December 31, 2016, are shown in Figures 10 through 12. The three traces shown in the figures depict the maximum, average, and minimum daily temperature based on the 10-minute average measurements. The average air temperature during CY2016 for Station 400 was 12.0 degrees Celsius (°C) (53.6 degrees Fahrenheit [°F]). The highest air temperature of 37.9 °C (100.2 °F) was recorded in July (July 28, 2016) and the lowest air temperature of -22.0 °C (-7.6 °F) was recorded in February (February 2, 2016). The highest average monthly air temperature of 25.4 °C (77.8 °F) was recorded in August and the lowest average monthly air temperature of -0.4 °C (31.2 °F) was recorded in January. Air temperatures at Stations 401 and 402 follow a very similar trend to Station 400 (Figure 13). The maximum observed air temperature at Station 401 was 38.4 °C (101.1 °F) in July and the lowest air temperature was -25.1 °C (-13.2 °F) in February. The average annual air temperature at Station 401 was 11.6 °C (52.9 °F). The maximum observed air temperature at Station 402 was 38.6 °C (101.4 °F) in July and the lowest air temperature was -26.3 °C (-15.3 °F) in February. The average annual air temperature at Station 402 was 11.4 °C (52.6 °F). It is important to note that small differences in air temperature readings may reflect an individual temperature sensor bias. The air temperature sensor used at the monitoring stations has a reported accuracy of ±0.5 °C for temperatures ranging from 5 and 40 °C (40 to 105 °F).

Figure 14 shows the daily average soil temperatures for all three TTR stations. Soil temperature is measured using temperature probes made of thermocouple wire that have been buried at a depth of 10 to 13 cm (4 to 5 in). Generally, there are minor differences in soil temperature readings between the stations. These minor differences may be explained in part by differences in local soil thermal conductivity, soil moisture, vegetation cover, and variations in probe burial depth. Station 400 generally indicates higher soil temperature compared with Stations 401 and 402. The disturbed gravel ground cover at Station 400 loses moisture more rapidly than the fine-grained soils at Stations 401 and 402. Low soil moisture at Station 400 allows the soil temperature to respond more quickly to changes in the air temperature compared to the responses observed at Stations 401 and 402, where soil moisture is more readily retained. The data from Station 401 (Figure 15) show the close relationship between soil temperature and air temperature.

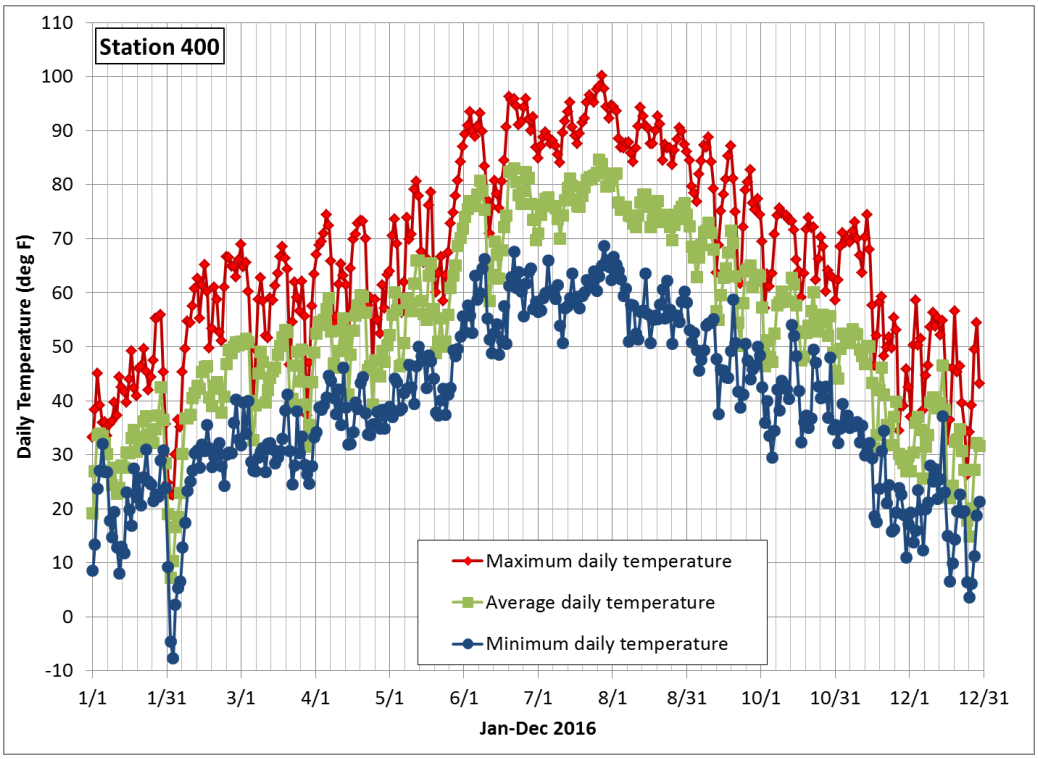

Figure 10. Ambient air temperature for Station 400 for CY2016.

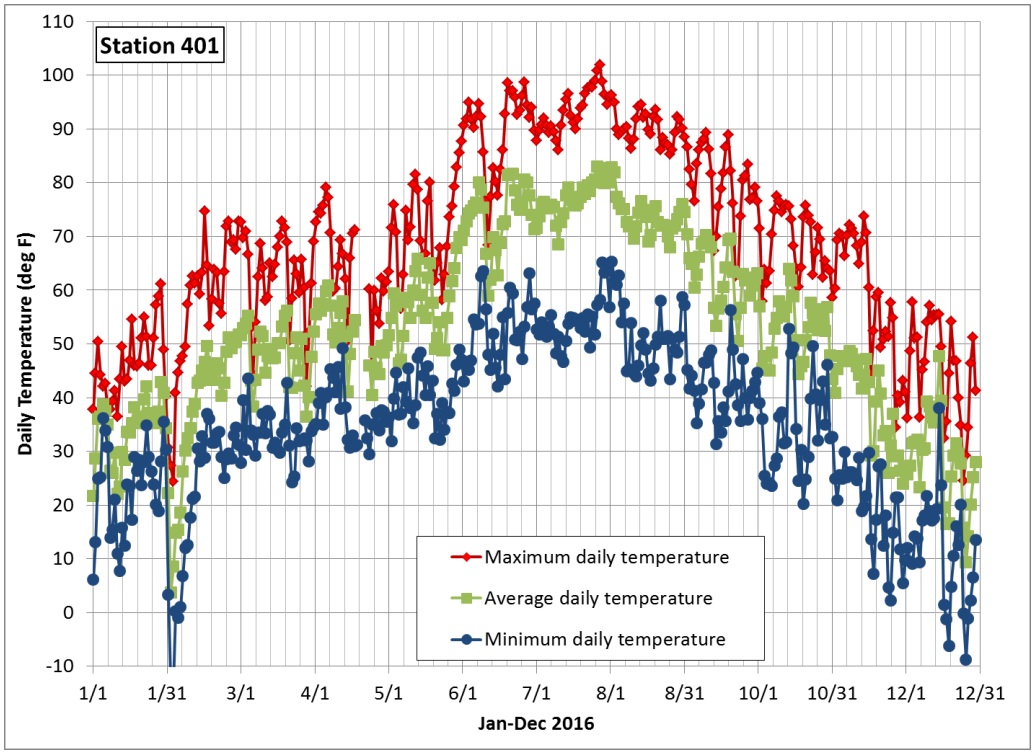

Figure 11. Ambient air temperature for Station 401 for CY2016.

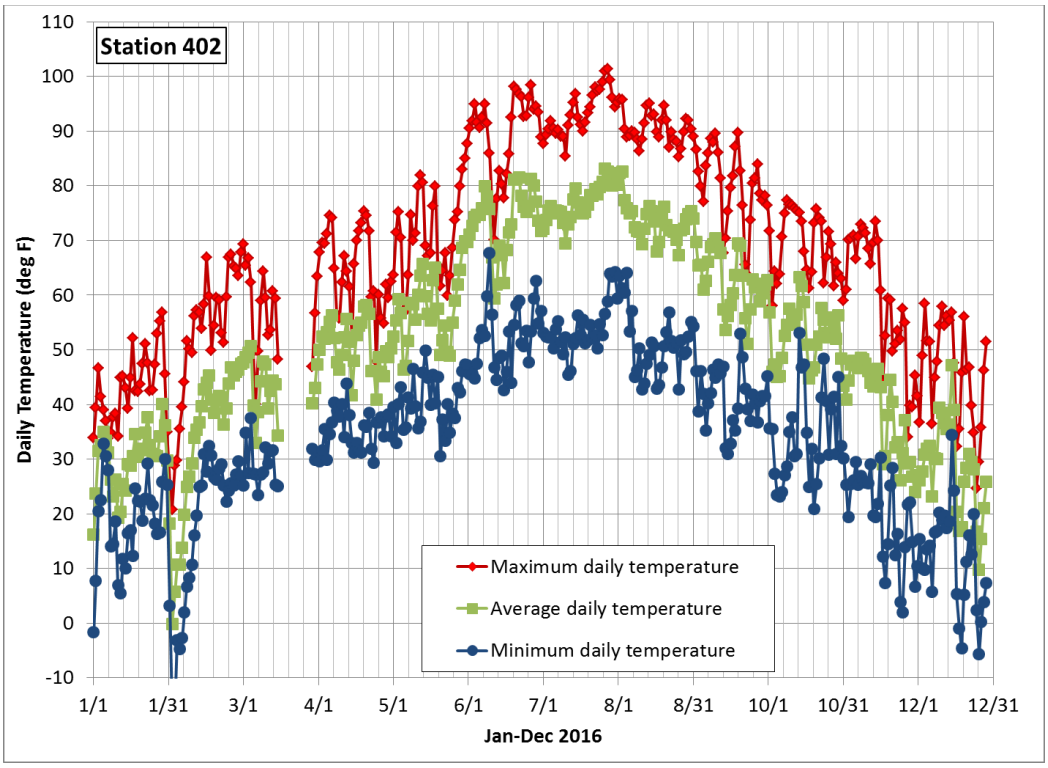

Figure 12. Ambient air temperature for Station 402 for CY2016. The data gap in August was because of equipment failure at the station.

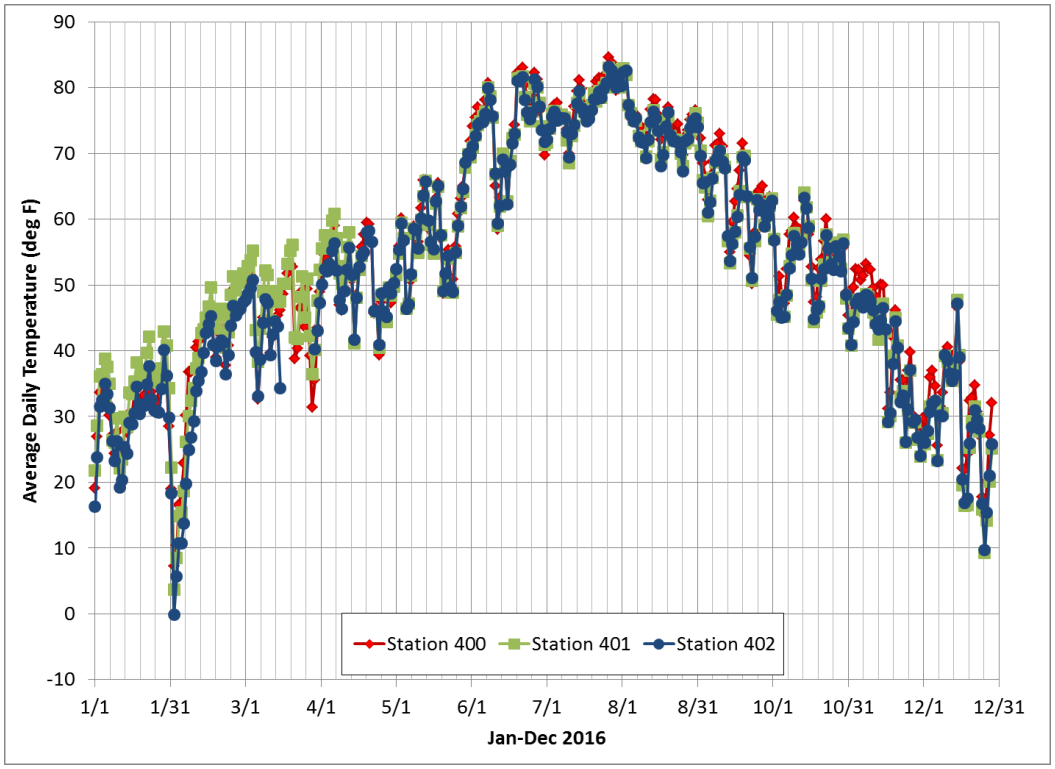

Figure 13. Average ambient air temperature for Stations 400, 401, and 402 for CY2016.

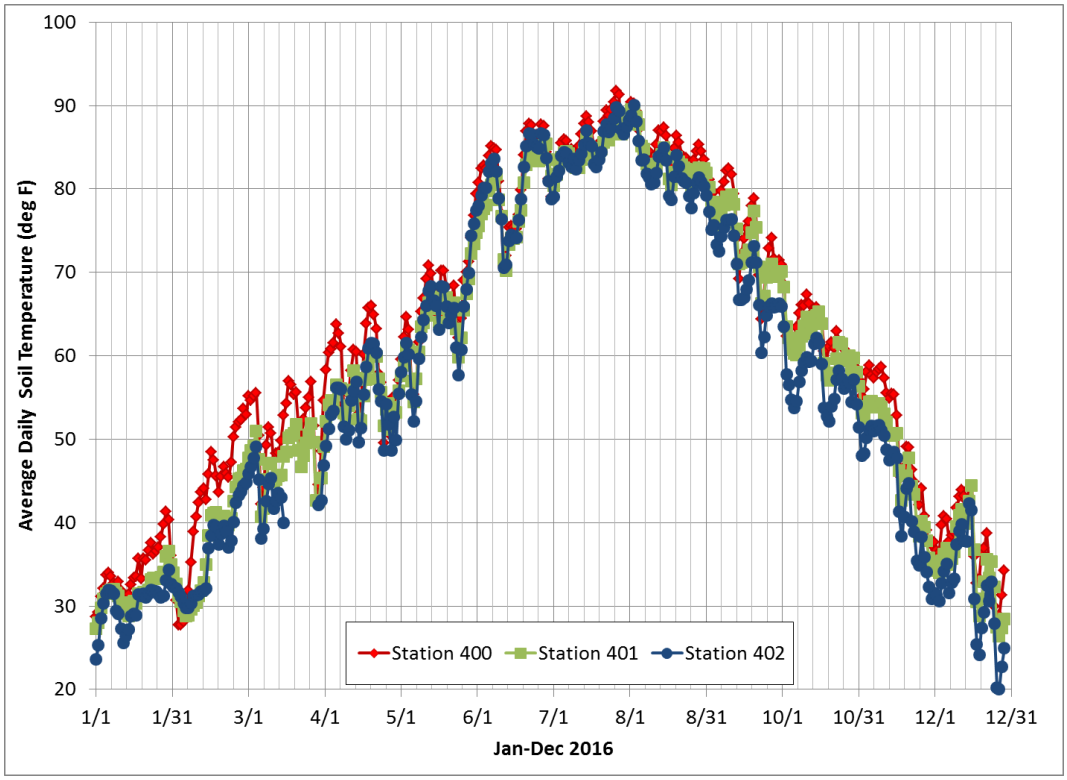

Figure 14. Average ambient soil temperature for Stations 400, 401, and 402 for CY2016.

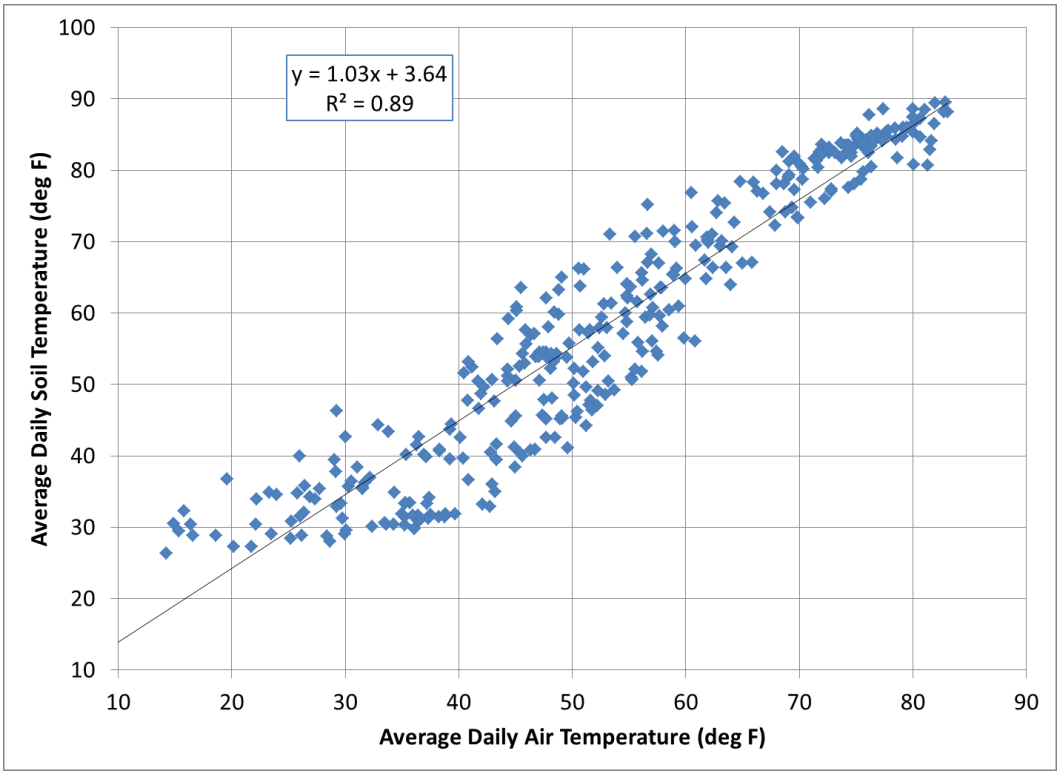

Figure 15. Comparison of average air and average soil temperatures by regression illustrates the close relationship between the two parameters at Station 401.

Figure 16 shows the total daily precipitation for Stations 400, 401, and 402 in the period between January 1, 2016, and December 31, 2016. Figure 17 shows the total cumulative precipitation for Stations 400, 401, and 402 for the period between January 1, 2016, and December 31, 2016. Precipitation for CY2016 totaled 84.3 mm (3.32 in) for Station 400 and 82.3 mm (3.24 in) for Station 401 and 74.4 mm (2.93 in) for Station 402. The similarities in these totals indicate that major precipitation events are widespread enough to be recorded by all three stations, even though rain intensity varies by station and event. The maximum total daily precipitation for Station 400 was 5.6 mm (0.22 in), which occurred on June 30, 2016. The maximum total daily precipitation for Station 401 was 8.4 mm (0.33 in), which occurred on January 31, 2016. The maximum total daily precipitation for Station 402 was 6.6 mm (0.26 in), which occurred on May 16, 2016. The May 16, 2016, rain event also registered significant precipitation at Station 400 (4.0 mm, 0.16 in) and Station 401 (7.4 mm, 0.29 in). Compared with previous years, there were no major rain events that resulted in more than 2.5 cm (one inch) of rain in a day between July and September.

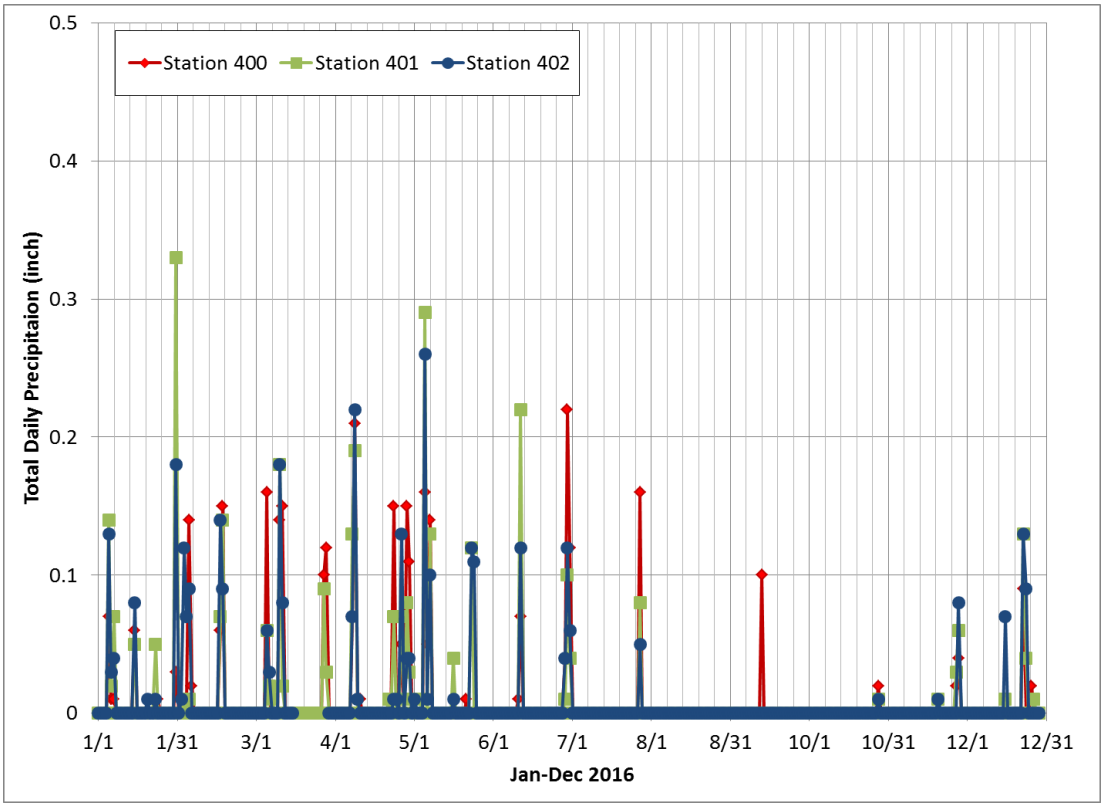

Figure 16. Total daily precipitation for Stations 400, 401, and 402 for CY2016.

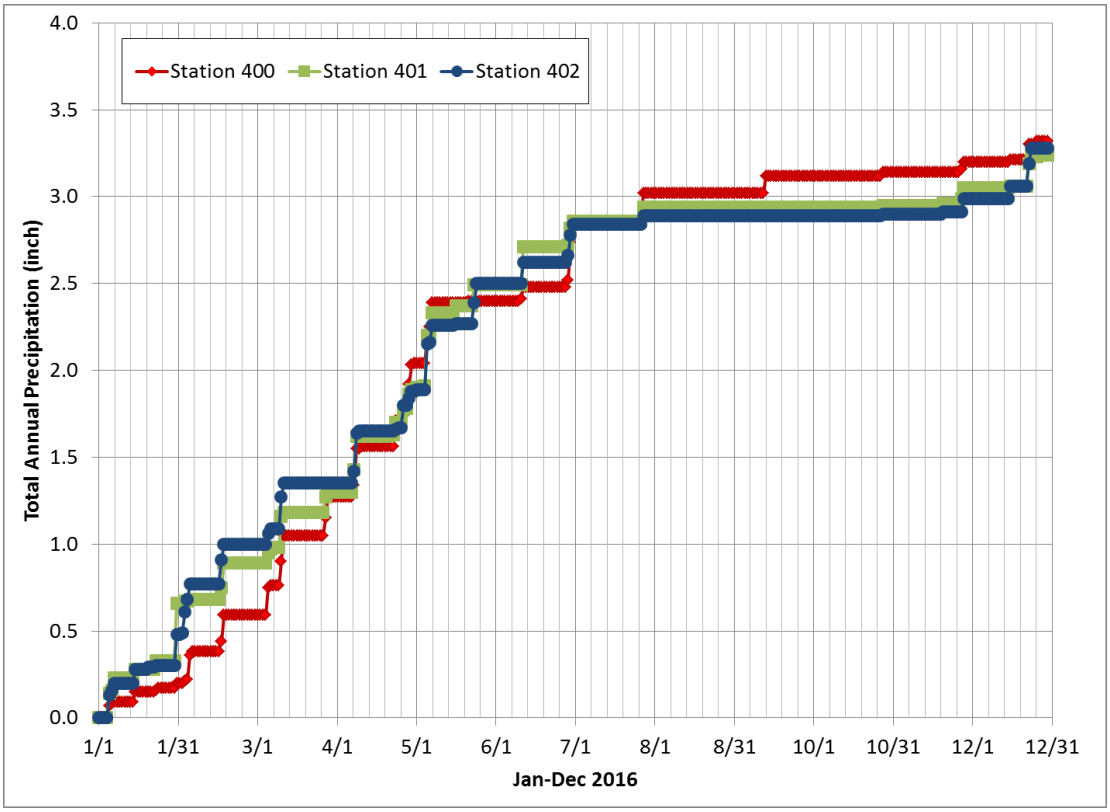

Figure 17. Cumulative precipitation for Stations 400, 401, and 402 for CY2016.

Total annual precipitation for each of the three stations during CY2016 averages 80.3 mm (3.16 in), which is well under the historic average annual precipitation of 129.03 mm (5.08 in) measured at the Tonopah Airport from 1954 through 2016 (www.wrcc.dri.edu/cgi-bin/cliMAIN.pl?nv8170, accessed May 30, 2017). The CY2016 average total annual precipitation is also below that measured at the stations in CY2014 (137.9 mm, 5.43 in) and CY2015 (142.7 mm, 5.62 in). Because non-heated rain gages are used at the three stations, snowfall may be underestimated if the gages froze or if snow was blown or sublimated out of the gage before it melted.

The water content of the top layer of soil is most relevant to soil migration by high winds. Sufficiently high soil-moisture content is expected to diminish the soil material available for wind transport because moisture helps bind the soil particles together. Soil volumetric water content (VWC) was monitored at all three stations in the top 5 cm (2 in) of soil using time domain reflectometry (TDR) probes installed at a shallow angle below ground surface. The TDR probes provide an estimate of soil water content based on the direct measurement of electrical soil conductivity. The TDR is a good indicator of relative changes in soil water content associated with precipitation and snowmelt events and drying periods. Absolute values of VWC are less meaningful without in-situ calibration. Even then, it can be difficult to relate the local TDR measurement to areal averages of soil moisture. Figure 18 shows the daily average VWC of the topsoil layer at Stations 400, 401, and 402 for the period between January 1, 2016, and December 31, 2016. Increases in soil VWC coincide with precipitation events and subsequent decreases in VWC correspond to drying periods.

The soil moisture was highest between January and May, when a series of minor but relatively frequent precipitation events and moderate spring air temperature resulted in elevated soil moisture. The soil moisture started to decrease from the middle of May and continued on this trend for the rest of the summer and fall with only a few minor precipitation events that very slightly elevated the measured soil moisture. The soil moisture was at its lowest in October and November 2016 before some rain at the end of November reversed the trend and resulted in an increase in soil moisture.

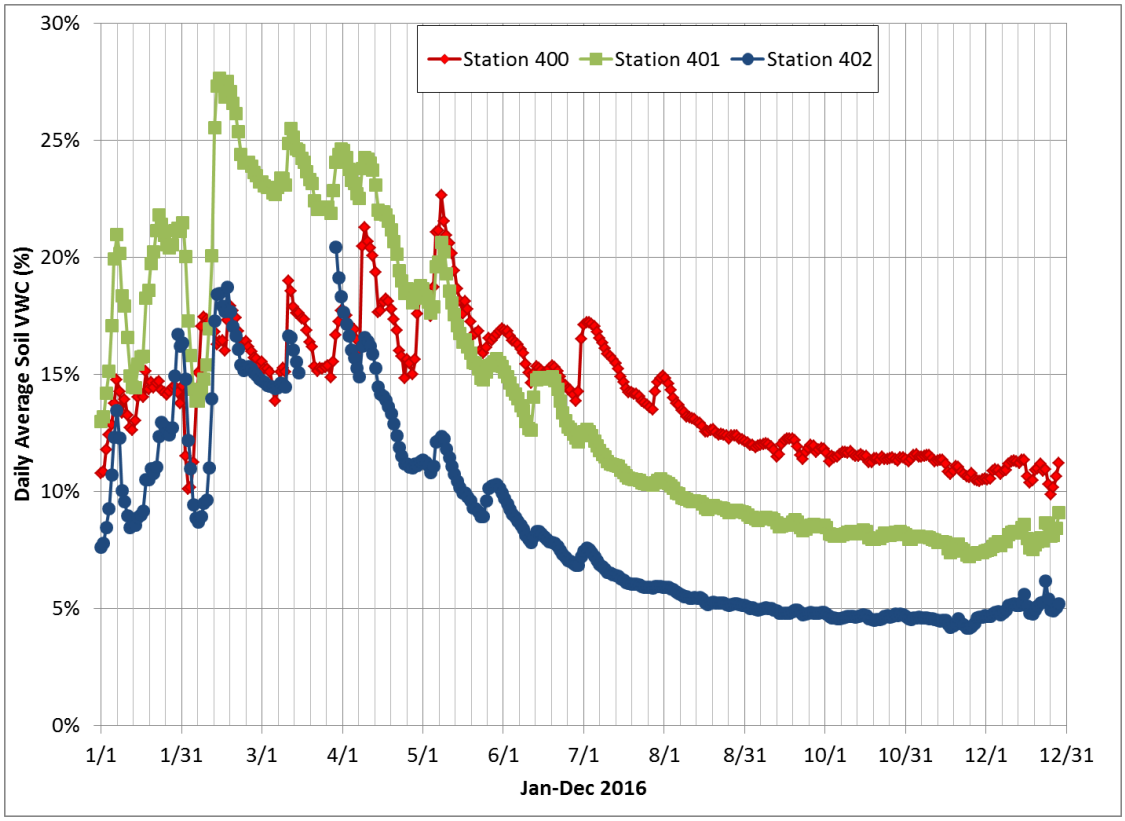

Figure 18. Soil volumetric water content for Stations 400, 401, and 402 for CY2016.

Figure 19 shows the daily average relative humidity for all stations for the monitoring period between January 1, 2016, and December 31, 2016. During precipitation events, the relative humidity increases to near the saturation value of 100 percent. The relative humidity at the TTR monitoring stations for a typical year is lowest between June and September, when precipitation events are rare and air temperature is high. The lowest monthly average relative humidity in 2016 was measured in August and was 17.4 percent, 17.7 percent, and 19.3 percent for Stations 400, 401, and 402, respectively (Appendix B). The highest monthly average relative humidity in 2016 was measured in January and was 71.3 percent, 77.6 percent, and 78.1 percent for Stations 400, 401, and 402, respectively (Appendix B).

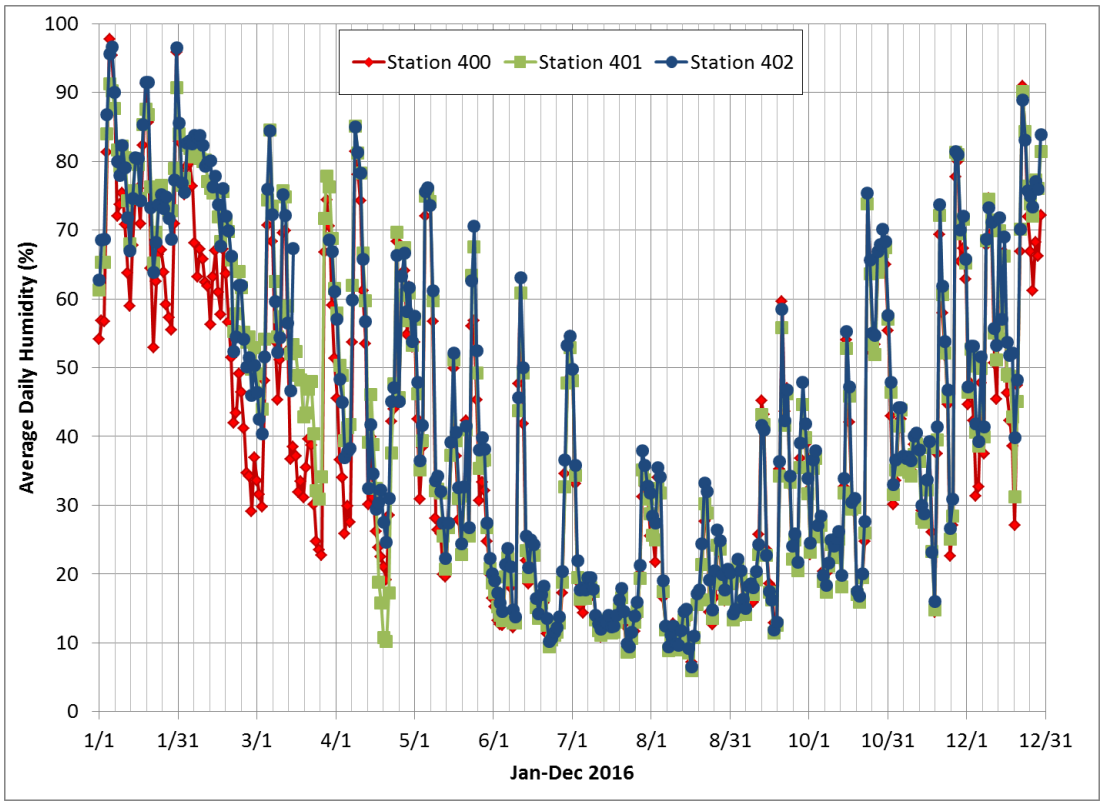

Figure 19. Average daily relative humidity for Stations 400, 401, and 402 for CY2016.

Because wind is an expected major driving force for soil transport at the Clean Slate sites, both wind speed and wind direction are collected at all TTR monitoring stations. Wind rose diagrams (Figures 20 and 21) have been developed for all three stations. Wind roses classify wind direction into sixteen directional classes that occupy 22.5 degrees and the different colors indicate different wind speed classes. The frequency of each wind speed class and wind direction is indicated by the length of each band. In Figure 20, each station has two wind roses that cover the same time period. The one on the left shows all wind speeds and their contribution to the overall wind rose and the one on the right shows only winds above 24 km/hr (15 mph) because this is typically the speed above which wind erosion has been observed at these sites (Mizell *et al.*, 2014).

In general, winds above 24 km/hr (15 mph) result in elevated PM_{10} (particulate matter of aerodynamic diameter of ≤ 10 µm) concentrations in the air. The PM_{10} concentration is an indicator of small particles that are suspended in the air and can be easily inhaled. It is estimated from the particle size distribution as measured by the Met One (Model 212) Particle Size Profiler, an instrument that uses the optical properties of particles to infer size and concentration. As seen in Figure 20, the most prevalent winds are from the south or northwest, especially for wind speeds above 24 km/hr (15 mph). The geographic context of the wind can be seen in Figure 21. Winds out of the southerly and northwesterly directions are predominant as well as the strongest, and are generally aligned with the valley topography.

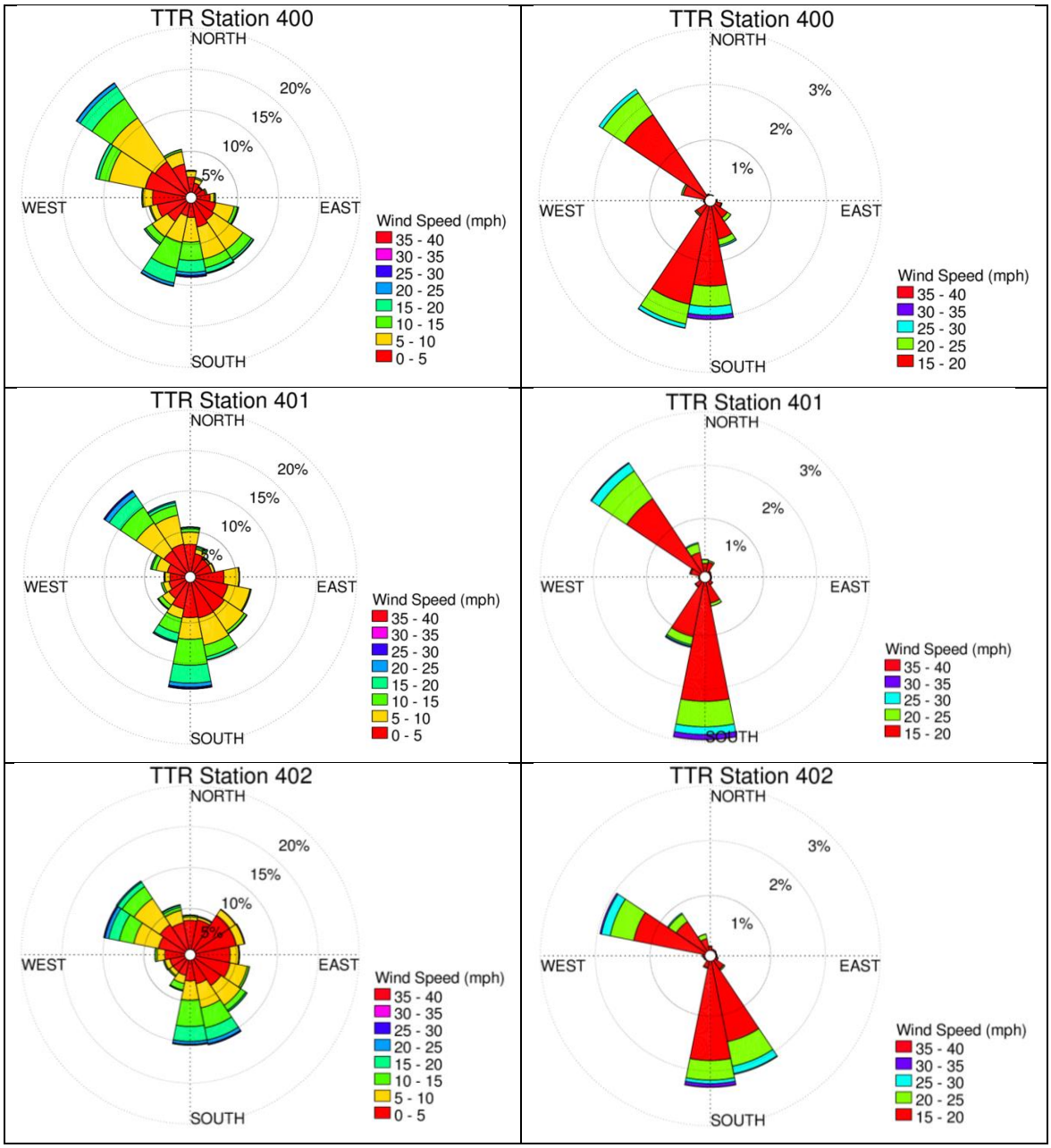

Figure 20. Annual wind roses for Stations 400, 401, and 402 for CY2016. Left panel: all winds. Right panel: winds greater than 24 km/hr (15 mph).

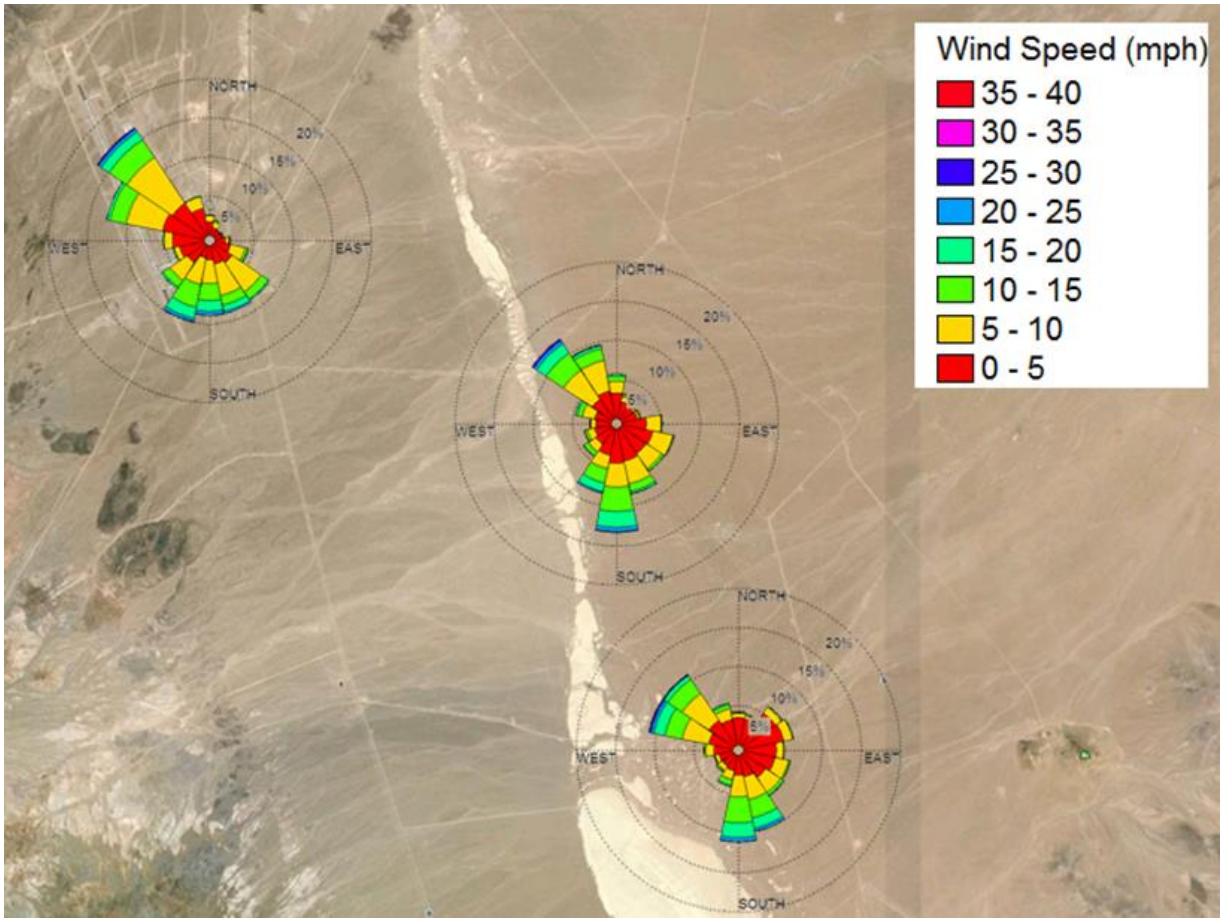

Figure 21. Annual wind rose diagrams for the TTR stations shown in map view.

Figure 22 shows the time series of average daily wind speed and shows a similar pattern for all three stations. The maximum average monthly wind speeds were recorded in April and were 13.1, 13.9, and 13.8 km/hr (8.2, 8.7, and 8.6 mph) at Stations 400, 401, and 402, respectively. In addition to March, April, and May being regularly windy months in 2016, October, which is a time of seasonal dry soil conditions, was above average in wind speed. The highest 10-minute interval sustained speeds were recorded in April and were 57.3, 57.9, and 58.6 km/hr (35.8, 36.2, and 36.6 mph) at Stations 400, 401, and 402 respectively. The highest three second interval wind speed gusts were also recorded in April and were 87.4, 85.6, and 86.5 km/hr (54.6, 53.5, and 54.1 mph) at Stations 400, 401, and 402, respectively. The annual average winds during CY2016 were 11.5, 10.6, and 10.1 km/hr (7.2, 6.6, and 6.3 mph) at Stations 400, 401, and 402, respectively (Appendix B).

Figure 23 shows the barometric pressure (atmospheric pressure) trends for Stations 400 and 402 (Station 401 is not equipped with the barometric pressure sensor). The fluctuations in barometric pressure can provide an indicator of the passage of weather fronts that can often cause high winds.

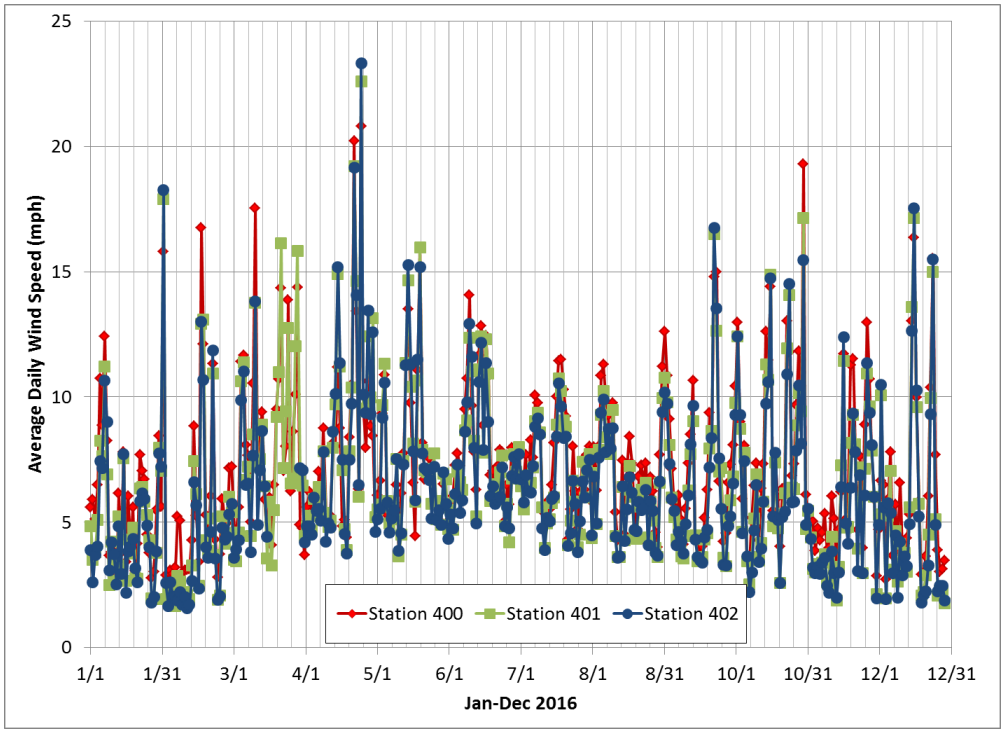

Figure 22. Average daily wind speed for Stations 400, 401, and 402 for CY2016.

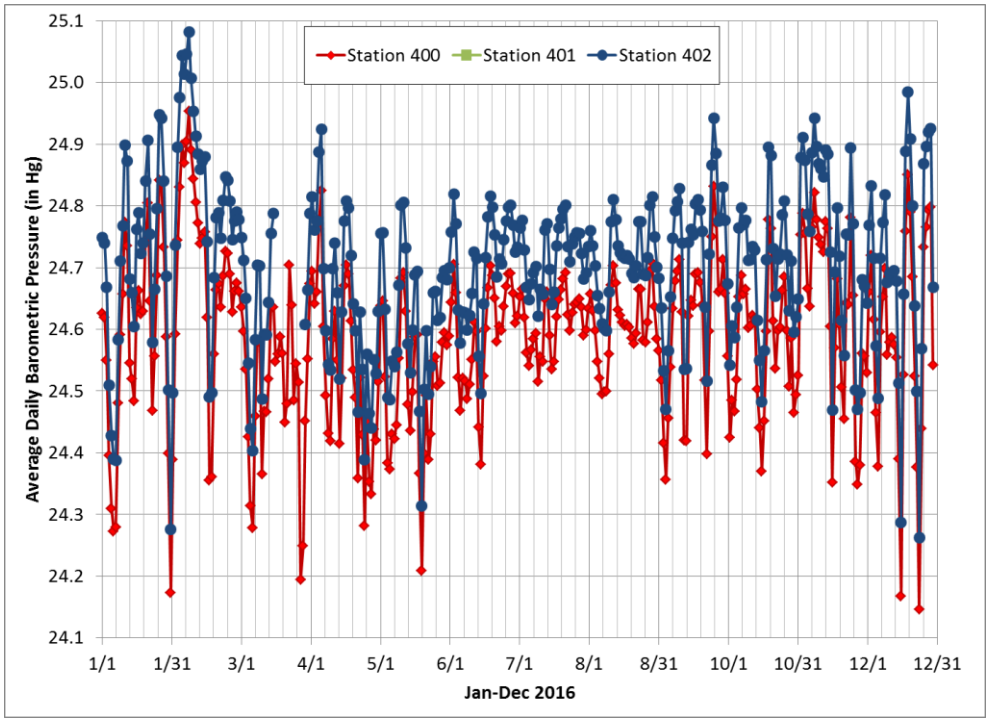

Figure 23. Average daily barometric pressure for Stations 400 and 402 for CY2016. Station 401 does not have a barometer.

RADIOLOGICAL ASSESSMENT OF AIRBORNE PARTICULATE MATERIAL

Airborne dust particles are collected continuously using Hi-Q^{TM} samplers located at each of the TTR air monitoring stations. A glass-fiber filter (diameter: 10 cm [4 in]; pore size: 0.3 µm) was used at all stations during CY2016. The Hi-Q^{TM} air sampling equipment draws ambient air through the filters at a rate of approximately 56.6 L/m (2 ft^3/m) and is designed to maintain the same flow rate as dust is collected on the filter. The total volume of air passed through the filter and the total hours of operation are recorded when filters are recovered from the monitoring stations and new filters are deployed every two weeks. Filters are weighed before and after deployment to determine the mass of particulate matter collected. Sample filters are accumulated and periodically submitted, or submitted as needed, to the RSL at the University of Nevada, Las Vegas, for gross alpha, gross beta, and gamma spectroscopy assessment. The gross alpha and gross beta observations for CY2016 are summarized below in Tables 3 and 4, respectively.

Filters collected during CY2016 were deployed between December 23, 2015, and December 21, 2016. This generated 26 particulate matter filter samples for each station. The mean annual gross alpha activity (Table 3) for the glass-fiber filter samples ranged from 1.67×10^{-15} µCi/mL at Station 401 to 2.01×10^{-15} µCi/mL at Station 402. The mean annual gross beta activity (Table 4) for the glass-fiber filter samples ranged from 1.37×10^{-14} µCi/mL at Station 401 to 1.84×10^{-14} µCi/mL at Station 402.

Table 5 gives the CY2016 gross alpha and gross beta concentrations reported for CEMP stations surrounding the TTR. Because glass-fiber filters are also used in the air samplers at the CEMP stations, useful comparisons can be made to the glass-fiber filter samples from the TTR. Mean annual gross alpha concentrations at the TTR monitoring stations are higher than the values at the surrounding CEMP stations with the exception of Sarcobatus Flats and Alamo (Figure 24). The maximum gross alpha value for 2016 of 5.70×10^{-15} µCi/ml was recorded at TTR Station 400. The Station 400 samples typically have a higher dust load than the other two stations, presumably because of soil disturbance by people and vehicles in the ROC area, and this may contribute to higher gross alpha and beta concentrations than would occur in an undisturbed background area.

Table 3. Gross alpha results for TTR sampling stations 2016.

Sampling Location	Number of Samples	Concentration ($\times 10^{-15}$ µCi/mL [3.7×10^{-5} Becquerel (Bq)/m^3])			
		Mean	Standard Deviation	Minimum	Maximum
Station 400	26	1.79	1.16	0.32	5.70
Station 401	26	1.67	1.02	0.27	3.50
Station 402	26	2.01	1.17	0.45	5.09

NOTES: Bq = Becquerel; m^3 = cubic meter; µCi/ml = microcuries per milliliter; TTR = Tonopah Test Range

Table 4. Gross beta results for TTR sampling stations 2016.

Sampling Location	Number of Samples	Concentration (× 10^{-14} µCi/mL [3.7 ×10^{-4} Becquerel (Bq)/m^3])			
		Mean	Standard Deviation	Minimum	Maximum
Station 400	26	1.56	0.44	0.92	2.91
Station 401	26	1.37	0.35	0.71	2.26
Station 402	26	1.84	0.51	1.09	3.06

NOTES: Bq = Becquerel; m^3 = cubic meter; µCi/ml = microcuries per milliliter; TTR = Tonopah Test Range

Table 5. Mean annual gross alpha and gross beta concentrations for 2016 reported at CEMP stations that surround the TTR.

Sampling Location	Gross alpha (× 10^{-15} µCi/mL)			Gross beta (× 10^{-14} µCi/mL)		
	Mean	Minimum	Maximum	Mean	Minimum	Maximum
Alamo	1.80	0.73	3.97	2.02	1.13	3.53
Beatty	1.19	0.51	2.43	1.80	1.13	3.28
Goldfield	1.13	0.56	2.44	1.73	1.10	2.98
Rachel	1.23	0.38	2.84	2.03	1.09	3.99
Sarcobatus Flats	1.90	0.57	4.88	1.97	1.22	3.57
Tonopah	1.02	0.44	1.82	1.64	1.12	3.20

The mean annual gross beta concentrations at the CEMP stations (Figure 25) are higher than those measured at the TTR stations with the exception of TTR Station 402, which falls in the middle of the CEMP range of values. All of the TTR maximum gross beta measurements are lower than the maximums measured at the surrounding CEMP stations with the exception of TTR Station 402 being higher than Goldfield.

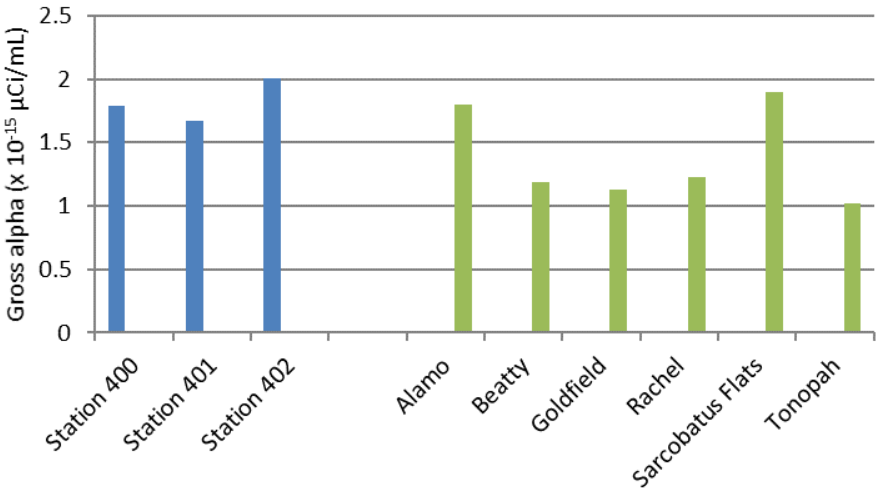

Figure 24. The mean annual gross alpha concentrations for the TTR samples (blue) compared with the mean annual gross alpha concentrations for samples collected at most of the surrounding CEMP stations (green).

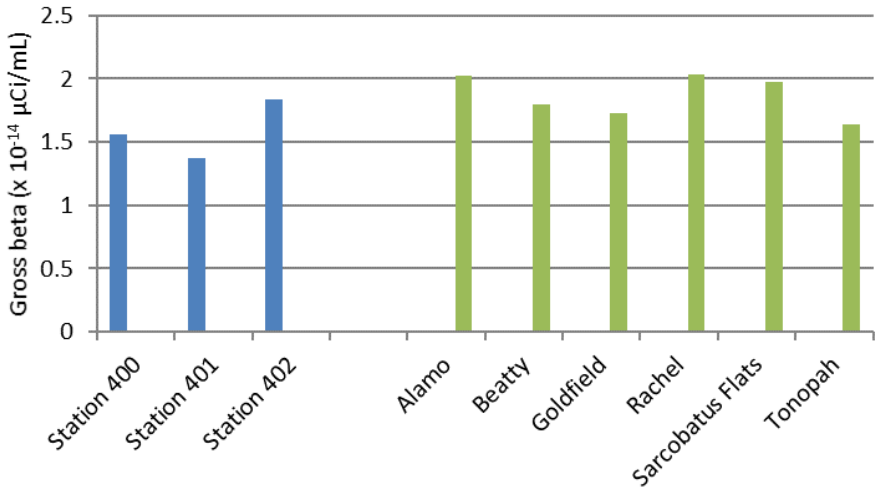

Figure 25. The mean annual gross beta concentrations for the TTR samples (blue) compared with the mean annual gross beta concentrations for samples collected at the surrounding CEMP stations (green).

Gamma spectroscopy identified only naturally occurring radionuclides in the particulate samples collected from TTR Stations 400, 401, and 402 during CY2016 (Table 6). The detected radionuclides occurred with varying frequency. Beryllium-7 and lead-210 were the most commonly detected. Americium-241, a product of ^{241}Pu decay, was not detected.

During 2016, alpha spectroscopy analysis for plutonium isotopes was conducted on air filters collected in 2015 and 2016 for comparison with analyses of soil collected from saltation traps (see later section). Two filters from each quarter of the year were selected and submitted to Test America Laboratories for alpha spectroscopy analysis. These quarterly samples include the sample with the highest gross alpha result plus one random sample from Stations 400, 401, and 402, for a total of eight samples per station. The previous gamma spectroscopy on the samples did not detect ^{241}Am.

Table 6. The number of CY2016 particulate samples in which naturally occurring radionuclides were identified by gamma spectroscopy varied by radionuclide and between stations.

Radionuclide	**Number of Samples**		
	Station 400	**Station 401**	**Station 402**
Beryllium-7 (Be-7)	26	26	26
Lead-210 (Pb-210)	7	6	9
Potassium-40 (K-40)	2	2	5
Lead-212 (Pb-212)	0	0	0
Bismuth-214 (Bi-214)	0	0	0
Protactinium-234m (Pa-234m)	0	1	1

Table 7 summarizes the results of alpha spectroscopy analyses for ^{238}Pu and $^{239/240}$Pu for filters selected from the CY2015 archive. Plutonium-238 was not identified above the minimum detectable concentration (MDC). Plutonium-239/240 was detected at the Clean Slate Stations 401 and 402, but not at Station 400, which is located at the ROC. The mean $^{239/240}$Pu activity at Station 401 was 1.69×10^{-16} µCi/mL, with a maximum of 3.66×10^{-16} µCi/mL, a minimum of 0.32×10^{-16} µCi/mL, and a standard deviation of 1.17×10^{-16} µCi/mL. The mean $^{239/240}$Pu activity at Station 402 was 1.52×10^{-16} µCi/mL, with a maximum of 4.34×10^{-16} µCi/mL, a minimum of 0.55×10^{-16} µCi/mL, and a standard deviation of 1.32×10^{-16} µCi/mL.

Table 8 summarizes the results of alpha spectroscopy analyses for ^{238}Pu and $^{239/240}$Pu for filters selected from CY2016. Plutonium-238 was not identified above the MDC. Plutonium-239/240 was detected at Clean Slate Stations 401 and 402, but not at Station 400. The mean $^{239/240}$Pu activity at Station 401 was 9.12×10^{-16} µCi/mL, with a maximum of 45.00×10^{-16}, a minimum of 0.61×10^{-16}, and a standard deviation of 17.63×10^{-16}. It is important to note that the mean and standard deviation are skewed because the maximum sample, which was collected between November 9 and 22, 2016, is an order of magnitude larger than the other samples. The mean $^{239/240}$Pu activity at Station 402 was 1.14×10^{-16}, with a maximum of 1.57×10^{-16}, a minimum of 0.71×10^{-16}, and a standard deviation of 0.61×10^{-16}.

Table 7. TTR alpha spectroscopy results for Stations 400, 401, and 402 for samples collected in 2015.

Sampling Location	Number of Samples > MDC Pu-238	Number of Samples >MDC Pu-239/240	Concentration ($\times 10^{-16}$ µCi/mL [3.7×10^{-6} Bq/m^3])		
			Mean ± S.D. Pu-239/240	Minimum Pu-239/240	Maximum Pu-239/240
400	0	0	n/a	n/a	n/a
401	0	7	1.69 ± 1.17	0.32	3.66
402	0	6	1.52 ± 1.32	0.55	4.34

n/a = not applicable; S.D. = standard deviation; MDC = minimum detectable concentration; MDC Pu-238 = 0.75 ± 0.16 µCi/mL $\times 10^{-16}$; MDC Pu-239/240 = 0.47 ± 0.22 µCi/mL $\times 10^{-16}$.

Table 8. TTR alpha spectroscopy results for Stations 400, 401, and 402 for samples collected in 2016.

Sampling Location	Number of Samples > MDC Pu-238	Number of Samples >MDC Pu-239/240	Concentration ($\times 10^{-16}$ µCi/mL [3.7×10^{-6} Bq/m^3])		
			Mean ± S.D. Pu-239/240	Minimum Pu-239/240	Maximum Pu-239/240
400	0	0	n/a	n/a	n/a
401	0	6	9.12 ± 17.63[a]	0.61	45.00
402	0	2	1.14 ± 0.61	0.71	1.57

n/a = not applicable; S.D. = standard deviation; MDC = minimum detectable concentration; MDC Pu-238 = 0.94 ± 0.13 µCi/mL $\times 10^{-16}$; MDC Pu-239/240 = 0.55 ± 0.09 µCi/mL $\times 10^{-16}$.

a) Data are skewed because of one sample collected between November 9 and 22, 2016.

GAMMA RADIATION OBSERVATIONS

Gamma radiation is measured using a PIC detector. A PIC detector is generally deployed to detect gamma radiation events that substantially exceed ambient radiation levels as a result of human activities. In the absence of such activities, ambient gamma radiation rates are recorded. These radiation values vary naturally among locations and reflect differences in altitude and latitude (cosmic radiation) and radioactivity in the soil (terrestrial radiation). Additionally, slight variations in gamma radiation at a single location may be caused by changes in weather (UNSCEAR, 2000).

The PIC data collected at the TTR air monitoring stations measure gamma radiation exposure every three seconds. These measurements are averaged every 10 minutes before being recorded in the station database. The 10-minute average gamma values for CY2016 recorded at TTR Stations 400, 401, and 402 are presented in Table 9 and Figure 26. Shown in Figure 26 shows the gamma record from each PIC as well as the mean of all CY2016 10-minute gamma values at that station and the PIC mean plus and minus two standard deviations.

Table 9. Gamma exposure rate at the TTR measured in 2016 by the PIC detectors.

Sampling Location	Average of 10-minute Gamma Exposure Rate (µR/hr)			
	Mean	Standard Deviation	Minimum	Maximum
Station 400	19.24	0.46	16.89	24.97
Station 401	20.26	1.19	15.50	25.52
Station 402	21.06	0.91	17.52	27.42

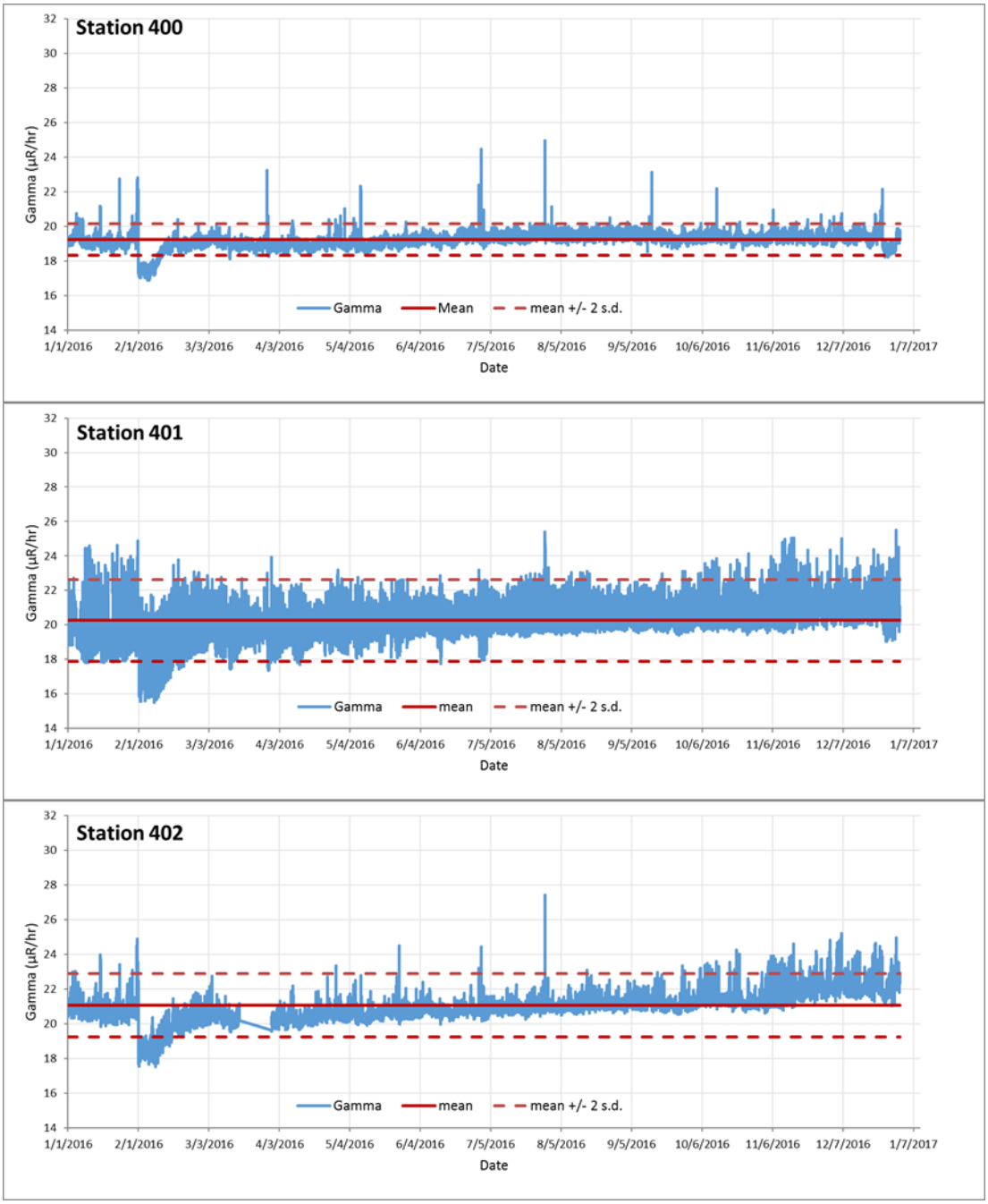

Figure 26. The CY2016 PIC gamma data for the TTR monitoring stations.

The average gamma exposure rates for the CEMP stations in the region are generally lower than the TTR stations with the exception of the CEMP station at Warm Springs Summit (Table 10). Mizell *et al.* (2014) examined atmospheric conditions coinciding with increases in gamma radiation. Observed meteorological conditions associated with intervals of increased gamma values commonly included increasing wind speeds, wind direction changes, increasing barometric pressure, increasing humidity, decreasing air temperature, and precipitation. These conditions also indicate a passing storm front, which suggests an

association between storm front passage and intervals of increased gamma values, one reason being precipitation washing dust from the atmosphere that often contains gamma emitting materials. Additionally, high dust counts observed prior to the intervals of increased gamma values are likely the result of the winds associated with these storm fronts. The 2013 analysis concluded that the observed intervals of increased gamma values were not associated with wind transport of radionuclide-contaminated soil material.

Table 10. Gamma exposure rate measured with PICs at CEMP stations in the TTR region in 2016.

Sampling Location	Average of 10-minute Gamma Exposure Rate (µR/hr)			
	Mean	Standard Deviation	Minimum	Maximum
Alamo	13.05	0.45	11.55	17.91
Beatty	16.59	0.42	13.53	22.35
Goldfield	15.63	0.78	13.49	19.97
Rachel	14.68	0.45	13.05	20.41
Sarcobatus Flats	16.58	0.39	15.50	22.97
Tonopah	16.11	0.51	13.95	21.28
Warm Springs Summit	19.28	0.70	16.14	27.67

A comparison of the CY2016 gamma measurements for Station 402 with precipitation measured at the monitoring station (Figure 27) reveals that many of the short-term gamma increases coincide with precipitation events. Comparisons of the TTR station precipitation measurements and the gamma record from the CEMP station at Warm Springs Summit also find coincidence between the timing of the gamma increases (Figure 28). These observations suggest that many of the higher gamma values are associated with precipitation or other widespread weather events, not the migration of contaminated material from the Clean Slate sites.

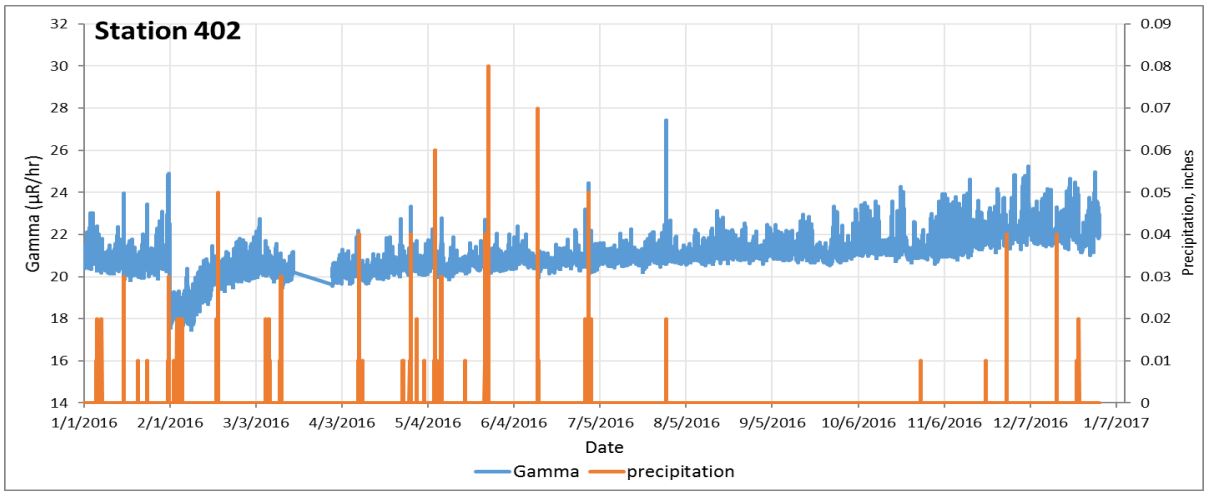

Figure 27. The CY2016 PIC gamma data and precipitation for TTR Station 402.

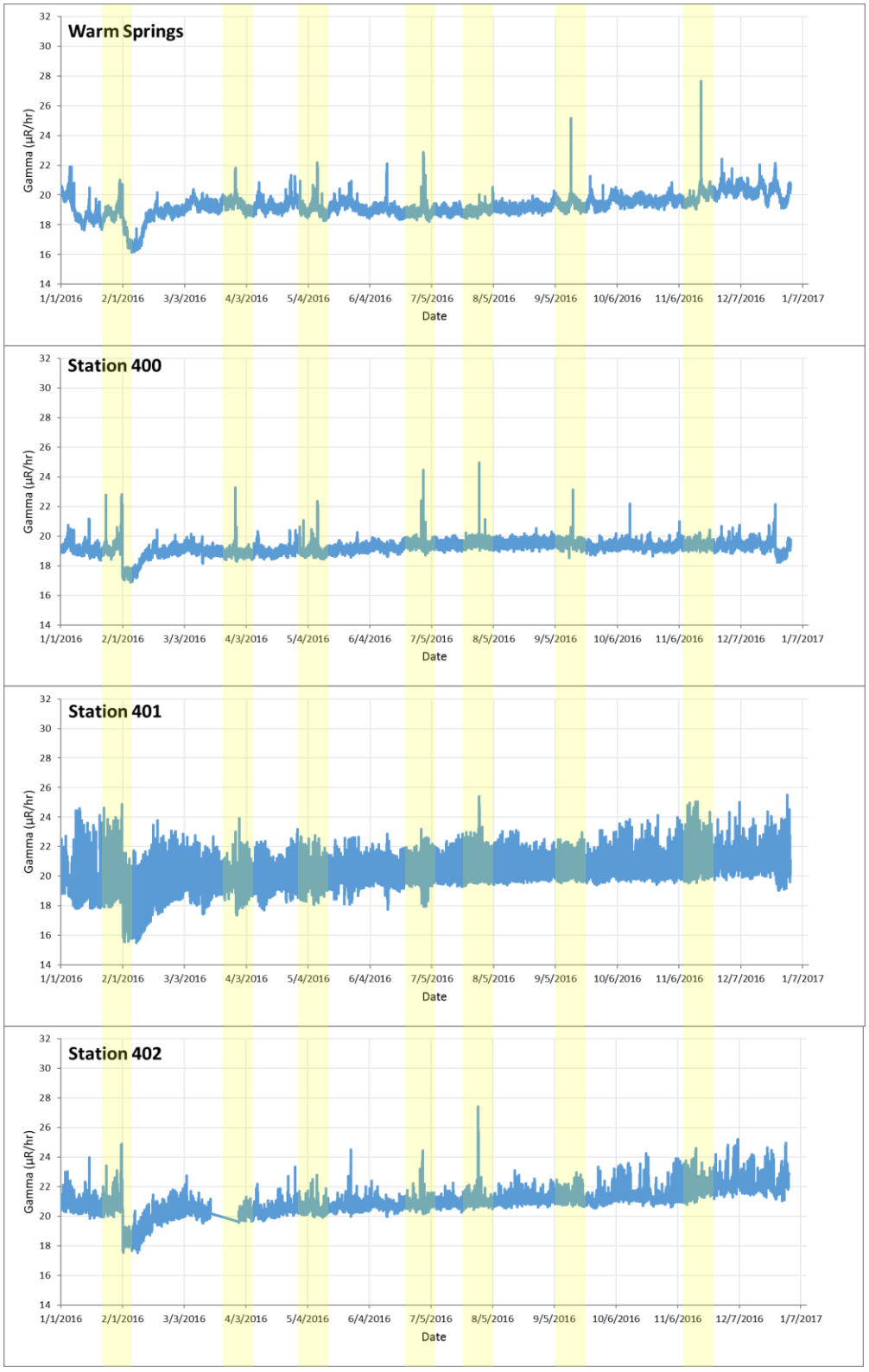

Figure 28. The CY2016 PIC gamma data for the CEMP station at Warm Springs Summit and the TTR stations that highlight select coincident times of increased values.

OBSERVATIONS OF SOIL TRANSPORT BY SALTATION

Saltation is the mechanism by which sand-sized soil particles are transported across the ground surface. Generally, saltation involves particle sizes greater than approximately 50 µm. Particles are dislodged and carried a small distance in the air before falling to the ground (Figure 29). Transport paths usually follow a parabolic trajectory; the particles essentially bounce across the ground. The amount of time the particles are in the air and the distances traveled are functions of wind speed and particle mass. Saltation is important because the impact of saltated particles dislodges smaller particles and ejects them into the air where the smaller particles are transported by suspension.

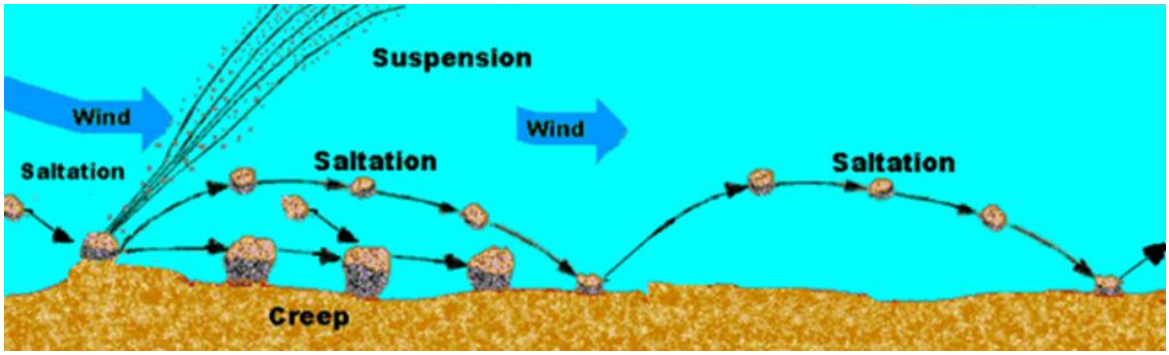

Figure 29. Diagram of the saltation process. The suspension of smaller particles ejected by the impact of a particle landing after saltation is depicted on the left.

Piezoelectric Sensor Results

The Sensit H11-LIN® (Sensit, Inc., Redlands, California) is deployed at TTR Stations 401 and 402 to measure the motion of soil particles saltating across the ground surface. The sensing area, which is set 10 cm (4 in) above the ground surface, wraps completely around the vertically oriented instrument and is capable of registering impacts from any direction. The sensing area is made of piezoelectric material that converts particle impacts to electrical impulses that are registered and summed over 10-minute intervals and subsequently stored on the station data logger. The saltation sensors are located in proximity to the meteorological towers at each station in areas that are free of recent disturbance and vegetation that might interfere with instrument operation. Windblown plant debris, such as tumbleweed, is cleared from the sensor area as needed. Raindrop impacts dislodge soil particles and eject particles, which may result in spurious impact counts on the saltation sensors during precipitation events. Therefore, saltation sensor data that are coincident with precipitation are not considered during data analyses.

Sand particle saltation is strongly dependent on wind speed (Table 11 and Figure 30). In contrast to previous years, there is no marked increase in saltation particle counts at wind speeds above 24 to 32 km/hr (15 to 20 mph) and, in particular, the particle counts at the highest wind speeds are significantly lower than recorded in 2015. For example, at Station 401, the saltation counts for winds of 57 to 64 km/hr (35 to 40 mph) were 133.8 counts/10 minutes in 2015, and 9 counts/10 minutes in 2016. Nonetheless, sand transport by saltation is more effective at wind speeds above 24 to 32 km/hr (15 to 20 mph)

because the average particle counts at lower wind speeds are very small. At all wind speeds, Station 402 consistently has higher particle counts than Station 401. There is a strong, linear relationship between average saltation counts and average PM_{10} concentration (Figure 31).

Table 11. Average saltation particle impact counts by wind speed class at TTR air monitoring Stations 401 and 402.

Wind Speed Class (mph)	Duration (hours)	Average Wind Speed (mph)	Average Particle Counts (count/10-min)
Station 401			
0-5	4,293.83	2.70	0.001
5-10	2,544.83	7.09	0.020
10-15	1,120.33	12.22	0.362
15-20	568.33	17.14	1.684
20-25	142.00	21.90	7.168
25-30	34.50	27.21	15.238
30-35	11.33	31.90	13.662
35-40	0.67	35.46	9.000
Total hours	8,715.8	n/a	n/a
Station 402			
0-5	4,350.00	2.71	0.030
5-10	2,126.83	7.10	0.694
10-15	1,048.00	12.27	3.871
15-20	501.50	17.06	13.091
20-25	132.67	21.86	22.059
25-30	33.67	27.18	22.386
30-35	8.00	31.65	48.146
35-40	1.17	35.69	42.571
Total hours	8,201.83	n/a	n/a

n/a = not applicable.

Note: mph can be converted to km/hr by multiplying by 1.6.

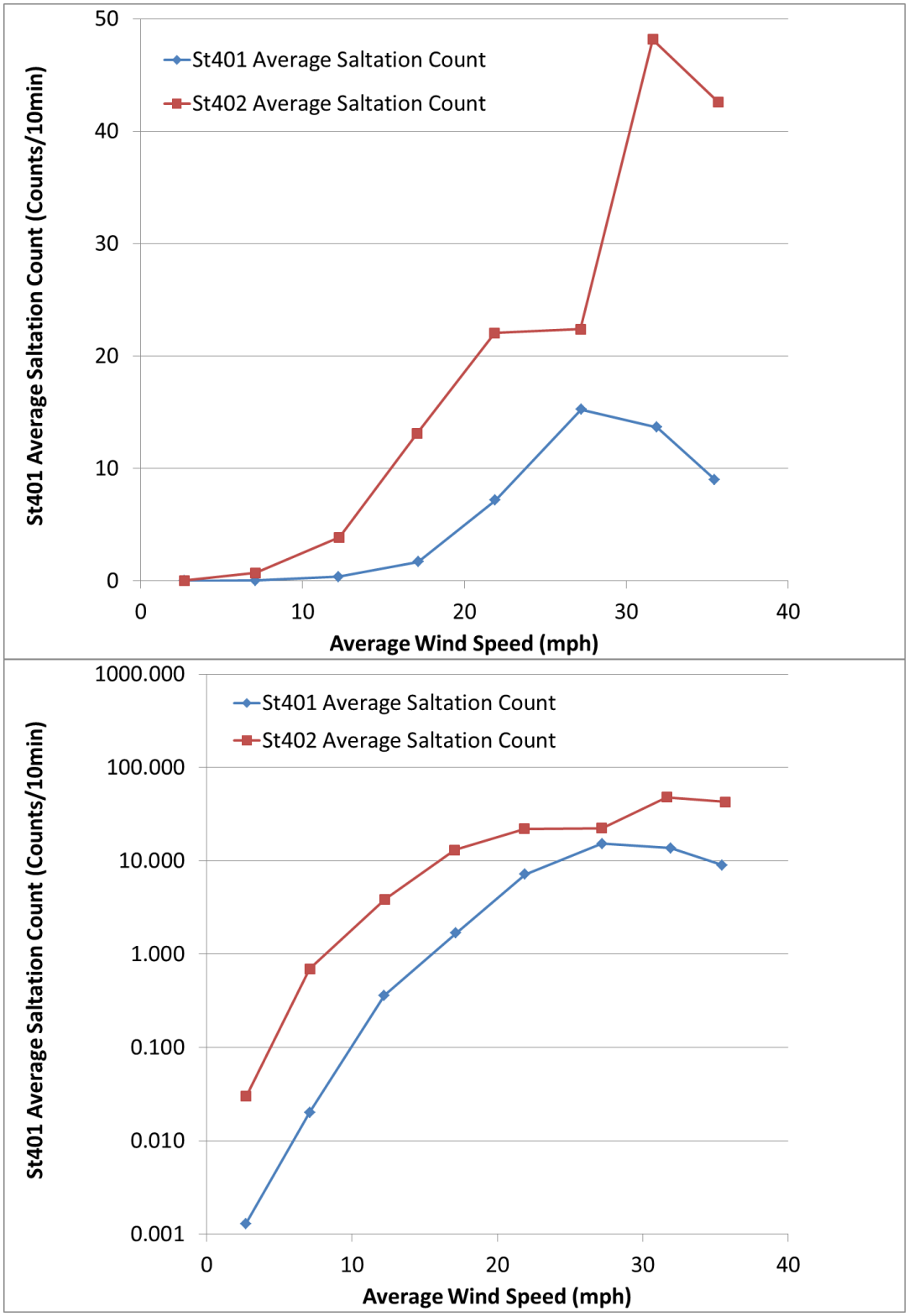

Figure 30. Linear (top) and log (bottom) scale relationships of particle counts and wind speed. Average saltation counts generally increase rapidly as the wind speed increases above 20 mph at both TTR Stations 401 and 402.

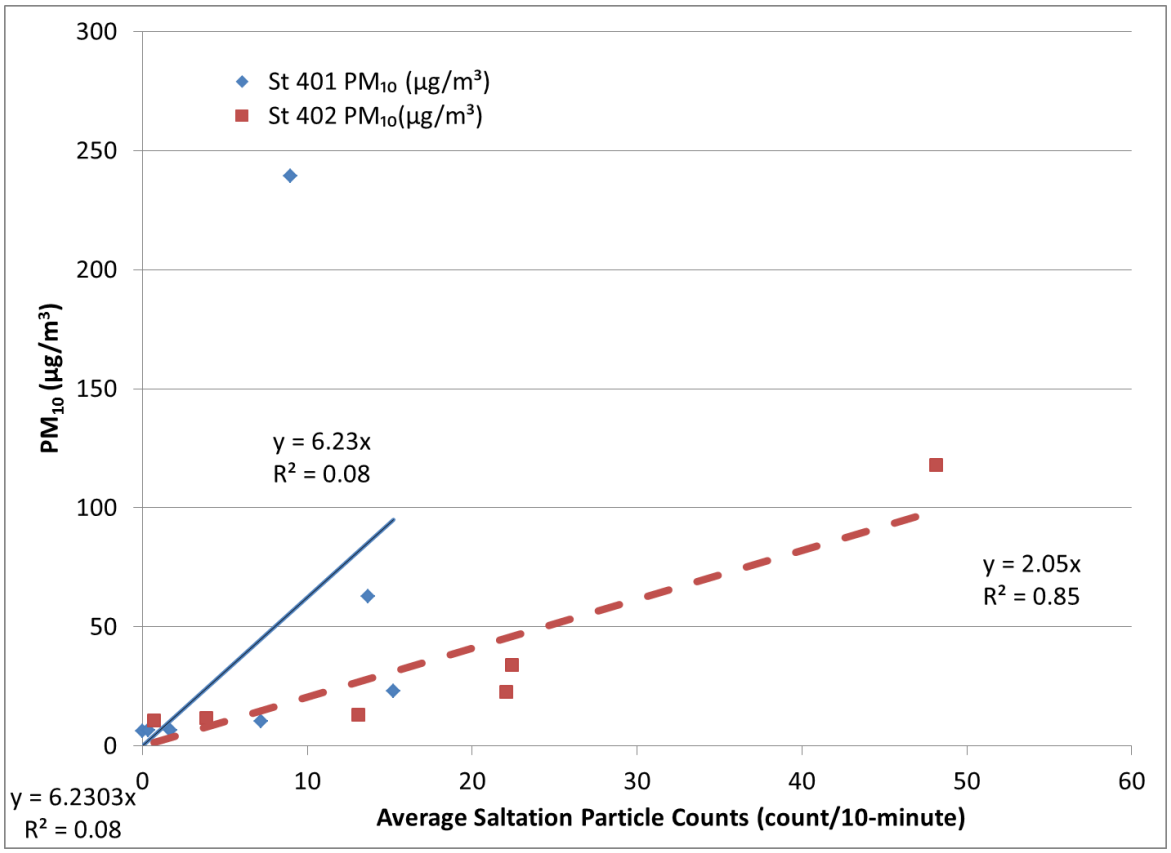

Figure 31. Regression of PM_{10} against saltation counts by wind speed class.

Saltation Trap Results

The Sensit® piezoelectric instruments record real-time saltation activity that can be used to identify transport events when analyzed in conjunction with wind speed data. One of the drawbacks of the Sensit® instrument is that it provides count information but not the transport mass flux. To estimate the transport mass flux, the BSNE traps were installed at TTR Stations 401 and 402 to provide integrated mass samples. The design and installation of the BSNE samplers is described in the section entitled BSNE Sand Trap Installation.

The BSNEs at the TTR Clean Slate I and III were originally installed on April 1, 2014. Each BSNE collector was sequentially numbered from 1 to 24. Odd numbered BSNEs are always oriented toward the south-southeast and even number BSNEs toward the north-northwest (see Figure 32 and 33). Therefore, the material transported from Clean Slate sites by southerly winds would be collected in odd numbered BSNEs and material transported by northwesterly winds would be collected by the even numbered BSNEs. Two sets of traps (numbers 1-12 and numbers 13-24) are used in rotation as sample collection occurs. The third BSNE sample collection occurred on October 19, 2016, when BSNEs 1-12 were collected from the Clean Slate I and III locations. Samplers 13-24 were emplaced at the same time. The first collection interval—between April 1, 2014, and June 24, 2015—was 449 days long. The second collection interval—between June 24, 2015, and February 16, 2016—was 237 days long. The third interval—between February 16, 2016, and October 19, 2016—was 245 days long.

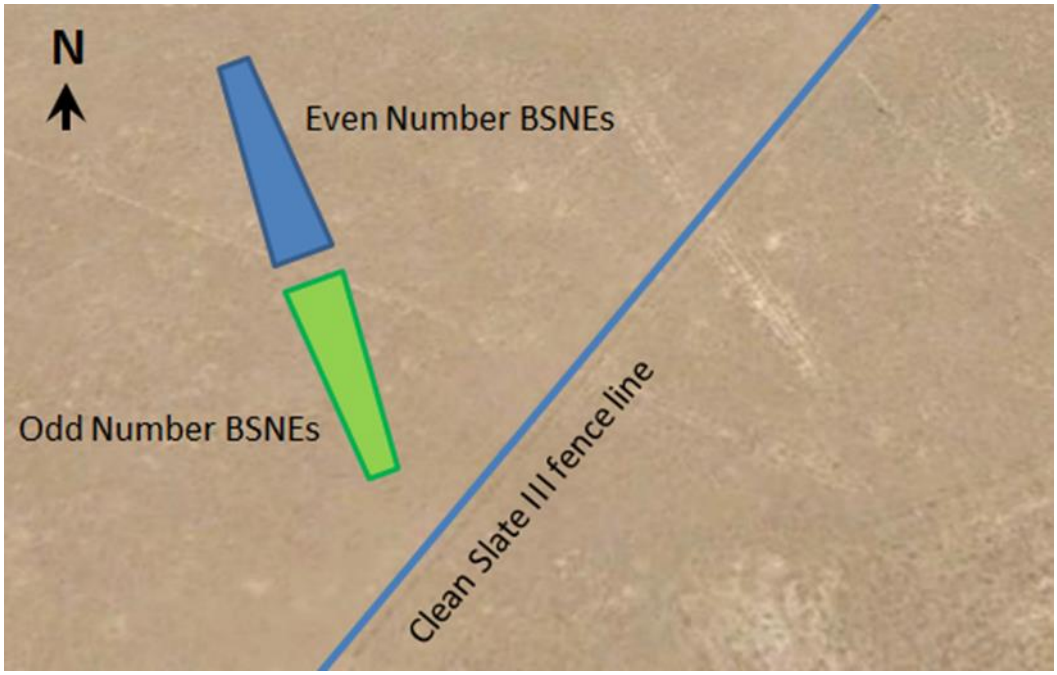

Figure 32. TTR Clean Slate III Station 401 BSNE alignment.

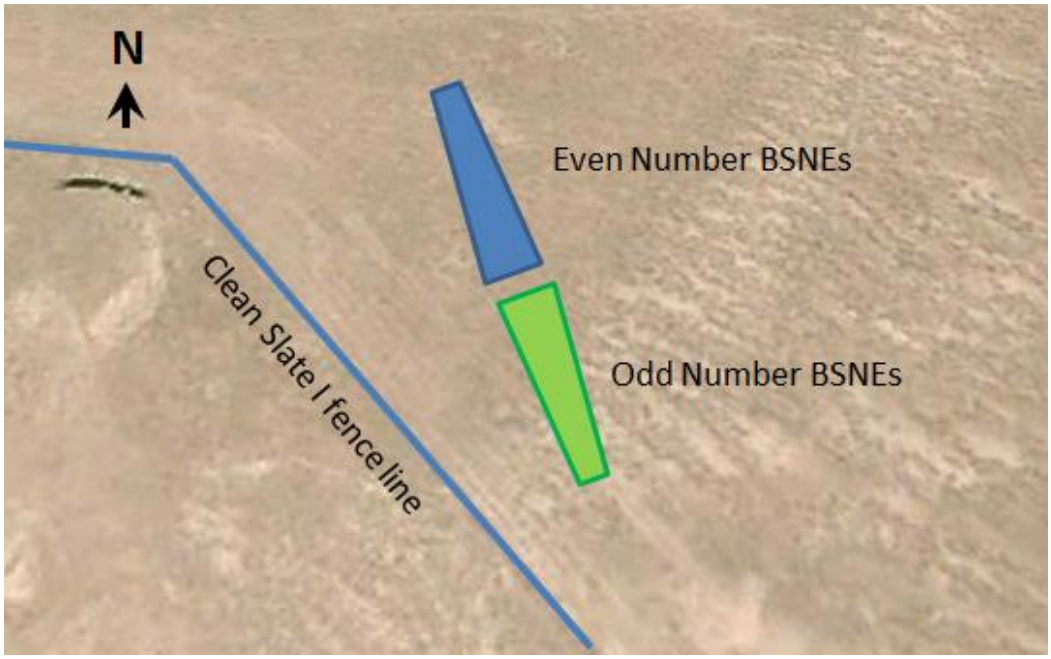

Figure 33. TTR Clean Slate I Station 402 BSNE alignment.

When the BSNEs were collected on October 19, 2016, the traps were processed and cleaned in the field and the samples were initially weighed and packaged for the radiological and soil size distribution lab analyses. To determine the collected weight, each BSNE was wiped on the outside to remove any rain splatter debris, the top section was removed (see Figure 34), and the collected sample in the bottom was inspected. The bottom of each BSNE containing the samples was weighed on a lab balance with a 0.1 g resolution and the weight was recorded in the field datasheet. After being cleaned and dried, the bottom of the BSNEs were weighed and the net collected soil weight was determined by subtracting the two measured weights (Table 12). Deionized water was used to carefully wash out the collected soil samples into 0.5 L plastic bottles (Figure 35). Samples from the three odd numbered BSNEs at each specific Clean Slate site were combined into one 0.5 L plastic bottle for lab analysis because of the relatively small amount of collected material. The same procedure was followed for the even numbered BSNEs at each location, which resulted in the collection of two composite samples for lab analyses for each Clean Slate site. The soil samples collected in October 2016 were separated by the laboratory into three size ranges for analysis: ≥ 250 μm, between 65 and 250 μm, and ≤ 63 μm in diameter. The results of the gravimetric analysis are shown in Table 13.

Table 12. Field weights of collected soil samples and collection dates/times.

Clean Slate Site	BSNE Number	Start Date	End Date	Net Weight (g)
Clean Slate III	T1	February 17, 2016	October 19, 2016	1.1
Clean Slate III	T3	February 17, 2016	October 19, 2016	0.9
Clean Slate III	T5	February 17, 2016	October 19, 2016	0.9
Clean Slate III	T2	February 17, 2016	October 19, 2016	2.8
Clean Slate III	T4	February 17, 2016	October 19, 2016	3.1
Clean Slate III	T6	February 17, 2016	October 19, 2016	2.6
Clean Slate I	T7	February 17, 2016	October 19, 2016	1.7
Clean Slate I	T9	February 17, 2016	October 19, 2016	2.4
Clean Slate I	T11	February 17, 2016	October 19, 2016	1.6
Clean Slate I	T8	February 17, 2016	October 19, 2016	2.1
Clean Slate I	T10	February 17, 2016	October 19, 2016	1.9
Clean Slate I	T12	February 17, 2016	October 19, 2016	2.2

Table 13. Gravimetric laboratory analysis.

BSNE #	Mass > 250 μm (g)	Mass 63-250 μm (g)	Mass < 63 μm (g)	Total Mass Lab (g)
TTR CS III Traps: 1, 3, 5	0.4804	1.9785	0.8911	3.3500
TTR CS III Traps: 2, 4, 6	1.9185	5.8158	1.4726	9.2069
TTR CS I Traps: 7, 9, 11	1.3626	3.6244	1.0528	6.0398
TTR CS I Traps: 8, 10, 12	0.9150	4.1421	1.5266	6.5837

Figure 34. TTR BSNE sample collection October 19, 2016.

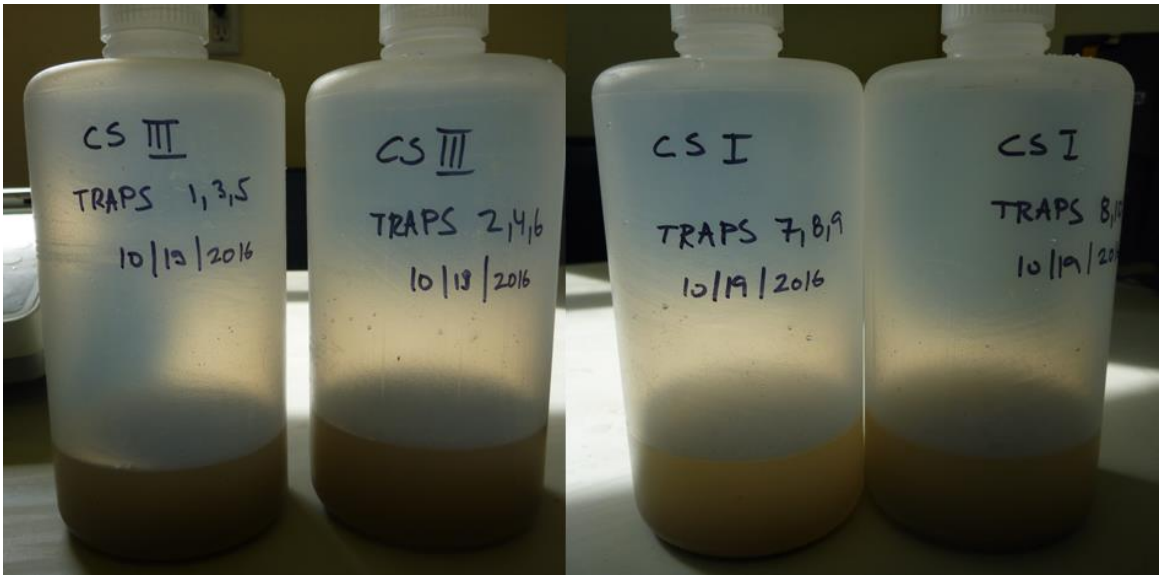

Figure 35. TTR BSNE samples collection October 19, 2016.

Figures 36 and 37 show the results of the soil particle size analysis for BSNE samples collected at the Clean Slate III and I sites between February 17, 2016, and October 19, 2016. For this collection period, net soil and dust transport at Clean Slate III is from the northwest toward the Clean Slate III site, whereas there is little difference between soil transport toward and away from the Clean Slate I site (Figure 36). The general size fraction characteristics are similar between Clean Slate I and III. Most of the saltating particles by weight are in the size fraction of 63 to 250 µm (more than 60 percent) (Figure 37).

Radiological analyses were performed for ^{238}Pu, $^{239+240}$Pu, and ^{241}Am (Table 14) for all BSNE samples. Trap location appears to be of greater importance to radionuclide concentration than trap orientation. Samples collected adjacent to Clean Slate III tend to have higher concentrations than those from Clean Slate I. An inlet orientation facing toward the adjacent Clean Slate site is not generally associated with higher concentrations than the material collected in the opposite orientation. At Clean Slate I, only five samples from odd-numbered traps (the inlet facing the site) had a higher concentration than the even-numbered traps for the nine pairs. At Clean Slate III, concentrations are consistently higher for the smallest size fraction of material collected from the traps oriented away from the site (even traps), than for samples collected facing toward the site.

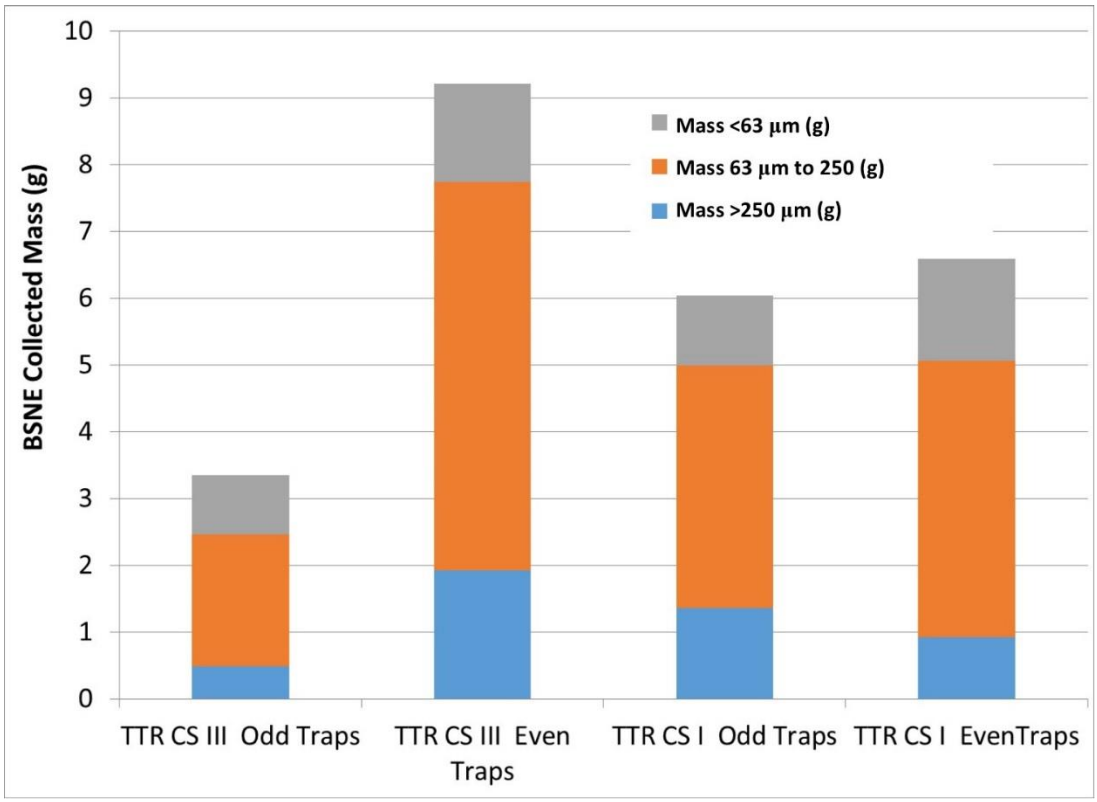

Figure 36. BSNE February 17, 2016, to October 19, 2016, collection period soil sample size distribution.

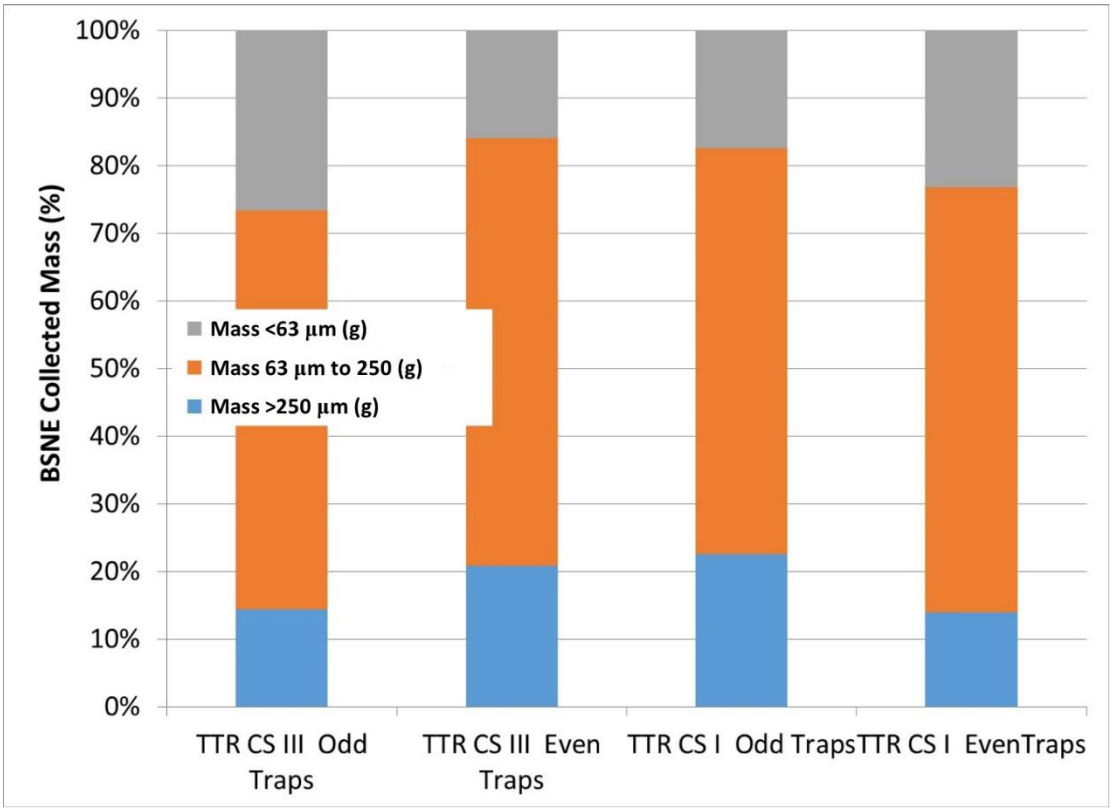

Figure 37. BSNE February 17, 2016, to October 19, 2016, collection period normalized soil sample size distribution.

Table 14. Alpha spectroscopy analytical results for samples collected in saltation traps.

BSNE #	Isotope Concentrations at Clean Slate Sites					
	Size Fraction					
	< 63 µm	TPU*	63-250 µm	TPU*	> 250 µm	TPU*
	Pu-239/240 (pCi/g)					
TTR CS I Traps: 7, 9, 11	23.2	2.94	9.38	1.24	8.27	1.09
TTR CS I Traps: 8, 10, 12	27.4	3.50	9.03	1.17	6.86	0.949
TTR CS III Traps: 1, 3, 5	50.7	6.43	61.9	7.76	8.49	1.23
TTR CS III Traps: 2, 4, 6	205	25.7	12.6	1.63	9.06	1.17
	Am-241 (pCi/g)					
TTR CS I Traps: 7, 9, 11	5.69	0.996	0.840	0.183	0.497	0.128
TTR CS I Traps: 8, 10, 12	2.20	0.409	0.755	0.162	0.952	0.224
TTR CS III Traps: 1, 3, 5	2.86	0.530	1.58	0.297	0.701	0.214
TTR CS III Traps: 2, 4, 6	20.0	3.24	1.15	0.214	0.771	0.165
	Pu-238 (pCi/g)					
TTR CS I Traps: 7, 9, 11	0.114	0.0505	0.0934	0.0378	0.0218	0.0263
TTR CS I Traps: 8, 10, 12	0.153	0.0539	0.0554	0.0269	0.0578	0.0432
TTR CS III Traps: 1, 3, 5	0.518	0.139	0.364	0.0810	0.105	0.0748
TTR CS III Traps: 2, 4, 6	1.30	0.218	0.0941	0.0368	0.0384	0.0226

*TPU = total propagated uncertainty.

The particle size fraction is an important factor in the results, with a strong correlation between smaller particle size and higher radionuclide concentration (Figures 38 through 40). With only one exception, the highest radionuclide concentration for each set of traps occurred in the size fraction below 63 µm. Similarly, the lowest concentrations tend to be associated with the size fraction larger than 250 µm.

The $^{239+240}$Pu concentrations for all of the composited samples are on the order of 500 to 15,000 times higher than background (assumed to be 0.014 pCi/g per Turner *et al.* [2003]), but 20 to 600 times lower than the 25 millirem per year action level established for environmental restoration of Soil Activity sites (equivalent to a $^{239+240}$Pu concentration of

4,120 pCi/g for an industrial area worker scenario) (U.S. DOE, 2014). The $^{239+240}Pu/^{238}Pu$ ratio is also two to twelve times higher than that from atmospheric weapons testing fallout in the northern hemisphere (fallout ratio of 30 per Turner *et al.* [2003]). The higher $^{239+240}Pu/^{238}Pu$ ratio indicates an additional source for $^{239+240}Pu$ and is consistent with the location adjacent to the Clean Slate safety tests.

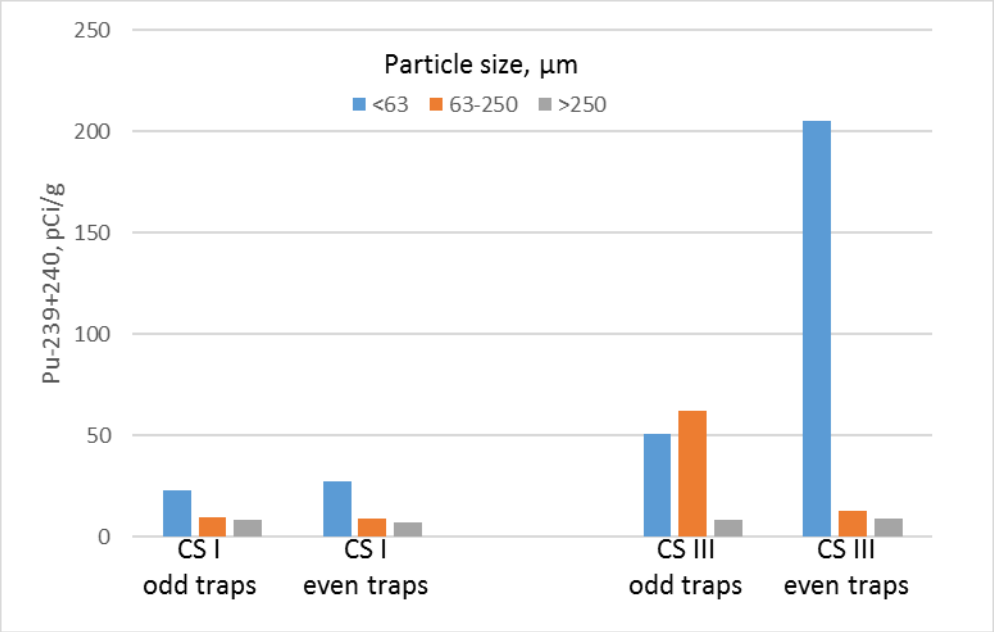

Figure 38. $^{239+240}Pu$ concentrations in samples from the saltation traps.

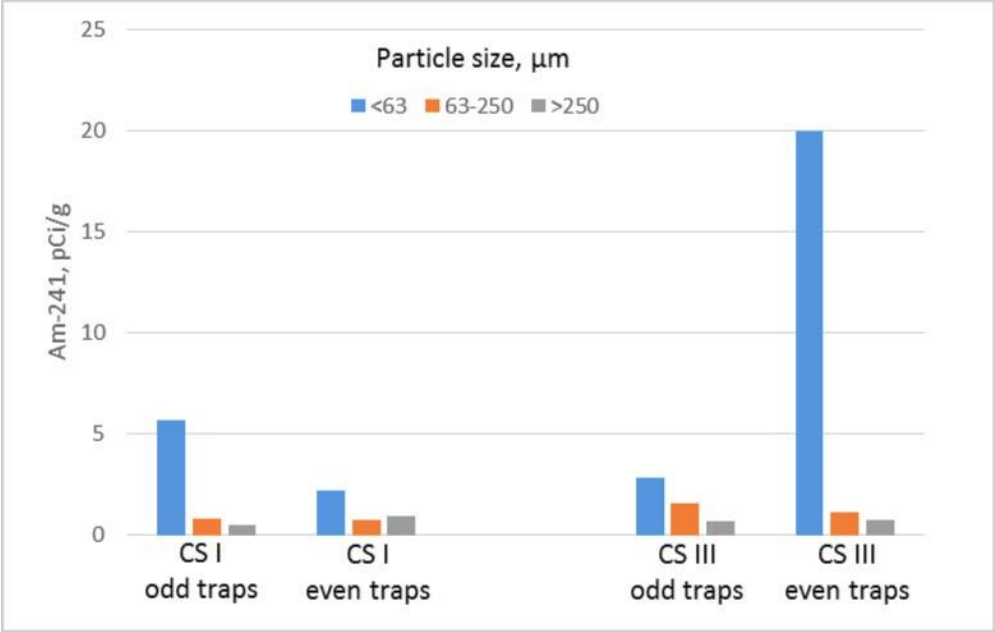

Figure 39. ^{241}Am concentrations in samples from the saltation traps.

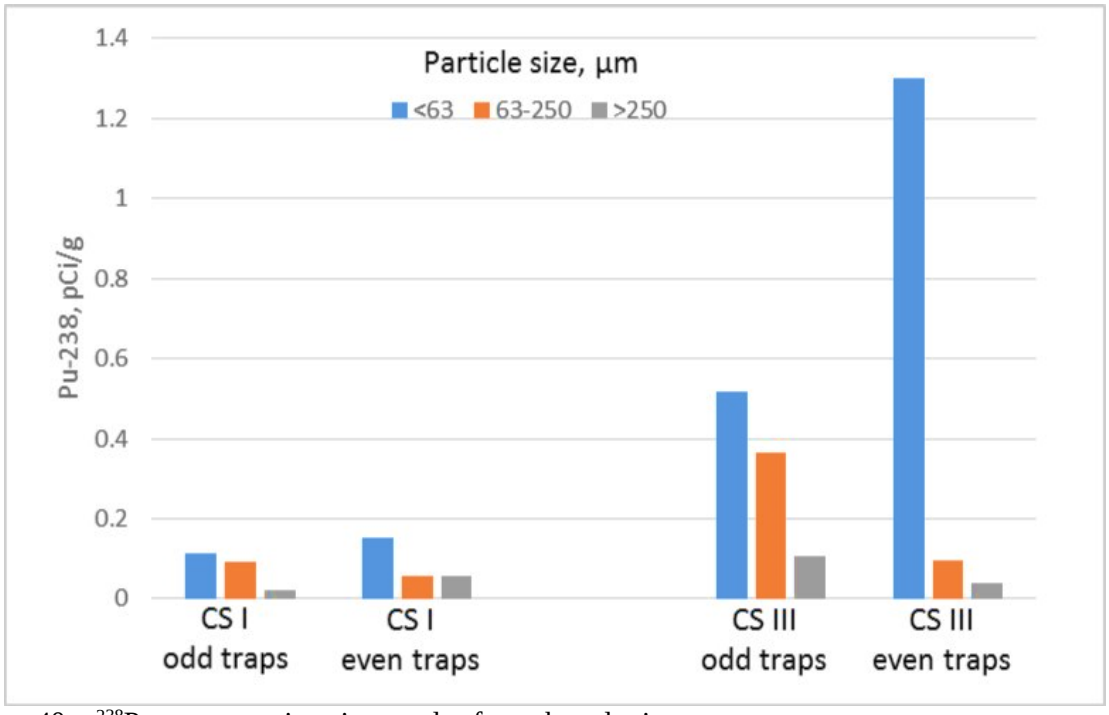

Figure 40. ^{238}Pu concentrations in samples from the saltation traps.

OBSERVATIONS OF SOIL TRANSPORT BY SUSPENSION

Table 15 summarizes wind speed and the corresponding PM_{10} concentration by wind speed class for Stations 400, 401, and 402. More than 90 percent of the time, the wind speed at all three stations is below 24 km/hr (15 mph) and the corresponding average PM_{10} concentrations are below 12 µg/m^3. Although PM_{10} concentrations generally increase as wind speed increases, the PM_{10} concentrations remain fairly low until winds exceed approximately 32 km/hr (20 mph). At Station 400, PM_{10} concentrations increase with increasing wind speed and exceed 66 µg/m^3 for the strongest winds between 57 and 64 km/hr (35 and 40 mph). At Stations 401 and 402, PM_{10} concentrations also increased consistently with increasing wind speed and reached a maximum of 240 and 476 µg/m^3 when winds were between 57 and 64 km/hr (35 and 40 mph), respectively. During CY2016, there was a somewhat similar frequency of winds over 57 km/hr (35 mph) compared with CY2015 (Nikolich *et al.*, 2016), and despite generally lower soil moisture in the summer, the PM_{10} concentrations were significantly lower compared to CY2015for those time periods when winds exceed 32 km/hr (20 mph).

Various wind speeds occur with similar frequencies at all stations (Figure 41). The small percentage of winds above 32 km/hr (20 mph) is responsible for dust events. Light winds (0 to 8 km/hr [0 to 5 mph]) are most common. Wind speeds in excess of 24 km/hr (15 mph) occur less than 10 percent of the time and wind speeds in excess of 32 km/hr (20 mph) occur less than 3 percent of the time. This low occurrence frequency of high winds and relatively low associated PM_{10} resulted in fewer dust transport events compared with previous years.

At Stations 400, 401, and 402, the average PM_{10} concentration increases in an approximately exponential pattern with linear increases in wind speed (Figure 42). All three monitoring stations show similar trends and dependence on wind speed when it comes to PM_{10} concentration. Figure 43 shows a similar trend between monitoring stations for $PM_{2.5}$ concentration (particulate matter of aerodynamic diameter ≤ 2.5 μm) and corresponding wind speed class.

Table 15. Summary of wind and PM_{10} data for Stations 400, 401, and 402 for CY2016.

Wind Speed Class (mph)	Duration (hours)	Frequency (%)	Cumulative Frequency (%)	Average Wind Speed (mph)	PM_{10} (μg/m^3)
Station 400					
0-5	3,589.50	41.62%	41.62%	3.16	8.66
5-10	3,072.33	35.62%	77.25%	7.11	9.13
10-15	1,217.83	14.12%	91.37%	12.22	11.40
15-20	576.17	6.68%	98.045%	17.02	10.81
20-25	130.17	1.51%	99.56%	21.84	18.27
25-30	30.50	0.35%	99.91%	26.89	21.57
30-35	7.50	0.09%	99.99%	32.19	30.57
35-40	0.33	0.00%	100.00%	36.53	55.23
Total hours	8,624.33	n/a	n/a	n/a	n/a
Station 401					
0-5	4,293.83	49.27%	49.27%	2.70	8.07
5-10	2,544.83	29.20%	78.46%	7.09	6.14
10-15	1,120.33	12.85%	91.32%	12.22	6.45
15-20	568.33	6.52%	97.84%	17.14	6.51
20-25	142.00	1.63%	99.47%	21.90	10.32
25-30	34.50	0.40%	99.86%	27.21	23.06
30-35	11.33	0.13%	99.99%	31.90	62.86
35-40	0.67	0.01%	100.00%	35.46	239.48
Total hours	8,715.8	n/a	n/a	n/a	n/a
Station 402					
0-5	4,350.00	53.04%	53.037%	2.71	9.75
5-10	2,126.83	25.93%	78.97%	7.10	10.77
10-15	1,048.00	12.78%	91.75%	12.27	11.81
15-20	501.50	6.11%	97.86%	17.06	12.88
20-25	132.67	1.62%	99.48%	21.86	22.79
25-30	33.67	0.41%	99.89%	27.18	34.06
30-35	8.00	0.10%	99.99%	31.65	117.80
35-40	1.17	0.01%	100.00%	35.69	475.70
Total hours	8,201.83	n/a	n/a	n/a	n/a

n/a = not applicable.

Note: mph can be converted to km/hr by multiplying by 1.6.

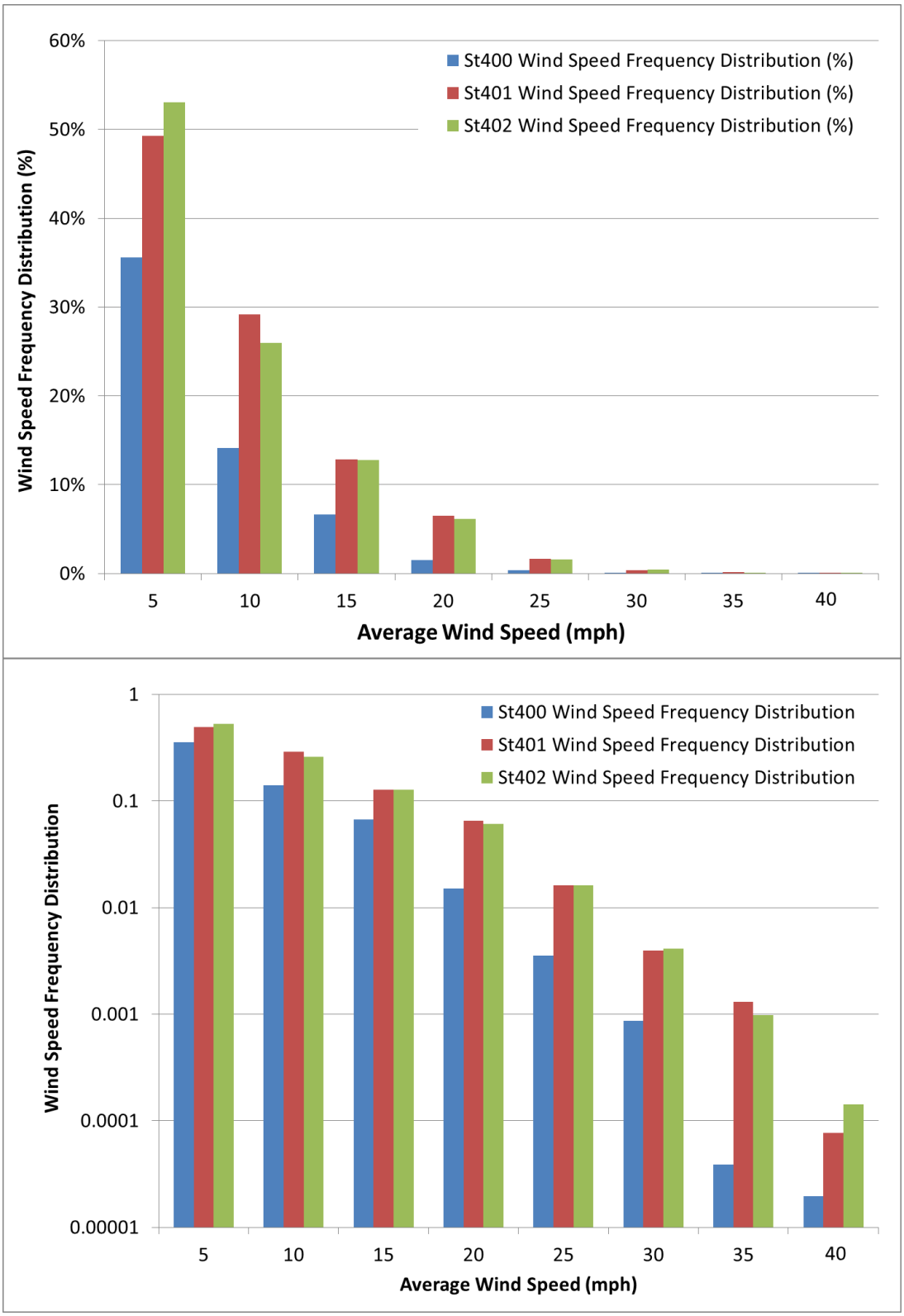

Figure 41. Wind speed frequency (top: linear scale; bottom: log scale) by wind class for Stations 400, 401, and 402 for CY2016. The portion of time wind speed falls within a given class is plotted against the average wind speed for that class.

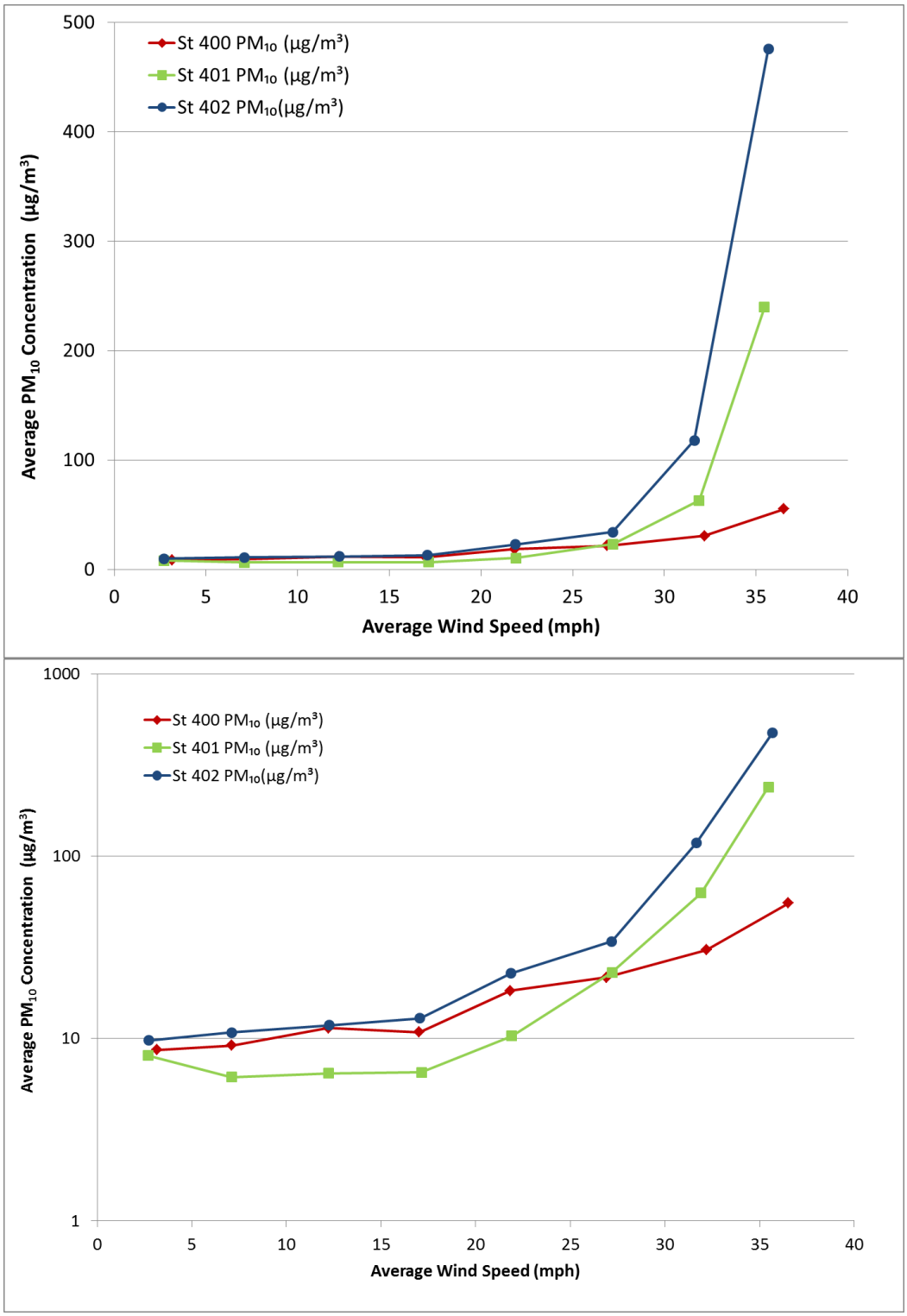

Figure 42. PM_{10} trends as a function of wind speed for Stations 400, 401, and 402 for CY2016; PM_{10} concentration is on a linear scale in (top) and log scale in (bottom).

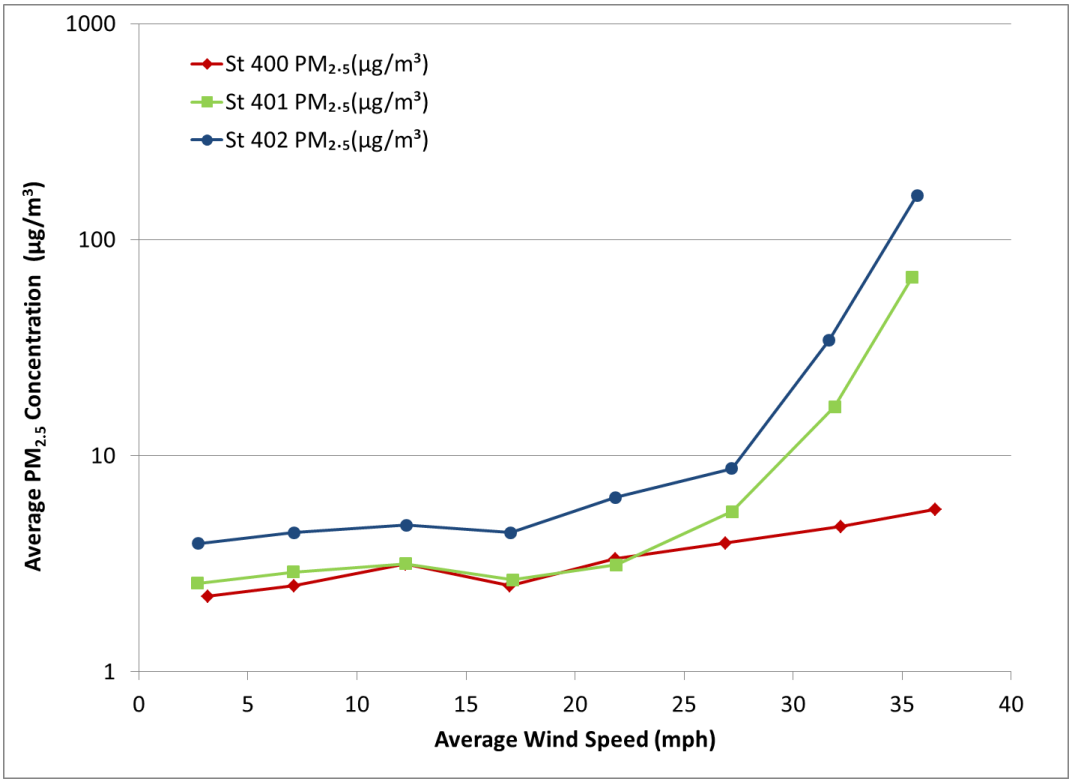

Figure 43. $PM_{2.5}$ trends as a function of wind speed for Stations 400, 401, and 402 for CY2016; $PM_{2.5}$ concentration plotted on a logarithmic scale to illustrate wide dynamic range of $PM_{2.5}$ concentrations.

OBSERVATIONS OF SOIL TRANSPORT BY SUSPENSION FROM SOUTH AND NORTHWEST DIRECTIONS

The PM_{10} transport has been evaluated previously (Mizell *et al.*, 2014; Nikolich *et al.*, 2015) by establishing relationships between different wind speed classes and the corresponding average PM_{10} concentration. These data indicate an exponential-type increase in PM_{10} concentration with a linear increase in wind speeds over 24 km/hr (15 mph). Table 16 shows the frequency of winds from the south and northwest compared with all winds based on wind speed class. For all three stations, winds from the south and northwest account for over 90 percent of winds above 24 km/hr (15 mph) (those that generally cause saltation and dust transport). Table 17 and Figures 44 through 46 show the average wind speed and the corresponding average PM_{10} concentration for southerly and northwesterly winds. Winds over 40 km/hr (25 mph) occurred more frequently out of the south than the northwest in 2016. The associated PM_{10} for south and northwest winds below 40 km/hr (25 mph) is comparable between the three monitoring stations. The associated PM_{10} for winds above 40 km/hr (25 mph) is significantly higher for south winds at Stations 401 and 402 in contrast to northwesterly winds, an observation accentuated by the near absence of winds from the northwest at speeds above 48 km/hr (30 mph). The CY2016 trend is a reversal from CY2015 (Nikolich *et al.*, 2016) when the highest winds observed were from the northwest, causing the greatest dust transport.

Table 16. Summary of wind speed, duration, and direction data for Stations 400, 401, and 402 for CY2016.

	Wind Speed Class (mph)	Total Duration (hours)	Duration from South (hours)	Duration from Northwest (hours)	Portion of Time from S and NW (%)
Station 400	0-5	3,655.17	558.67	1,751.50	63.2%
	5-10	3,121.33	905.50	1,295.00	70.5%
	10-15	1,250.50	605.00	413.50	81.4%
	15-20	587.67	340.67	195.50	91.2%
	20-25	130.83	75.50	45.17	92.2%
	25-30	30.50	22.50	7.00	96.7%
	25-30	7.50	7.33	0.00	97.8%
	30-35	0.33	0.33	0.00	100.0%
	Total hours	8,783.83	2515.50	3,707.67	n/a
Station 401	0-5	4,337.00	1,080.00	1,407.33	57.4%
	5-10	2,552.67	616.67	1,035.33	64.7%
	10-15	1,128.67	579.50	423.33	88.9%
	15-20	575.17	326.17	225.00	95.8%
	20-25	143.83	60.83	80.83	98.5%
	25-30	34.50	15.83	18.17	98.6%
	30-35	11.33	9.83	1.50	100.0%
	>35	0.67	0.67	0.00	100.0%
	Total hours	8,783.83	2,689.50	3,191.50	n/a
Station 402	0-5	4,535.17	617.33	1,625.00	49.4%
	5-10	2,161.33	515.83	845.83	63.0%
	10-15	1,060.33	535.67	377.83	86.2%
	15-20	512.83	283.67	195.50	93.4%
	20-25	133.67	69.00	60.00	96.5%
	25-30	33.67	16.83	16.17	98.0%
	30-35	8.00	5.67	2.33	100.0%
	30-35	1.17	1.17	0.00	100.0%
	Total hours	8,446.17	2,045.17	3,122.67	n/a

n/a = not applicable.

Note: mph can be converted to km/hr by multiplying by 1.6.

Table 17. Summary of wind and PM_{10} data for Stations 400, 401, and 402 for CY2016.

	Wind Speed Class (mph)	South Average Wind Speed (mph)	Northwest Average Wind Speed (mph)	Average PM_{10} for South wind ($\mu g/m^3$)	Average PM_{10} for Northwest Wind ($\mu g/m^3$)
Station 400	0-5	3.27	3.16	8.43	8.54
	5-10	7.33	7.11	9.41	8.92
	10-15	12.39	12.12	10.33	13.83
	15-20	17.00	17.08	9.88	12.84
	20-25	21.81	21.91	13.59	26.73
	25-30	27.09	26.07	17.05	36.38
	30-35	32.23	none	31.08	none
	35-40	36.53	none	55.23	none
Station 401	0-5	2.70	2.68	8.49	8.04
	5-10	7.47	7.23	5.91	5.72
	10-15	12.41	12.10	6.08	6.73
	15-20	17.12	17.21	6.64	5.94
	20-25	21.85	21.95	9.71	10.45
	25-30	27.14	27.29	26.99	19.20
	30-35	32.13	30.40	68.11	28.43
	35-40	35.46		239.48	none
Station 402	0-5	2.50	2.65	7.23	10.35
	5-10	7.59	7.22	12.16	9.23
	10-15	12.42	12.18	15.09	7.03
	15-20	16.98	17.20	13.53	10.87
	20-25	21.91	21.81	25.38	19.61
	25-30	27.13	27.32	41.02	26.21
	30-35	32.07	30.61	158.50	18.96
	35-40	35.69	none	475.70	none

Note: mph can be converted to km/hr by multiplying by 1.6.

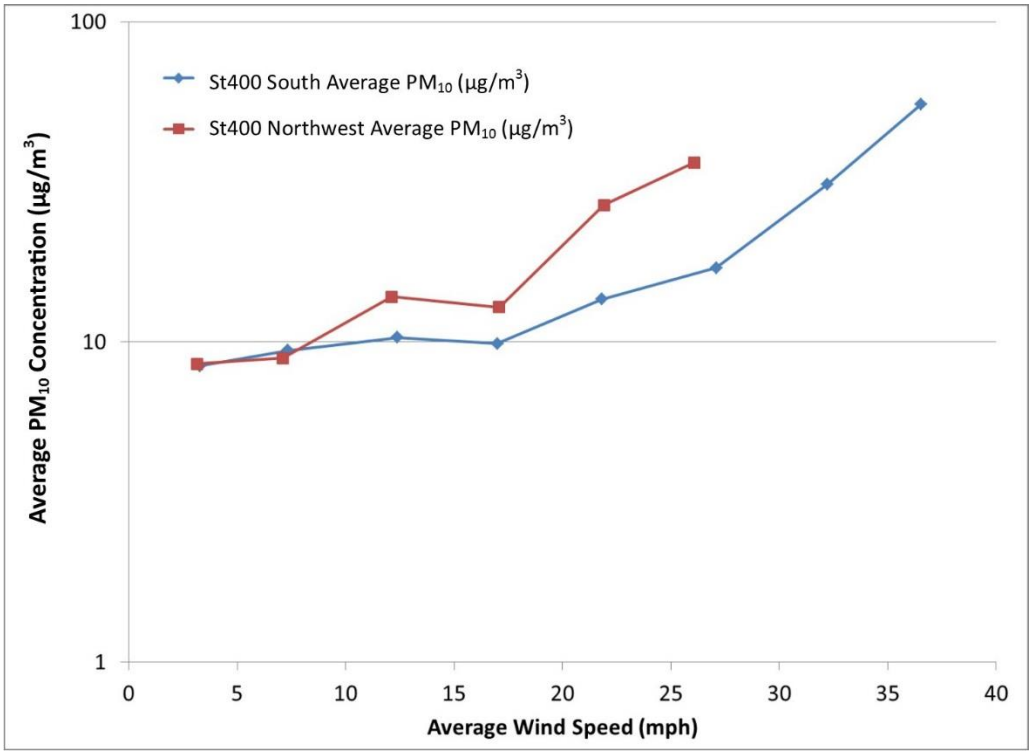

Figure 44. PM_{10} trends as a function of wind speed for Station 400 for CY2016. PM_{10} concentration plotted on a logarithmic scale to show a wide dynamic range of PM_{10} concentrations.

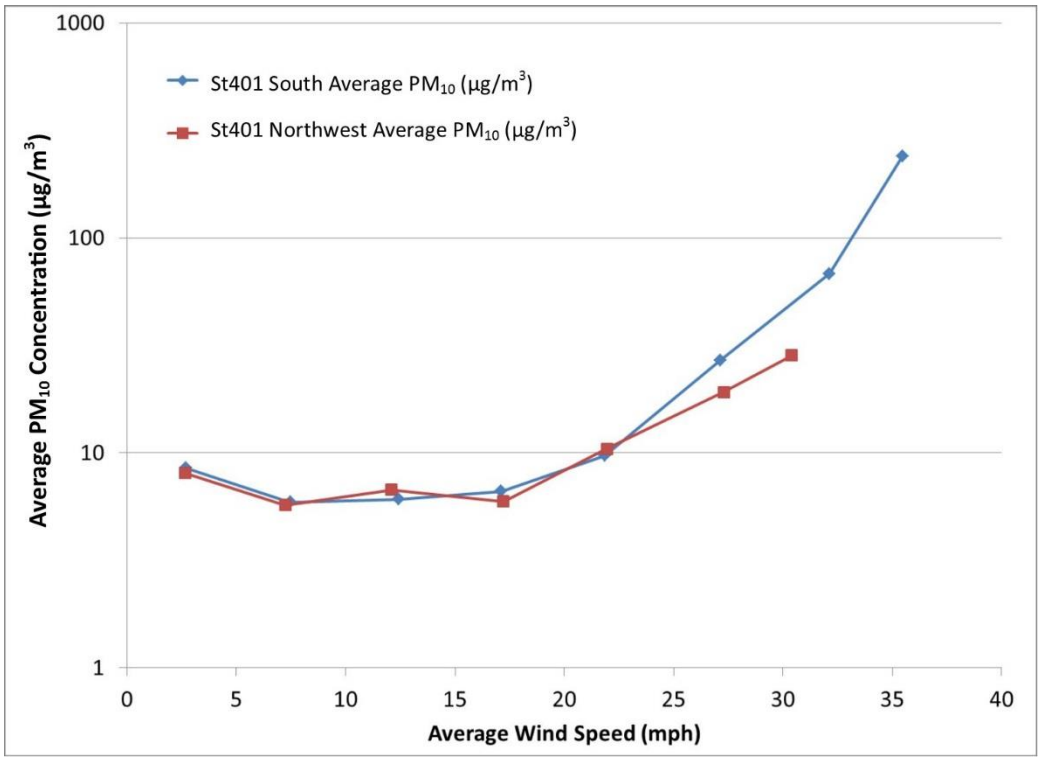

Figure 45. PM_{10} trends as a function of wind speed for Station 401 for CY2016. PM_{10} concentration plotted on a logarithmic scale to show a wide dynamic range of PM_{10} concentrations.

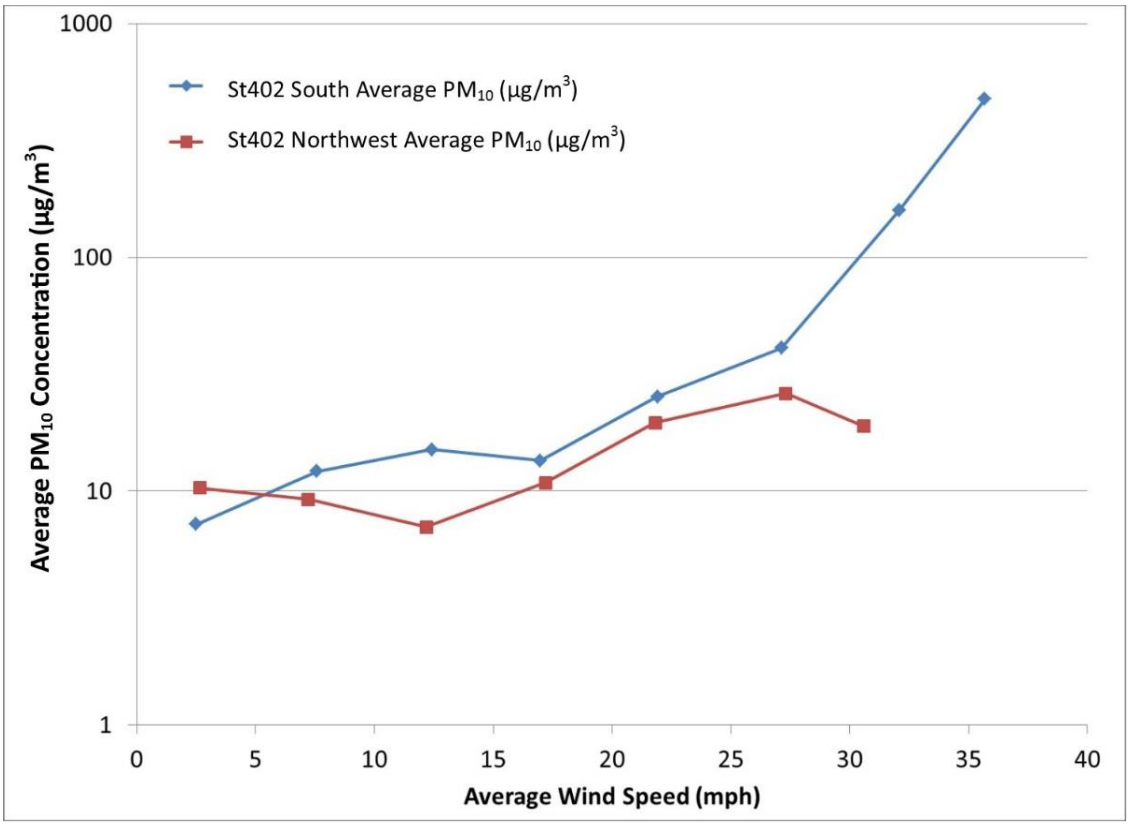

Figure 46. PM_{10} trends as a function of wind speed for Station 402 for CY2016. PM_{10} concentration plotted on a logarithmic scale to show a wide dynamic range of PM_{10} concentrations.

WIND EVENT OF APRIL 22, 2016

Most dust transport occurs during high wind events that tend to be short in duration. The strongest wind events usually occur between March and May (see Tables B-1, B-2, and B-3 in Appendix B) and it is also during this time period that the highest PM_{10} concentrations are recorded. Figure 47 shows the wind rose graphs for all three monitoring stations at TTR for April 22, 2016. This was the day with the strongest and most sustained winds, which lasted around 10 hours at all three monitoring stations. The wind roses show the maximum wind gusts based on the three second readings saved every 10 minutes. Wind roses show that the strongest winds during this wind event came from the south direction with a less strong and much less frequent component from the northwest. The wind gusts were over 64 km/hr (40 mph) between roughly 10:50 and 17:40 h Pacific Daylight Saving Time (PDST). A wind gust reached the maximum speed of over 80 km/hr (50 mph) between 14:20 and 14:40 h. The sustained winds were well over 48 km/hr (30 mph) between 11:40 and 17:20 h. Figures 48 through 50 show detailed time series of wind speed and PM_{10} concentration. All three monitoring stations experienced very similar wind conditions and showed similar increases in PM_{10} mass concentrations. Station 400 PM_{10} concentration peaked at 220 µg/m^3 at approximately 19:20 h as winds slowed down and shifted from the south to the northwest. The PM_{10} concentration at Stations 401 and 402 peaked at 688 and 724 µg/m^3 respectively around 14:20 h when winds were the strongest. Higher PM_{10} concentration at Stations 401 and 402 compared with Station 400 were because of winds blowing directly from the south

transporting dust from dry playas directly upwind of Stations 401 and 402. It is also interesting to note that the average PM_{10} concentration at Station 402 was significantly higher compared with Station 401, presumably because of the closer proximity to the large dry playa.

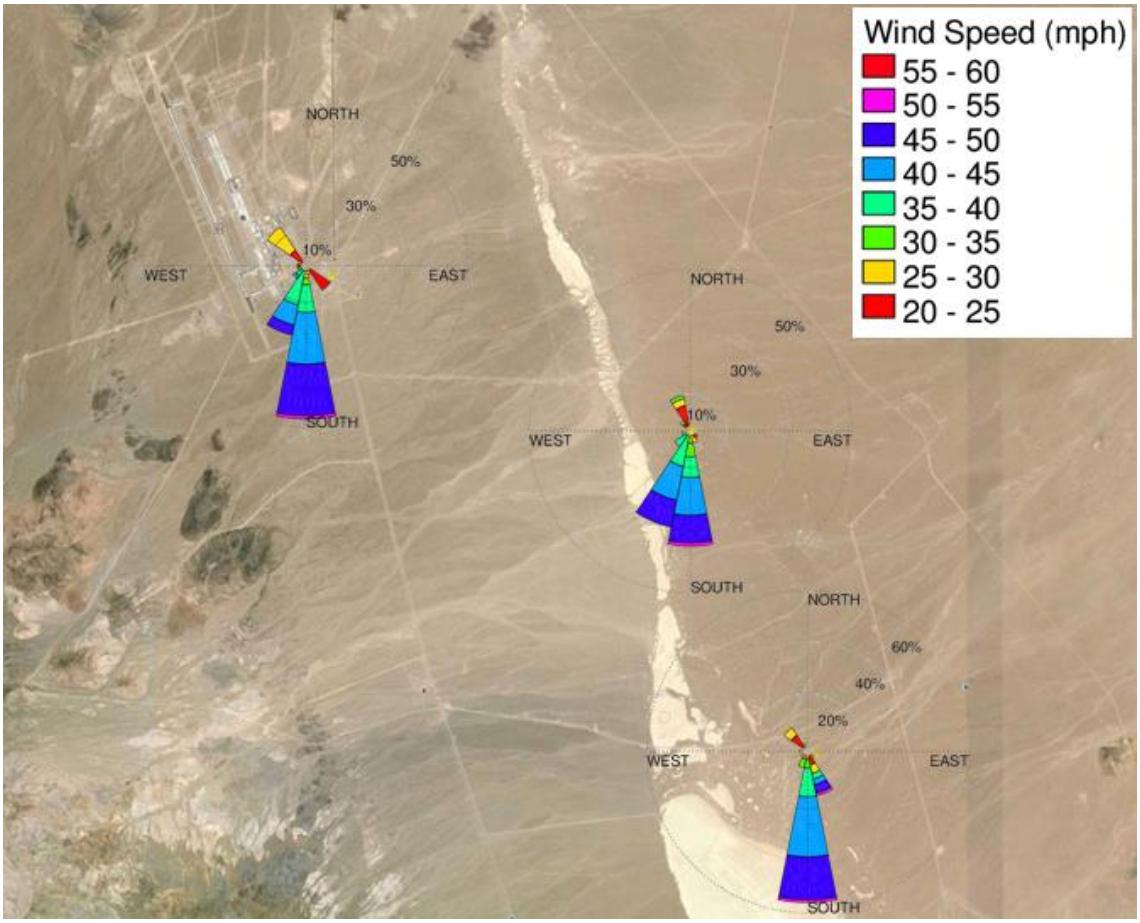

Figure 47. Wind roses based on the maximum wind-speed gust for 10-minute intervals at the monitoring stations on April 22, 2016 for the period between 06:00 and 21:00 hr.

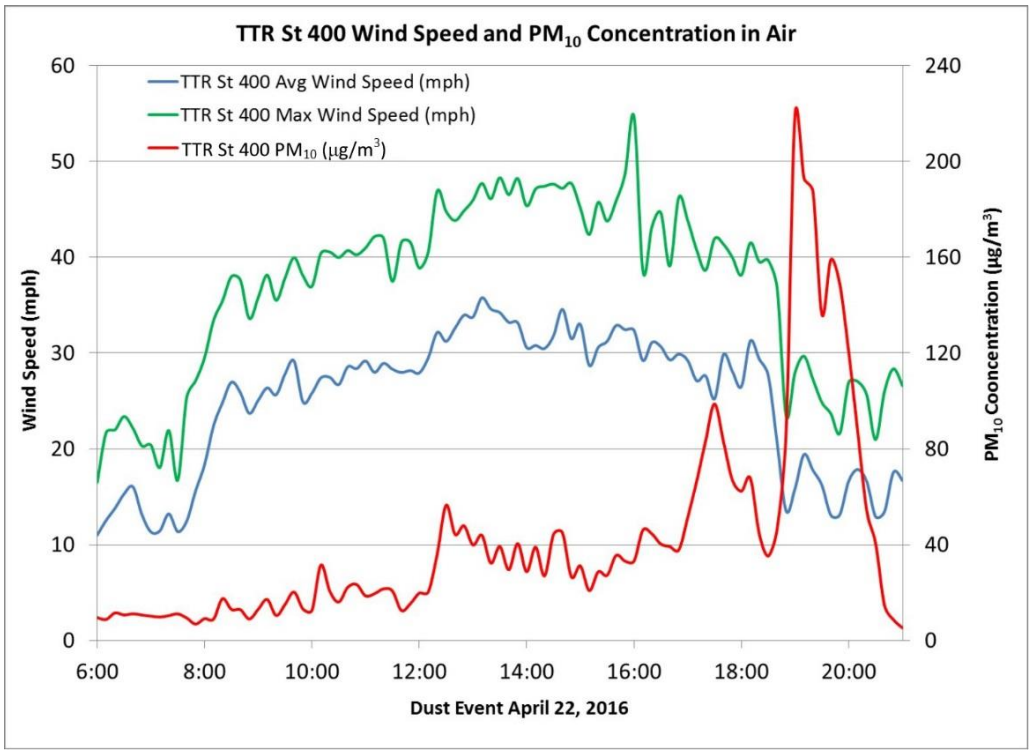

Figure 48. Wind speed and PM_{10} concentration at Station 400 on April 22, 2016.

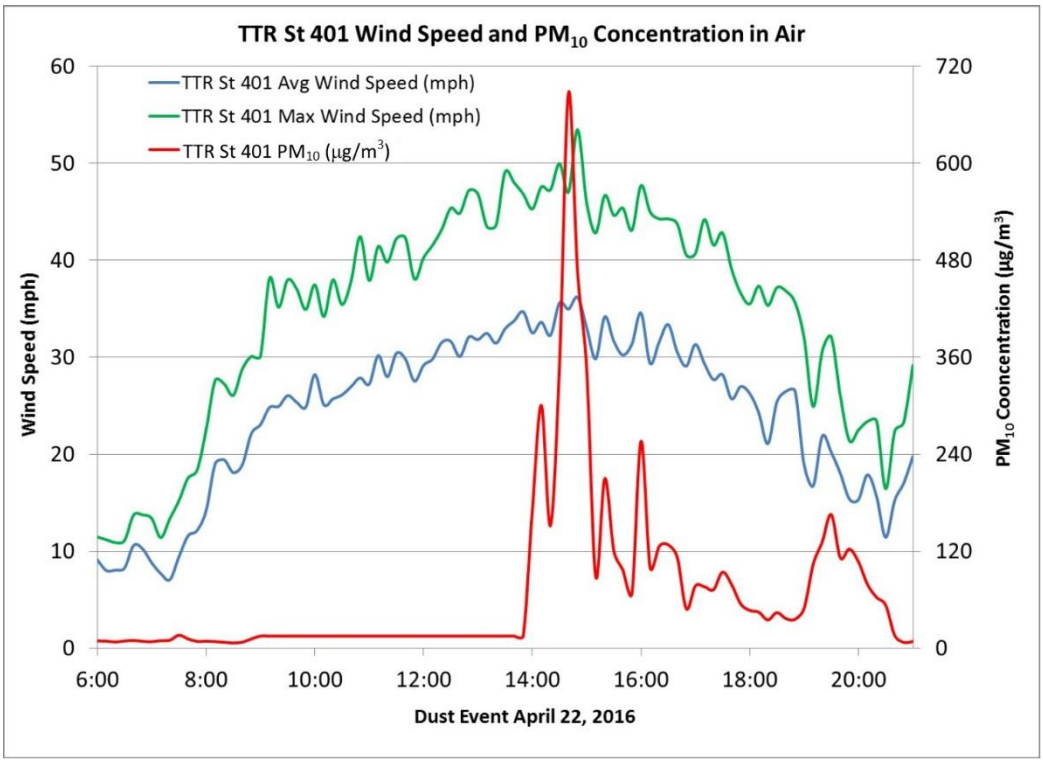

Figure 49. Wind speed and PM_{10} concentration at Station 401 on April 22, 2016.

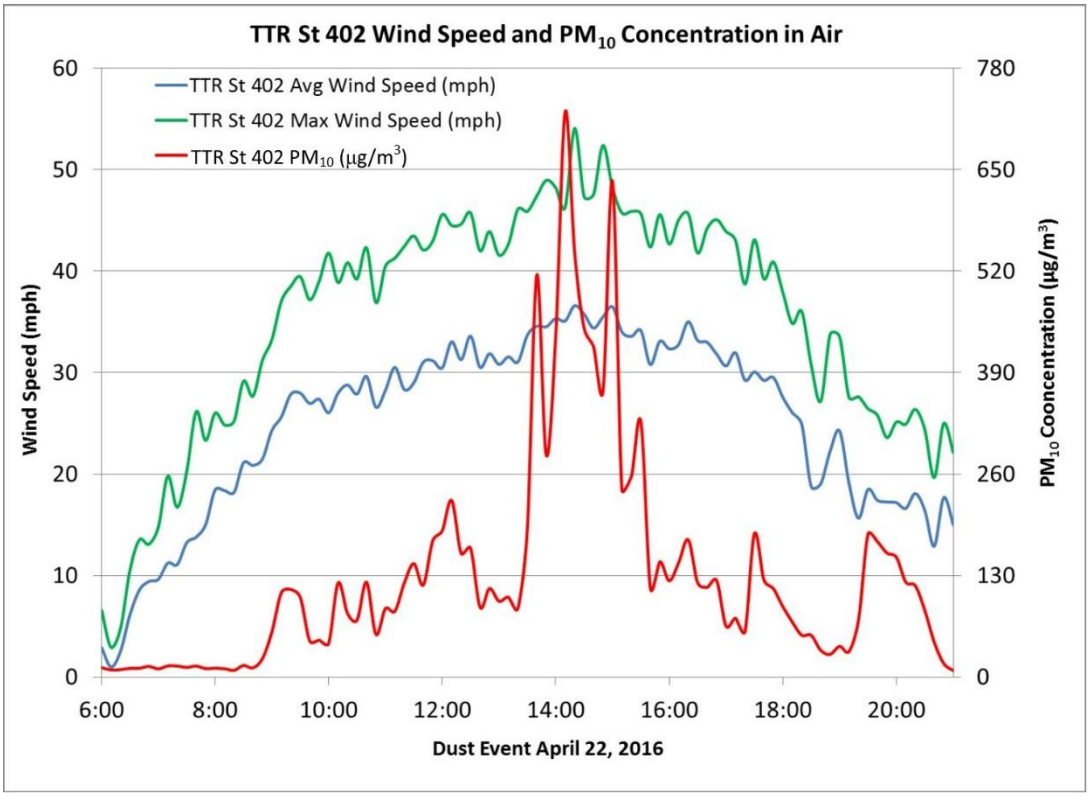

Figure 50. Wind speed and PM_{10} concentration at Station 402 on April 22, 2016.

DISCUSSION

Particle movement by saltation and suspension continues to be recorded at the TTR stations. Saltation counts and PM_{10} concentrations both increase significantly at wind speeds greater than 32 km/hr (20 mph). Winds of this speed occur less than two percent of the time at the three sample sites. High winds are predominantly (more than 90 percent of the time) from either the south or northwest. In 2016, the highest winds were observed from the south, in contrast to 2015 when the highest winds were observed from the northwest. Station 402 had a somewhat higher saltation rate and higher PM_{10} concentrations than Station 401 in 2016. At both sites, the highest PM_{10} concentrations occurred during wind events from the south, again in contrast to 2015 when the highest concentrations occurred during northwesterly winds.

To determine if radiological contaminants are being transported by wind from the Clean Slate sites, the gamma exposure rate is measured by PIC instruments, and dust collected by air filters at the monitoring stations is analyzed for gross alpha, gross beta, and gamma spectroscopy. Select filters are analyzed by alpha spectroscopy. Soil samples collected in saltation traps are also analyzed by alpha spectroscopy.

Gamma exposure rates measured by the PICs are similar to those measured at the CEMP station at Warm Springs Summit—although they are higher than rates at other CEMP stations—and within the range observed nationally for background levels of environmental (terrestrial and cosmic) gamma exposure rates in the United States (5.6 to 28.2 µR/hr; National Academy of Sciences, 1980). Most intervals of increased gamma values are

coincident among the three TTR stations and also coincident with the Warm Springs Summit measurements. Many of these intervals coincide with precipitation events, which suggests that resuspended plutonium particles are washed down from the atmosphere during rainfall and snowfall (Thakur *et al*., 2017).

Samples collected on the air filters show that the highest mean gross alpha and mean gross beta activities, as well as the highest mean gamma exposure rate, were observed at Station 402, which is adjacent to Clean Slate I. Values reported for Station 400 (at the ROC) are slightly lower than the Station 402 values. The maximum individual gross alpha measurement was from Station 400 and is attributed to the higher dust loads on the filters from this disturbed location (which is adjacent to frequent vehicle traffic). The mean gross alpha values for the TTR stations are higher than those observed at four CEMP stations in the region but comparable to two others. The mean gross beta measurements at Stations 400 and 401 are lower than the regional CEMP stations, and Station 402 is lower than three of the six CEMP stations that were compared. Only naturally occurring radionuclides were identified by gamma spectroscopy analyses for all three sites.

In contrast, the alpha spectroscopy analyses indicate the presence of $^{239+240}$Pu at concentrations above background in the environment immediately adjacent to Clean Slate I and III. Alpha spectroscopy is more sensitive than gamma spectroscopy because it can measure a narrower window of energy specific to plutonium isotopes. Background is represented by $^{239+240}$Pu concentrations measured during continuous air monitoring at the TTR airport (northwest of the ROC) in 1996 and 1997, which was reported as an average concentration of 9.5×10^{-19} µCi/ml (SNL, 1998). Alpha spectroscopy of the Station 400 filters (which were collected at the ROC at discrete times during 2015 and 2016) did not measure $^{239+240}$Pu above the minimum detectable level, which is consistent with background conditions. Adjacent to Clean Slate I and Clean Slate III, the minimum values measured on the air filters from Stations 401 and 402 are over an order of magnitude higher than the TTR airport mean value, and the maximum concentration from Station 401 of 4.5×10^{-15} µCi/ml is four orders of magnitude higher.

In terms of the soil samples collected from the saltation traps, the $^{239+240}$Pu concentrations are 500 to 15,000 times higher than background (assumed to be 0.014 pCi/g [Turner *et al*., 2003]). The alpha spectroscopy results for the saltation samples from Stations 401 and 402 are consistent with site radiological surveys that note the existence of "substantial areas of contamination…outside the fence" (EG&G, 1979). The 2016 samples are similar to the previous two saltation sample analysis periods in that there is no consistent bias for higher concentrations in the traps collecting material downwind of the Clean Slate sites compared with the companion traps collecting material coming from the upwind direction. Contaminant concentrations are apparently elevated in the entire area adjacent to the traps, and the entry into the passive traps demonstrates that winds are moving plutonium particles in the environment. These data indicate that movement is both toward and away from Clean Slate I and Clean Slate III, but they are not sufficient to determine if there is an overall predominant migration direction. The above-background presence of $^{239+240}$Pu on the Station 401 and 402 air filters indicates that movement is also occurring by suspension processes.

The CAU closure strategy uses a risk-based approach, whereby acceptable contaminant concentrations are determined as a function of anticipated human exposure. Therefore, the fence lines at the Clean Slate sites encircle areas of higher concentration and the presence of contamination outside of the fences is expected, albeit at lower concentrations. The $^{239+240}$Pu concentrations measured in the trap samples are all below the risk-based action level.

CONCLUSIONS

The combined results of the meteorological and particle monitoring suggest that conditions for wind-borne contaminant migration exist at the Clean Slate sites. Plutonium above background was collected during 2016 by saltation traps and was detected on select air filters from monitoring stations adjacent to the sites. Plutonium was not found above detection limits on filters from the ROC station.

As in previous years, the comparison of the gross alpha, gross beta, and gamma exposure rate data from the TTR stations with those from regional CEMP stations suggest that the TTR results for those analytes reflect natural background conditions. Similarly, gamma spectroscopy identified only naturally occurring radionuclides with no detection of ^{241}Am (which is used as an indicator of plutonium isotopes), although the more sensitive alpha spectroscopy analysis of select air filters measured $^{239+240}$Pu concentrations at Stations 401 and 402 above background (which was determined by previous air sampling at the TTR airport). Alpha spectroscopy results for filters from Station 400 are below detection limits. Alpha spectroscopy of material accumulated in saltation traps adjacent to Clean Slate I and III identified $^{239+240}$Pu at concentrations above background, but below risk-based action levels. The presence of plutonium in traps collecting material both upwind and downwind of the fenced sites is consistent with previous radiological survey results showing low-level contamination dispersed outside the fenced area. Given this, the collection of plutonium within the traps does not necessarily reflect transport of material beyond the fenced area, but it does demonstrate that plutonium is moving by saltation in the environment. Similarly, the $^{239+240}$Pu detected on air filters from the Clean Slate stations demonstrates plutonium movement by suspension.

High saltation values and high PM_{10} values are correlated with strong winds. However, wind speeds in excess of 32 km/hr (20 mph) occurred less than two percent of the time and occurred predominantly from the south or northwest. During 2016, the highest wind speeds were associated with the southerly direction. Annual precipitation averaged for the three stations in 2016 was 80.3 mm (3.16 in), which was below the long-term annual average measured at the Tonopah Airport (129.03 mm; 5.08 in). The annual amount varied from 74.4 mm (2.93 in) at Station 402 to 84.3 mm (3.32 in) at Station 400.

RECOMMENDATIONS

Several previous recommendations for Clean Slate monitoring have been followed and those results are contained in this report. These include analyzing select air filters using alpha spectroscopy for comparison with the saltation data and collecting the saltation trap samples more frequently. These activities will be continued in the following year.

Another recommendation is currently being implemented at the Clean Slate sites. The observation of very strong wind events from both the south and north-northwest directions led to a recommendation to monitor downwind of both directions. Monitoring of Clean Slate III by Station 401 has been augmented by adding Station 403 on the south end of the site. Two stations, Stations 404 and 405, are being placed at the north and south sides of Clean Slate II, respectively. The increased monitoring coincides with plans for remediation at the two locations. Station 402, located on the north end of the remediated Clean Slate I site, has been decommissioned.

The last analysis of multiyear data collected at the TTR monitoring stations included data collected from inception in 2008 to the end of 2012. With another five years of data collection by the end of 2017, another multiyear analysis should be considered. Of particular note will be the inclusion of the saltation data and the related alpha spectroscopy results, which were not available for the previous multiyear report.

REFERENCES

Dick, J.L., J.D. Shreve, and J.S. Iveson, 1963. Operation Roller Coaster, Interim Summary Report (II). POIR-2500 (Volume 1) Defense Atomic Support Agency predecessor to Defense Threat Reduction Agency, Washington, D.C.

Duncan, D., W. Forston, and R. Sanchez, 2000. 1999 Annual Site Environmental Report Tonopah Test Range, Nevada. SAND2000-2229, Sandia National Laboratories, Albuquerque, NM.

EG&G, 1979. An Aerial Radiological Survey of Clean Slates 1, 2, and 3, and Double Track, Test Range. EGG-1183-1737, Energy Measurement Group, EG&G, Las Vegas, NV.

Engelbrecht, J.P., I.G. Kavouras, D. Campbell, S.A. Campbell, S. Kohl, D. Shafer, 2008. Yucca Mountain Environmental Monitoring System Initiative, Air Quality Scoping Study for Tonopah Airport, Nye County, Nevada, Letter Report DOE/NV/26383-LTR2008-04.

Fryrear, D.W., 1986. A field dust sampler. *Journal of Soil and Water Conservation*, v. 41, pp. 117-120.

Helsel, D.R., and R.M. Hirsch. 1995. Statistical Methods in Water Resources. Studies in Environmental Science 49, Elsevier, New York, 529pp.

Johnson, W.G., and S.R. Edwards, 1996. A historical evaluation of Operation Roller Coaster, Stonewall and Cactus Flats, Nellis Air Force Range and Tonopah Test Range, Nye County, Nevada. NTS Project #9649MA, Historic Evaluation Short Report #SR090996-1, prepared by Desert Research Institute for U.S. Department of Energy, Nevada Operations Office, Las Vegas, Nevada.

Mizell, S.A., and C. Shadel, 2016. Radiological results for samples collected on paired glass- and cellulose-fiber filters at the Sandia complex, Tonopah Test Range, Nevada. Desert Research Institute Publication No. 45265, DOE/NV/0000939-29.

Mizell, S.A., V. Etyemezian, G. McCurdy, G. Nikolich, C. Shadel, and J. Miller, 2014. Radiological and environmental monitoring at the Clean Slate I and III Sites, Tonopah Test Range, Nevada, with emphasis on the implications for off-site transport. Desert Research Institute Publication No. 45257, DOE/NV/0000939-19.

National Academy of Sciences, 1980. The Effects on Populations of Exposure to Low Levels of Ionizing Radiation, BEIR III. Washington, D.C.

Nikolich, G., C. Shadel, J. Chapman, S. Mizell, G. McCurdy, V. Etyemezian, and J. Miller, 2015. Tonopah Test Range Air Monitoring: CY 2014 Meteorological, Radiological, and Airborne Particulate Observations. Desert Research Institute Publication No. 45271, DOE/NV/0000939-37.

Nikolich, G., C. Shadel, J. Chapman, G. McCurdy, V. Etyemezian, J. Miller and S. Mizell, 2016. Tonopah Test Range Air Monitoring: CY 2015 Meteorological, Radiological, and Airborne Particulate Observations. Desert Research Institute Publication No. 45263, DOE/NV/0000939-26.

NSTec, 2013. Nevada National Security Site Environmental Report 2012. DOE/NV/25946-1856, prepared by National Security Technologies, LLC for the US Department of Energy, National Nuclear Security Administration, Nevada Site Office.

Proctor, A.E., and T.J. Hendricks, 1995. An aerial radiological survey of the Tonopah Test Range including Clean Slate 1, 2, 3, Roller Coaster, Decontamination area Cactus Springs Ranch Target areas Central Nevada. EGG 11265-1145, The Remote Sensing Laboratory, EG&G Energy Measurements prepared for the US Department of Energy.

Sandia National Laboratory (SNL), 2014. Calendar Year 2013 Annual Site Environmental Report for Sandia National Laboratories' Tonopah Test Range, Nevada and Kauai Test Facility, Hawaii. SAND2014-16456R, Sandia National Laboratories, Albuquerque, NM.

Sandia National Laboratory (SNL), 2012. Calendar Year 2011 Annual Site Environmental Report for Tonopah Test Range, Nevada and Kauai Test Facility, Hawaii. SAND2012-7341P, Sandia National Laboratories, Albuquerque, NM.

Sandia National Laboratory (SNL), 1998. 1997 Annual Site Environmental Report, Tonopah Test Range, Nevada. SAND98-1832, Sandia National Laboratories, Albuquerque, NM.

Thakur, P., H. Khaing, and S. Salminen-Paatero, 2017. Plutonium in the atmosphere: a global perspective. *Journal of Environmental Radioactivity*, v.175-176, pp. 39-51.

Turner, M., M. Rudin, J. Cizdziel, and V. Hodge, 2003. Excess Plutonium in Soil near the Nevada Test Site, USA. *Environmental Pollution*, v. 125, pp. 193-203.

UNSCEAR, 2000. Sources and effects of ionizing radiation, Annex B: Exposures from natural radiation sources. United Nations Scientific Committee on the Effects of atomic Radiation. Available May 6, 2013 at: http://www.unscear.org/unscear/publications/2000_1.html.

U.S. Department of Energy, 2014. Soils Risk-Based Corrective Action Evaluation Process. Nevada Field Office, DOE/NV--1475-REV.1.

U.S. Department of Energy, 1996. Clean Slate Corrective Action Investigation Plan. Nevada Operations Office, DOE/NV--456.

U.S. Nuclear Regulatory Commission, 1979. Regulatory Guide 8.12 Health physics surveys for byproduct material at NRC-licensed processing and manufacturing plants, subsection 1.12 Calibration of radiation safety instruments. U.S. Nuclear Regulatory Commission, Office of Standards Development, Washington, D.C.

APPENDIX A: Quality Assurance Program

Although the current data collected for the TTR air monitoring study are considered for informational purposes to support conceptual models or guide investigations, the U.S. Department of Energy, National Nuclear Administration, Nevada Field Office (DOE/NNSA/NFO), Soils Activity Quality Assurance Plan (QAP) (2012) was used as a guideline to collect and analyze radiological data presented in the Radiological Assessment of Airborne Particulate Material section of this report. This QAP and the Desert Research Institute Quality Assurance Program Manual for the DOE Program (2010) ensures compliance with U.S. Department of Energy Order DOE O 414.1D, "Quality Assurance," which implements a quality management system to ensure the generation and use of quality data. The following items are addressed by the aforementioned QA documents:

- Data quality objectives (DQOs)
- Sampling plan development appropriate to satisfy the DQOs
- Environmental health and safety
- Sampling plan execution
- Sample analyses
- Data review
- Continuous improvement

Data Quality Objectives (DQOs)

The DQO process is a strategic planning approach that is used to plan data collection activities. It provides a systematic process for defining the criteria that a data collection design should satisfy. These criteria include when and where samples should be collected, how many samples to collect, and the tolerable level of decision errors for the study. The DQOs are unique to the specific data collection or monitoring activity and their defined level of use (in this case, informational purposes).

Measurement Quality Objectives (MQOs)

The MQOs are basically equivalent to DQOs for analytical processes. The MQOs provide direction to the laboratory concerning performance objectives or requirements for specific method performance characteristics. Default MQOs are established in the subcontract with the laboratory but can be altered to satisfy changes in the DQOs. The MQOs for the TTR air monitoring study are described in terms of precision, accuracy, representativeness, completeness, and comparability requirements. These terms are defined and discussed in the DOE/NNSA/NFO QAP.

Sampling Quality Assurance Program

Quality assurance (QA) in field operations for the TTR air monitoring study includes sampling assessment, surveillance, and oversight of the following supporting elements:

- The sampling plan, DQOs, and field data sheets accompanying the sample package.

- Database support for field and laboratory results, including systems for long-term storage and retrieval.
- Qualified personnel able and available to perform the required tasks.

Sample packages include the following items:

- Field notes confirming all observable information pertinent to sample collection.
- An Air Surveillance Network Sample Data form documenting air sampler parameters, collection dates and times, and total sample volumes collected.
- Chain-of-custody forms that also include some of the elements of the field notes.

This managed approach to sampling ensures that the sampling is traceable and enhances the value of the final data available to the project manager. The sample package also ensures that the field personnel responsible for sample collection have followed proper procedures for sample collection.

Data obtained in the course of executing field operations are entered in the documentation accompanying the sample package during sample collection and in the TTR Study database along with analytical results on their receipt and evaluation.

Hard copies of the completed sample packages are kept in the archived files. The analytical reports are kept in dedicated and secure archival systems that are protected and maintained in accordance with the Desert Research Institute's Computer Protection Program and hard copies are kept in the file archives.

Laboratory QA Oversight

Although the data for the TTR air monitoring study are for informational purposes, the main aspects of the DOE O 414.1D requirements are used as guidelines to evaluate laboratory services through review of the vendor laboratory policies formalized in a Laboratory Quality Assurance Plan (LQAP). The TTR study is assured of obtaining quality data from laboratory services through a multifaceted approach that involves specific procurement protocols, the conduct of quality assessments, and requirements for selected laboratories to have an acceptable QA Program. These elements are discussed below.

Procurement

Laboratory services are procured through subcontracts that establish the technical specifications required of the laboratory to provide the basis for determining compliance with those requirements and for evaluating overall performance. A subcontract is usually awarded on a "best value" basis determined by pre-award audits, but because of the specific requirement requested for gamma spectroscopy analysis (24 hour count duration) for the TTR study, the laboratory was procured on a sole proprietor basis. The laboratory was required to provide a review package that included the following items:

- All procedures pertinent to subcontract scope
- Environment, Health, and Safety Plan
- LQAP
- Example deliverables (hard copy and/or electronic)
- Proficiency testing (PT) results from the previous year from recognized PT programs

- Résumés
- Accreditations and certifications
- Licenses

Continuing Assessment

A continuing assessment of the selected laboratory involves ongoing monitoring of the laboratory's performance against the contract terms and conditions, part of which are the technical specifications. The following tasks support continuing assessment:

- Tracking schedule compliance.
- Reviewing analytical data deliverables.
- Monitoring the laboratory's adherence to the LQAP.
- Monitoring for continued successful participation in approved PT programs.

Data Review

Essential components of process-based QA are data checks, verification, validation, and data quality assessment to evaluate data quality and usability.

Data checks: Data checks are conducted to ensure accuracy and consistency of field data collection operations prior to and upon data entry into the TTR databases and data management systems.

Data verification: Data verification is defined as a compliance and completeness review to ensure that all laboratory data and sample documentation are present and complete. Sample preservation, chain-of-custody, and other field sampling documentation shall be reviewed during the verification process. Data verification ensures that the reported results entered in the TTR databases correctly represent the sampling and/or analyses performed and includes evaluation of quality control (QC) sample results.

Data validation: Data validation is the process of reviewing a body of analytical data to determine if it meets the data quality criteria defined in operating instructions. Data validation ensures that the reported results correctly represent the sampling and/or analyses performed, determines the validity of the reported results, and assigns data qualifiers (or "flags") if required. The process of data validation consists of the following:

- Evaluating the quality of the data to ensure that all project requirements are met.
- Determining the effect of not meeting those requirements on data quality.
- Verifying compliance with QA requirements.
- Checking QC values against defined limits.
- Applying qualifiers to analytical results in the TTR databases for the purposes of defining the limitations in the use of the reviewed data.

Operating instructions, procedures, applicable project-specific work plans, field sampling plans, QA plans, analytical method references, and laboratory statements of work may all be used in the data validation process. Documentation of data validation includes checklists, qualifier assignments, and summary forms.

Data quality assessment (DQA): The DQA is the scientific evaluation of data to determine if the data obtained from environmental data operations are of the right type, quality, and quantity to support their intended use. The DQA review is a systematic review against pre-established criteria to verify that the data are valid for their intended use.

2016 Sample QA Results

Assessments of QA were performed by the TTR air monitoring study, including the laboratories responsible for sample analyses. These assessments ensure that sample collection procedures, analytical techniques, and data provided by the subcontracted laboratory complies with TTR study requirements. Data were provided by the University of Nevada, Las Vegas, Radiation Services Laboratory for gross alpha, gross beta, and gamma spectroscopy analyses and TestAmerica, Inc., for alpha spectroscopy analyses. A brief discussion of the 2016 results for laboratory duplicates, control samples, blank analyses, and interlaboratory comparison studies is provided along with summary tables in this section.

Laboratory Duplicates (Precision)

A laboratory duplicate is a sample that is handled and analyzed following the same procedures as the primary analysis. The relative percent difference (RPD) between the initial result and the corresponding duplicate result is a measure of the variability in the analytical process of the laboratory, mainly overall measurement uncertainty. The average absolute RPD was determined for calendar year 2016 samples and is listed in Table A-1. An RPD of zero indicates a perfect duplication of results of the duplicate pair, whereas an RPD greater than 100 percent generally indicates that a duplicate pair falls beyond QA requirements and is not considered valid for use in data interpretation. These samples are further evaluated to determine the reason for QA failure and if any corrective actions are required. Overall, the RPD values for all analyses indicate very good results with no samples exceeding an RPD of 100 percent.

Table A-1. Summary of laboratory duplicate samples for the TTR air monitoring study in 2016.

Analysis	Matrix	Number of Samples Reported[(a)]	Number of Samples Reported Above MDC[(b)]	Average Absolute RPD of Those Above MDC (%)[(c)]
Gross Alpha	Air	9	9	14.4
Gross Beta	Air	9	9	3.4
Gamma – Beryllium-7	Air	7	7	10.3
Gamma – Lead-210	Air	7	0	na
Alpha Spectroscopy	Air	2	2	3.7

(a) Represents the number of laboratory duplicates reported for the purpose of monitoring precision.
(b) Represents the number of laboratory duplicate result sets reported above the minimum detectable concentration (MDC). If either the original laboratory analysis or its duplicate was reported below the detection limit, the precision was not determined.
(c) Reflects the average absolute RPD calculated for those field duplicates reported above the MDC.
na = not applicable.

The absolute RPD calculation is as follows:

$$Absolute\ RPD = \frac{|LD - LS|}{(LD + LS)/2} X\ 100\% \quad (1)$$

where: LD = Laboratory duplicate result

LS = Laboratory sample result

Laboratory Control Samples (Accuracy)

Laboratory control samples (LCSs) (also known as matrix spikes) are performed by the subcontract laboratory to evaluate analytical accuracy, which is the degree of agreement of a measured value with the true or expected value. Samples of known concentration are analyzed using the same methods used for the project samples. The results are determined as the measured value divided by the true value, expressed as a percentage. To be considered valid, the results must fall within established control limits (or percentage ranges) for further analyses to be performed. The LCS results obtained for 2016 are summarized in Table A-2. The LCS results were satisfactory, with all samples falling within control parameters for the air sample matrix.

Table A-2. Summary of laboratory control samples for the TTR air monitoring study in 2016.

Analysis	Matrix	Number of LCS Results Reported	Number Within Control Limits[(a)]
Gross Alpha	Air	16	16
Gross Beta	Air	16	16
Gamma	Air	10	10
Alpha Spectroscopy	Air	4	4

(a) Control limits are as follows: 78% to 115% for gross alpha, 87% to 115% for gross beta, 90% to 115% for gamma (^{137}Cs, ^{60}Co, ^{241}Am).

Laboratory Blank Analyses

Laboratory blank sample analyses are essentially the opposite of the LCSs discussed above. These samples do not contain any of the analyte of interest. Results of these analyses are expected to be "zero," or more accurately, below the MDC of a specific procedure. Blank analysis and control samples are used to evaluate overall laboratory procedures, including sample preparation and instrument performance. The laboratory blank sample results obtained for 2016 are summarized in Table A-3. The laboratory blank results were satisfactory with all samples falling within control parameters for the air sample matrix.

Table A-3. Summary of laboratory blank samples for the TTR air monitoring study in 2016.

Analysis	Matrix	Number of Blank Results Reported	Number within Control Limits[a]
Gross Alpha	Air	16	16
Gross Beta	Air	16	16
Gamma	Air	10	10
Alpha Spectroscopy	Air	2	2

(a) Control limit is less than the MDC.

Interlaboratory Comparison Studies

Interlaboratory comparison studies are conducted by the subcontracted laboratories to evaluate their performance relative to other laboratories providing the same service. These types of samples are commonly known as "blind" samples, in which the expected values are known only to the program conducting the study. The analyses are evaluated and if found satisfactory, the laboratory is certified that its procedures produce reliable results. The interlaboratory comparison sample results obtained for 2016 are summarized in Table A-4.

Table A-4 shows the summary of interlaboratory comparison sample results for the subcontract radiochemistry laboratory. The laboratories participated in the QA Program administered by the Mixed Analyte Performance Evaluation Program (MAPEP) for gross alpha, gross beta, and gamma analyses and Environmental Research Associates (ERA) for alpha spectroscopy analyses. The subcontracted laboratory performed very well during the year by passing all of the parameters analyzed.

Table A-4. Summary of interlaboratory comparison samples of the radiochemistry laboratory for the TTR air monitoring study in 2016.

Analysis	Matrix	MAPEP and ERA Results	
		Number of Results Reported	Number Within Control Limits[a]
Gross Alpha	Air	2	2
Gross Beta	Air	2	2
Gamma	Air	2	2
Alpha Spectroscopy	Air	1	

(a) Control limits are determined by the individual interlaboratory comparison study.

REFERENCES

Desert Research Institute, 2010. Desert Research Institute Quality Assurance Program Manual for the DOE Program, October 2010.

U.S. Department of Energy, 2011. Quality Assurance. DOE O 414.1D.

U.S. Department of Energy, 2012. Soils Activity Quality Assurance Plan. National Nuclear Security Administration, Nevada Site Office report DOE/NV--1478.

APPENDIX B: Summaries of Meteorological Data

Table B-1. Station 400 summary of monthly and annual meteorological data from CY2016.

Month	Jan	Feb	Mar	Apr	May	Jun	Jul	Aug	Sep	Oct	Nov	Dec	ANNUAL	VALUE
Wind Speed Avg (mph)	5.7	5.7	8.4	8.2	7.3	8.1	7.5	7.1	7.3	8.4	6.3	6.0	**AVG**	**7.2**
Wind Speed Max (mph)	19.0	18.0	26.8	27.1	27.2	27.3	27.5	26.6	22.9	25.4	21.7	19.5	**MAX**	**27.5**
Wind Speed Gust (mph)	32.3	45.2	46.9	54.7	41.0	39.2	42.1	37.6	37.9	54.4	42.7	41.0	**MAX**	**54.7**
***Wind Freq from S**	52%	26%	48%	30%	25%	45%	62%	71%	52%	68%	58%	34%	**AVG**	**47.6%**
****Wind Freq from NW**	34%	63%	44%	48%	44%	34%	16%	11%	29%	18%	27%	53%	**AVG**	**35.2%**
Air Temperature Avg (deg F)	31.2	37.0	45.1	51.0	57.4	74.6	77.8	75.3	64.9	54.8	42.7	31.3	**AVG**	**53.6**
Air Temperature Min (deg F)	7.0	-7.6	24.5	31.9	37.0	48.5	50.7	50.6	37.6	29.5	10.9	3.6	**MIN**	**-7.6**
Air Temperature Max (deg F)	55.9	66.6	69.0	74.4	84.3	96.3	100.2	94.6	88.8	75.7	74.4	58.6	**MAX**	**100.2**
Relative Humidity Avg (%)	71.3	59.5	46.4	44.6	39.3	20.5	18.7	17.4	26.4	36.4	42.5	57.3	**AVG**	**40.0**
Relative Humidity Min (%)	21	11	8	7	8	5	5	4	6	8	8	9	**MIN**	**4**
Relative Humidity Max (%)	100	100	100	97	97	83	83	68	85	99	98	100	**MAX**	**100**
Total Precipitation (inch)	0.20	0.39	0.68	0.76	0.37	0.34	0.28	0.00	0.10	0.02	0.06	0.12	**TOTAL**	**3.32**
Max Daily Precipitation (inch)	0.07	0.15	0.16	0.21	0.16	0.22	0.16	0.00	0.10	0.02	0.04	0.09	**MAX**	**0.22**
Soil Temperature Avg (deg F)	34.3	42.0	51.4	58.3	65.8	81.7	86.2	85.4	75.7	63.1	50.7	37.3	**AVG**	**61.0**
Soil Temperature Min (deg F)	25	25	37	43	46	62	69	73	59	52	31	24	**MIN**	**24**
Soil Temperature Max (deg F)	48	62	69	77	89	98	102	100	92	78	67	50	**MAX**	**102**
Soil Vol. Water Content Avg	0.14	0.16	0.16	0.18	0.18	0.15	0.15	0.13	0.12	0.11	0.11	0.11	**AVG**	**0.14**
Soil Vol. Water Content Min	0.09	0.09	0.13	0.14	0.15	0.13	0.13	0.12	0.11	0.11	0.10	0.09	**MIN**	**0.09**
Soil Vol. Water Content Max	0.16	0.20	0.21	0.24	0.25	0.19	0.19	0.16	0.13	0.13	0.12	0.12	**MAX**	**0.25**
Solar Radiation Avg (ly/day)	110	205	250	294	352	389	401	357	293	208	151	116	**AVG**	**261**
Solar Radiation Max (ly/day)	162	253	326	382	425	437	429	395	342	270	195	139	**MAX**	**437**
Barometric P. Avg (in Hg)	24.58	24.70	24.51	24.54	24.51	24.59	24.61	24.61	24.61	24.57	24.63	24.58	**AVG**	**24.59**
Barometric P. Min (in Hg)	24.17	24.35	24.19	24.28	24.21	24.38	24.52	24.50	24.36	24.37	24.35	24.15	**MIN**	**24.15**
Barometric P. Max (in Hg)	24.84	24.95	24.70	24.82	24.69	24.71	24.69	24.71	24.83	24.78	24.82	24.85	**MAX**	**24.95**

*Wind Freq from S (indicates aggregate frequency for winds over 5 mph coming from south direction).

**Wind Freq from NW (indicates aggregate frequency for winds over 5 mph coming from northwest direction).

Table B-2. Station 401 summary of monthly and annual meteorological data from CY2016.

Month	Jan	Feb	Mar	Apr	May	Jun	Jul	Aug	Sep	Oct	Nov	Dec	ANNUAL	VALUE
Wind Speed Avg (mph)	5.0	4.8	8.0	8.7	7.5	7.5	6.8	6.2	6.4	7.6	5.3	5.4	**AVG**	**6.59**
Wind Speed Max (mph)	17.7	16.6	26.0	27.6	26.6	27.1	27.5	25.4	23.3	24.5	21.2	17.0	**MAX**	**27.6**
Wind Speed Gust (mph)	29.0	46.3	46.0	53.5	41.2	36.2	49.2	39.0	37.3	48.4	41.1	34.6	**MAX**	**53.5**
Wind Freq from S*	41%	23%	36%	21%	28%	45%	57%	48%	42%	59%	41%	26%	**AVG**	**38%**
Wind Freq from NW**	39%	59%	45%	47%	44%	29%	10%	9%	27%	16%	36%	54%	**AVG**	**35%**
Air Temperature Avg (deg F)	33.8	36.8	48.1	51.5	56.8	73.8	76.84	73.8	63.14	53.2	39.4	28.2	**AVG**	**52.95**
Air Temperature Min (deg F)	6.2	-13.2	24.2	29.5	31.9	42.0	46.7	43.2	31.3	20.2	2.2	-8.7	**MIN**	**-13.2**
Air Temperature Max (deg F)	61.1	74.7	72.8	79.1	85.5	98.7	101.9	96.2	89.3	77.5	73.7	56.8	**MAX**	**101.9**
Relative Humidity Avg (%)	77.6	71.2	55.8	48.3	41.9	23.2	19.0	17.7	25.8	36.3	43.3	61.2	**AVG**	**43.3**
Relative Humidity Min (%)	29	16	13	6	6	3	3	1	4	5	7	8	**MIN**	**1**
Relative Humidity Max (%)	93	92	97	100	100	96	92	65	86	100	97	99	**MAX**	**100**
Total Precipitation (inch)	0.66	0.23	0.41	0.59	0.60	0.33	0.12	0.00	0.00	0.01	0.10	0.19	**TOTAL**	**3.24**
Max Daily Precipitation (inch)	0.33	0.14	0.18	0.19	0.29	0.22	0.08	0.00	0.00	0.01	0.06	0.14	**MAX**	**0.33**
Soil Temperature Avg (deg F)	31.6	36.6	47.4	55.0	63.7	79.1	84.7	83.6	74.2	61.5	47.6	34.7	**AVG**	**58.34**
Soil Temperature Min (deg F)	24	27	37	41	48	62	73	72	59	49	29	22	**MIN**	**22**
Soil Temperature Max (deg F)	40	52	60	67	81	93	96	97	89	77	61	47	**MAX**	**97**
Soil Vol. Water Content Avg	0.18	0.22	0.23	0.22	0.17	0.14	0.11	0.10	0.09	0.09	0.08	0.08	**AVG**	**0.14**
Soil Vol. Water Content Min	0.12	0.13	0.21	0.17	0.14	0.12	0.10	0.09	0.08	0.08	0.07	0.07	**MIN**	**0.07**
Soil Vol. Water Content Max	0.23	0.29	0.26	0.26	0.22	0.16	0.13	0.11	0.10	0.09	0.09	0.12	**MAX**	**0.29**

*Wind Freq from S (indicates aggregate frequency for winds over 5 mph coming from south direction).

**Wind Freq from NW (indicates aggregate frequency for winds over 5 mph coming from northwest direction).

Table B-3. Station 402 summary of monthly and annual meteorological data from CY2016.

Month	Jan	Feb	Mar	Apr	May	Jun	Jul	Aug	Sep	Oct	Nov	Dec	ANNUAL	VALUE
Wind Speed Avg (mph)	4.8	4.5	6.9	8.6	7.3	7.3	6.7	6.1	6.3	7.3	5.1	5.2	**AVG**	**6.3**
Wind Speed Max (mph)	18.0	15.5	24.5	27.5	27.3	27.1	27.1	25.2	22.3	24.1	21.4	16.9	**MAX**	**27.5**
Wind Speed Gust (mph)	30.5	38.6	46.5	54.1	46.5	35.8	42.6	31.5	37.6	44.0	42.7	39.2	**MAX**	**54.1**
Wind Freq from S*	32%	26%	47%	19%	26%	46%	68%	61%	44%	64%	42%	28%	**AVG**	**42%**
Wind Freq from NW**	47%	63%	32%	53%	42%	26%	11%	8%	29%	20%	37%	53%	**AVG**	**35%**
Air Temperature Avg (deg F)	29.8	32.6	43.9	50.6	57.1	73.6	76.8	73.8	63.1	53.1	39.4	28.4	**AVG**	**52.6**
Air Temperature Min (deg F)	-1.7	-15.3	23.5	29.4	30.5	42.7	45.5	42.7	31.0	20.9	1.9	-5.6	**MIN**	**-15.3**
Air Temperature Max (deg F)	56.8	67.5	69.3	75.4	85.0	98.4	101.4	95.9	89.8	77.3	73.5	58.5	**MAX**	**101.4**
Relative Humidity Avg (%)	78.1	71.4	59.7	49.6	43.3	22.8	20.2	19.3	26.9	37.8	44.7	62.7	**AVG**	**43.3**
Relative Humidity Min (%)	24.8	12	8	4	6	3	3	1	4	5	7	8	**MIN**	**1**
Relative Humidity Max (%)	100	100	100	99	100	97	94	72	83	100	97	99	**MAX**	**100**
Total Precipitation (inch)	0.48	0.52	0.35	0.53	0.62	0.28	0.11	0.00	0.00	0.01	0.09	0.29	**TOTAL**	**2.93**
Max Daily Precipitation (inch)	0.18	0.14	0.18	0.22	0.26	0.12	0.06	0.00	0.00	0.01	0.08	0.13	**MAX**	**0.26**
Soil Temperature Avg (deg F)	30.1	35.7	43.8	53.9	63.6	80.3	84.7	82.6	70.5	57.4	44.2	31.4	**AVG**	**57.7**
Soil Temperature Min (deg F)	18.8	28.9	35.0	38.3	44.3	59.4	68.0	67.7	54.4	44.0	24.7	14.6	**MIN**	**14.6**
Soil Temperature Max (deg F)	37.4	49.4	53.1	72.6	85.1	95.9	100.7	99.8	86.6	70.6	58.5	45.8	**MAX**	**100.7**
Soil Vol. Water Content Avg	0.11	0.14	0.15	0.14	0.10	0.08	0.06	0.05	0.05	0.05	0.04	0.05	**AVG**	**0.08**
Soil Vol. Water Content Min	0.07	0.08	0.10	0.11	0.09	0.07	0.06	0.05	0.05	0.04	0.04	0.04	**MIN**	**0.04**
Soil Vol. Water Content Max	0.17	0.20	0.21	0.19	0.13	0.10	0.08	0.06	0.05	0.05	0.05	0.07	**MAX**	**0.21**
Solar Radiation Avg (ly/day)	206	391	435	605	690	758	733	666	554	403	297	228	**AVG**	**497**
Solar Radiation Max (ly/day)	324	486	550	710	795	821	798	753	656	516	378	280	**MAX**	**821**
Barometric P. Avg (in Hg)	24.69	24.83	24.63	24.65	24.61	24.70	24.72	24.72	24.72	24.69	24.75	24.70	**AVG**	**24.71**
Barometric P. Min (in Hg)	24.27	24.49	24.40	24.39	24.31	24.50	24.62	24.60	24.47	24.48	24.47	24.26	**MIN**	**24.26**
Barometric P. Max (in Hg)	24.95	25.08	24.78	24.92	24.81	24.82	24.80	24.82	24.94	24.90	24.94	24.99	**MAX**	**25.08**

*Wind Freq from S (indicates aggregate frequency for winds over 5 mph coming from south direction).

**Wind Freq from NW (indicates aggregate frequency for winds over 5 mph coming from northwest direction).

APPENDIX C: Daily Average Meteorological and Environmental Data for TTTR Monitoring Stations 400, 401, and 402 during CY2016

Tonopah Test Range Station 400 CY2016

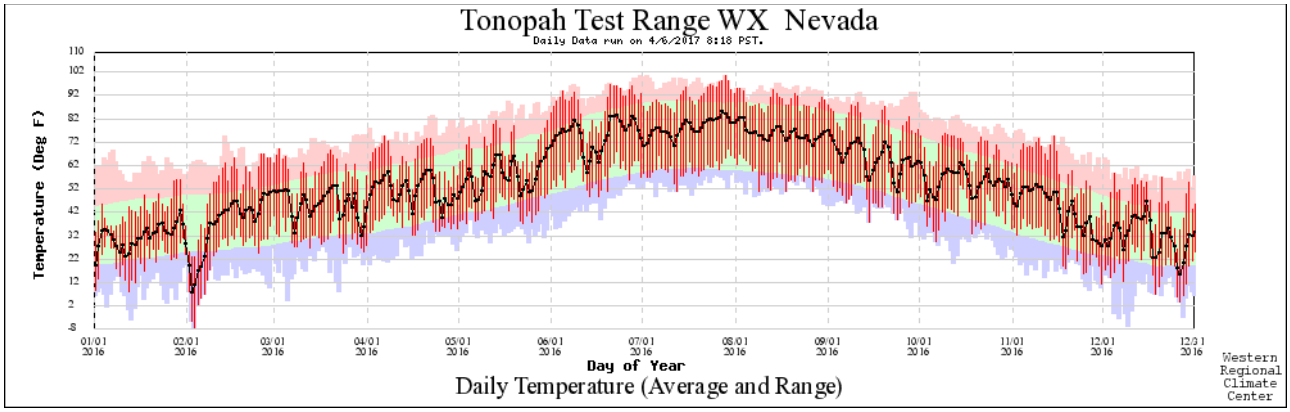

Figure C-1. Graphical summary of temperature data collected by the TTR 400 station from January 1, 2016, until December 31, 2016. Underlying pastel colors represent the period-of-record extremes (red and blue) and averages (green).

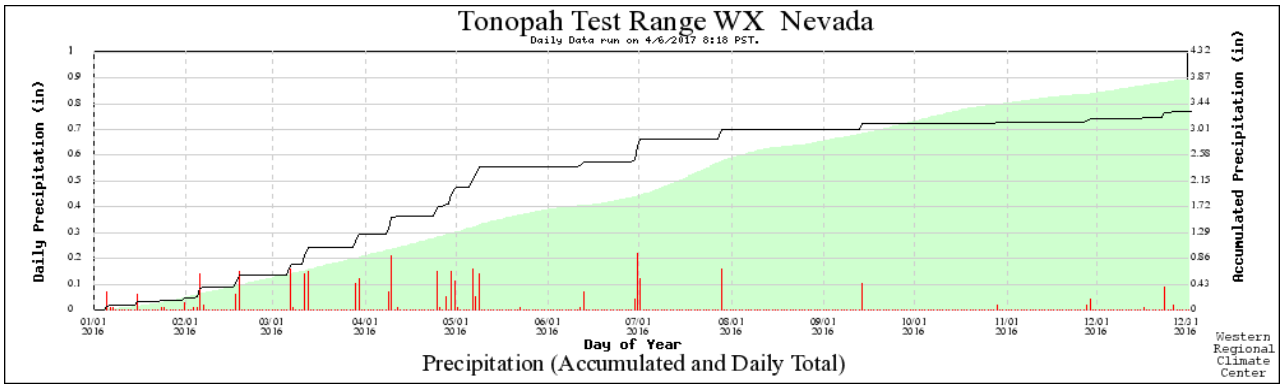

Figure C-2. Graphical summary of precipitation data, daily total (red bars) and accumulated (black line), collected by the TTR 400 station from January 1, 2016, until December 31, 2016. Underlying light green shaded area represents the station period-of-record average precipitation accumulation.

Tonopah Test Range Station 400 CY2016

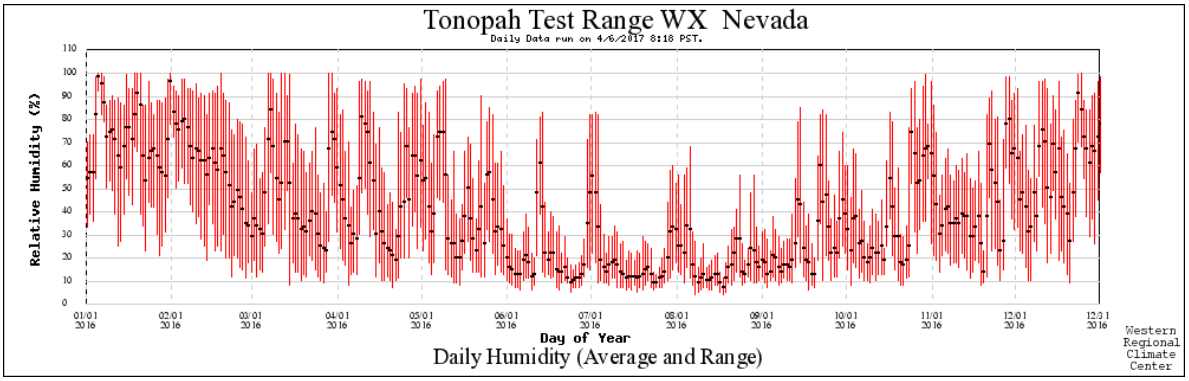

Figure C-3. Graphical summary of the humidity data, daily maximum, minimum (red bar) and average (black mark), collected by the TTR 400 station from January 1, 2016, until December 31, 2016.

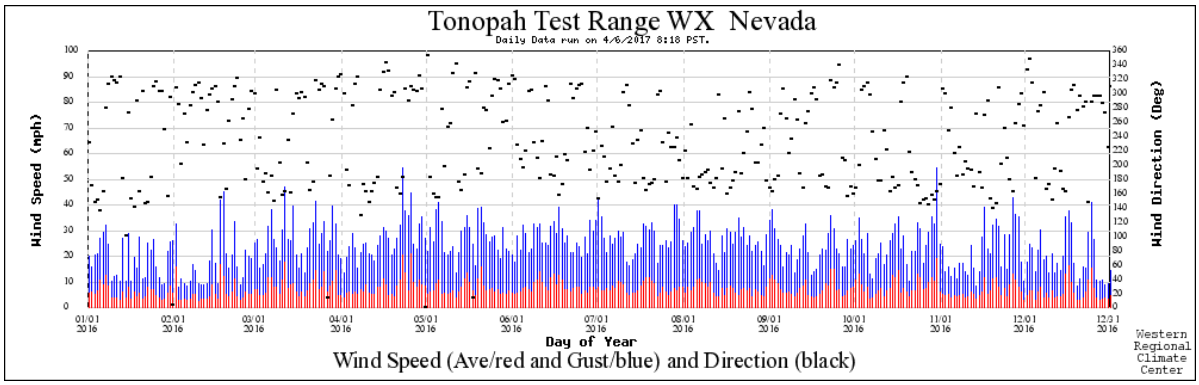

Figure C-4. Graphical summary of wind speed (daily average: red; daily peak gust: blue) and direction (black marks) data collected by the TTR 400 station from January 1, 2016, until December 31, 2016.

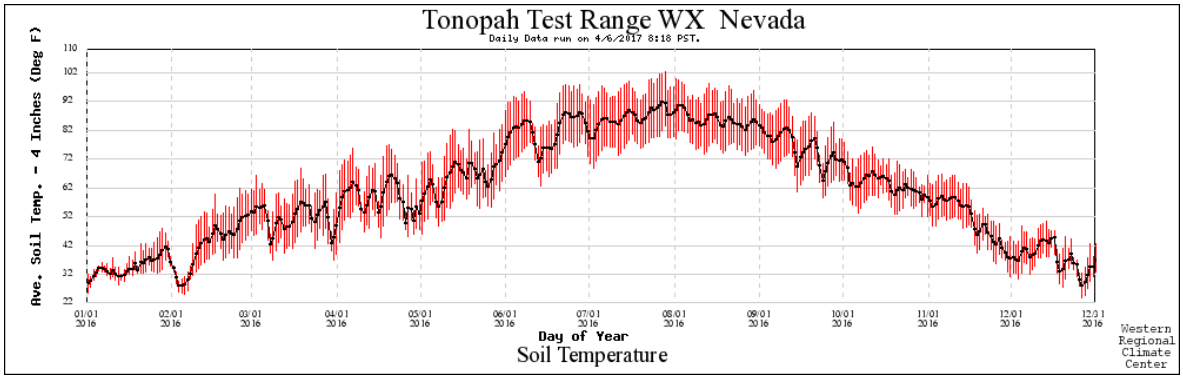

Figure C-5. Graphical summary of soil temperature data, daily maximum, minimum (red bar) and average (black line), collected by the TTR 400 station from January 1, 2016, until December 31, 2016.

Tonopah Test Range Station 400 CY2016

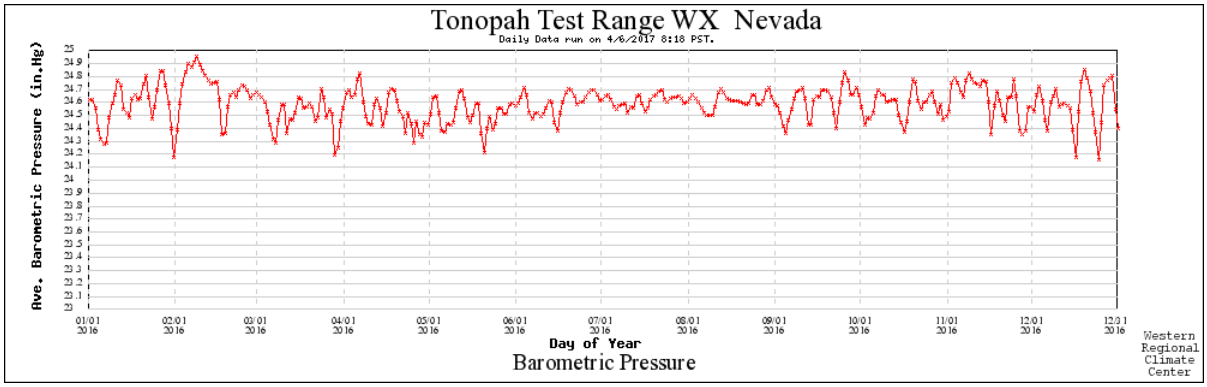

Figure C-6. Graphical summary of the daily average barometric pressure data collected by the TTR 400 station from January 1, 2016, until December 31, 2016.

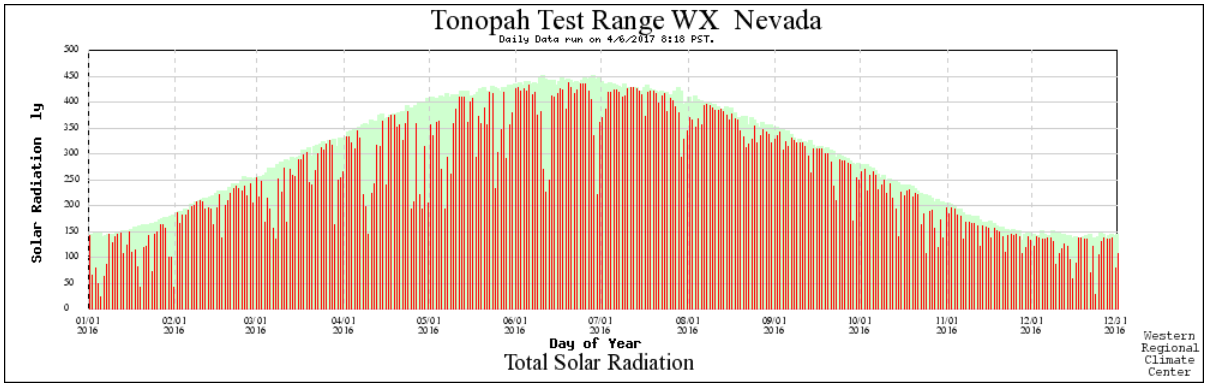

Figure C-7. Graphical summary of daily total solar radiation (red bar) data collected by the TTR 400 station from January 1, 2016, until December 31, 2016. Underlying light green shaded area represents the station period-of-record maximum daily solar radiation.

Clean Slate III Station 401 CY2016

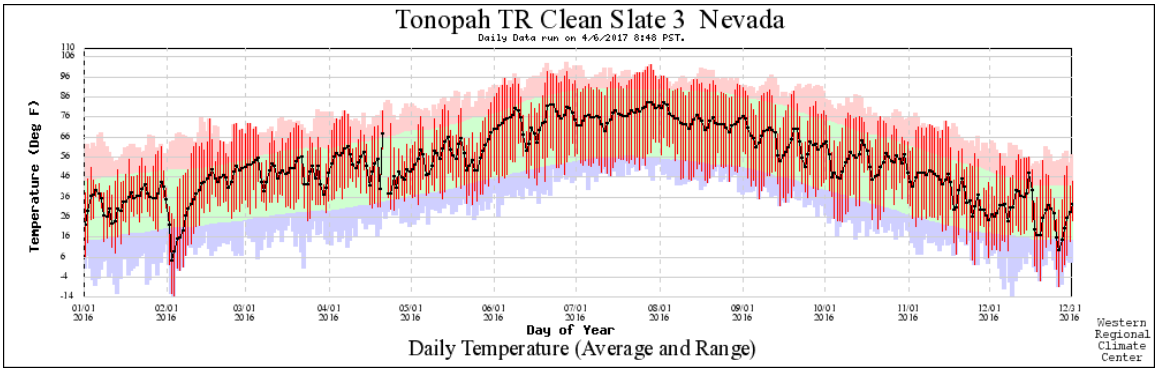

Figure C-8. Graphical summary of temperature data collected by the Clean Slate III station from January 1, 2016, until December 31, 2016. Underlying pastel colors represent the period-of-record extremes (red and blue) and averages (green).

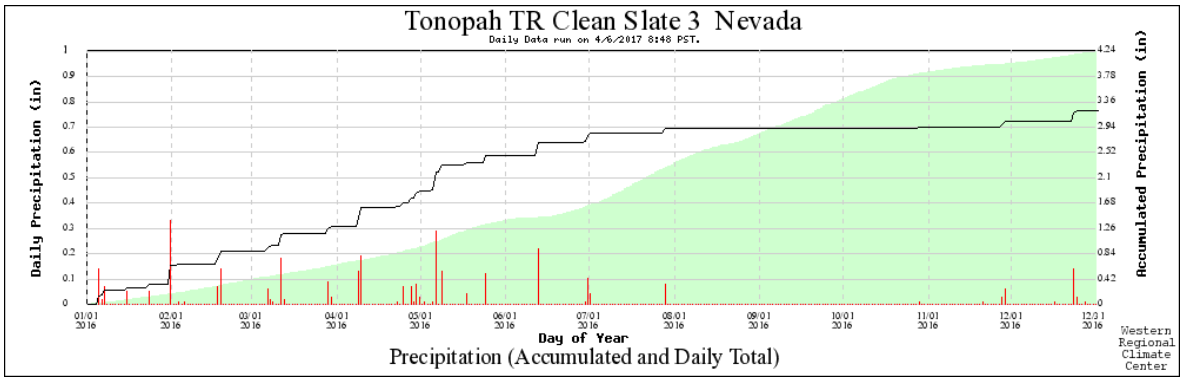

Figure C-9. Graphical summary of precipitation data, daily total (red bars) and accumulated (black line), collected by the Clean Slate III station from January 1, 2016, until December 31, 2016. Underlying light green shaded area represents the station period-of-record average precipitation accumulation.

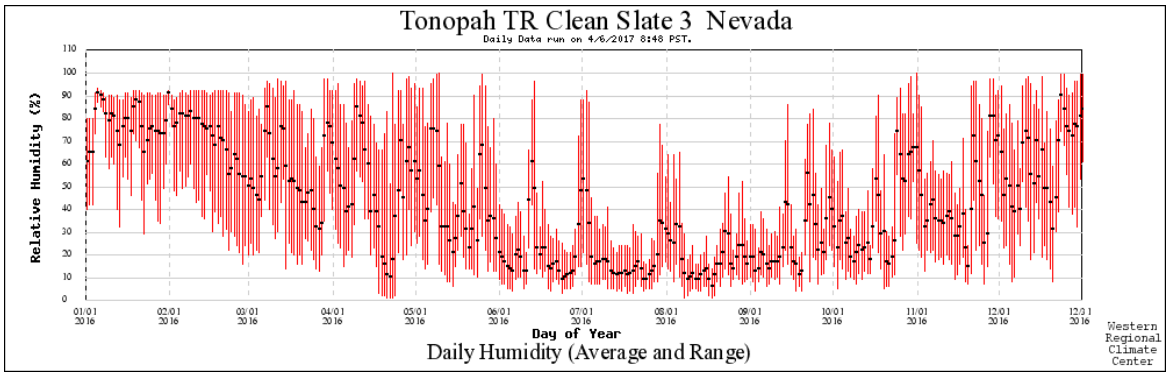

Figure C-10. Graphical summary of the humidity data, daily maximum, minimum (red bar), and average (black mark) collected by the Clean Slate III station from January 1, 2016, until December 31, 2016.

Clean State III Station 401 CY2016

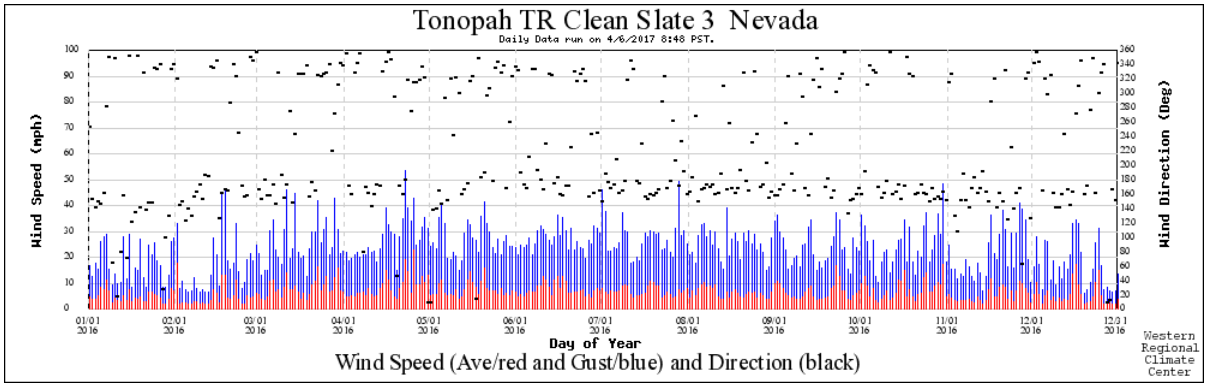

Figure C-11. Graphical summary of wind speed (daily average, red; daily peak gust, blue) and direction (black marks) data collected by the Clean Slate III station from January 1, 2016, until December 31, 2016.

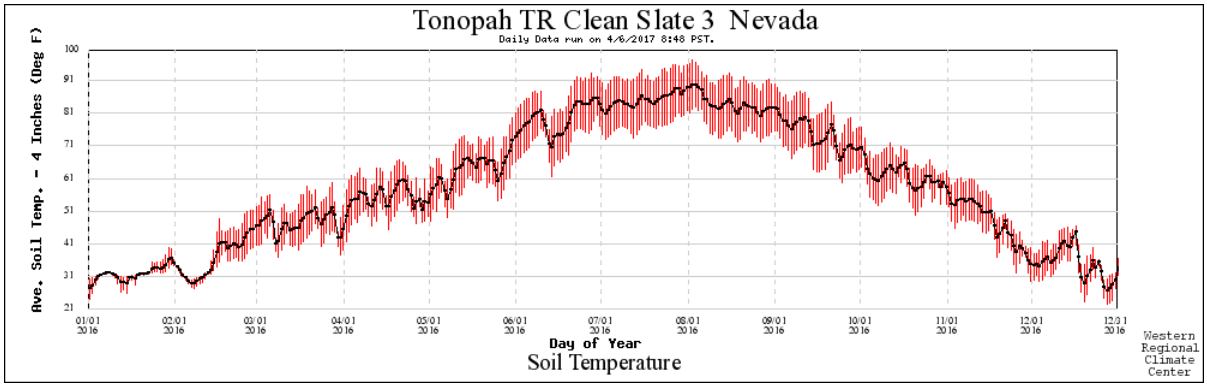

Figure C-12. Graphical summary of soil temperature data, daily maximum, minimum (red bar) and average (black line), collected by the Clean Slate III station from January 1, 2016, until December 31, 2016.

Clean Slate I Station 402 CY2016

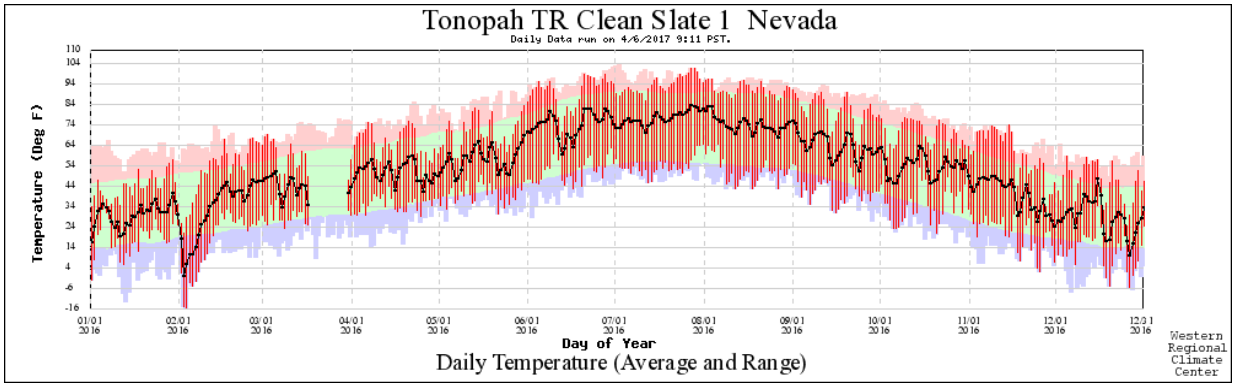

Figure C-13. Graphical summary of temperature data collected by the Clean Slate I station from January 1, 2016, until December 31, 2016. Underlying pastel colors represent the period-of-record extremes (red and blue) and averages (green). The data gap from March 17 to 29, 2016 was because of a communication problem.

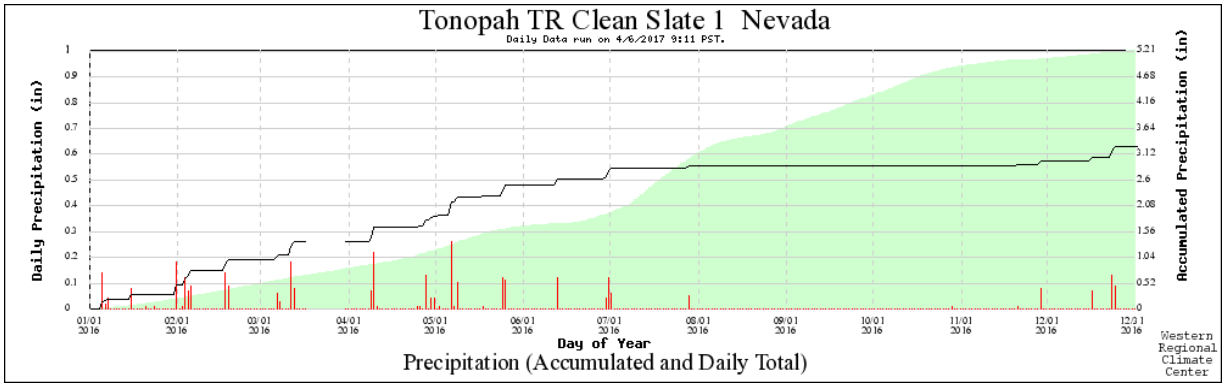

Figure C-14. Graphical summary of precipitation data, daily total (red bars) and accumulated (black line), collected by the Clean Slate I station from January 1, 2016, until December 31, 2016. Underlying light green shaded area represents the station period-of-record average precipitation accumulation. The data gap from March 17 to 29, 2016 was because of a communication problem.

Clean Slate I Station 402 CY2016

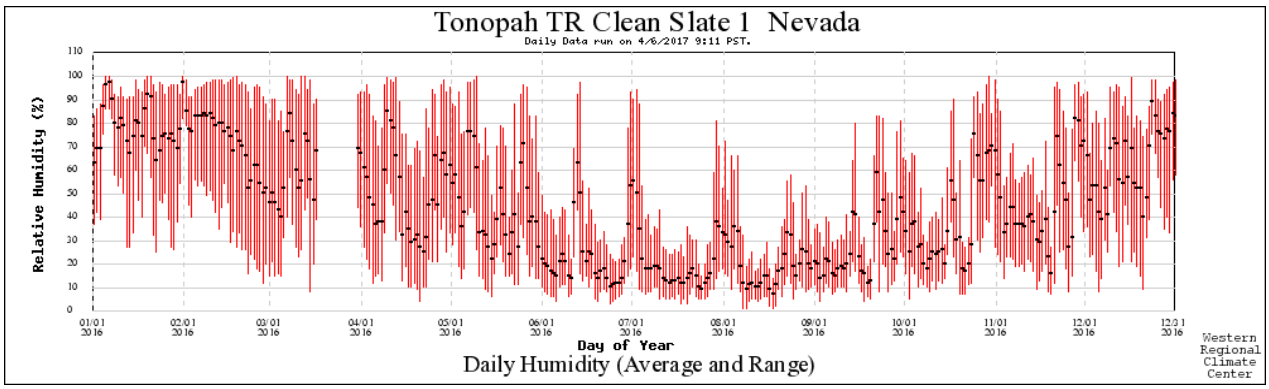

Figure C-15. Graphical summary of the humidity data, daily maximum, minimum (red bar) and average (black mark), collected by the Clean Slate I station from January 1, 2016, until December 31, 2016. The data gap from March 17 to 29, 2016 was because of a communication problem.

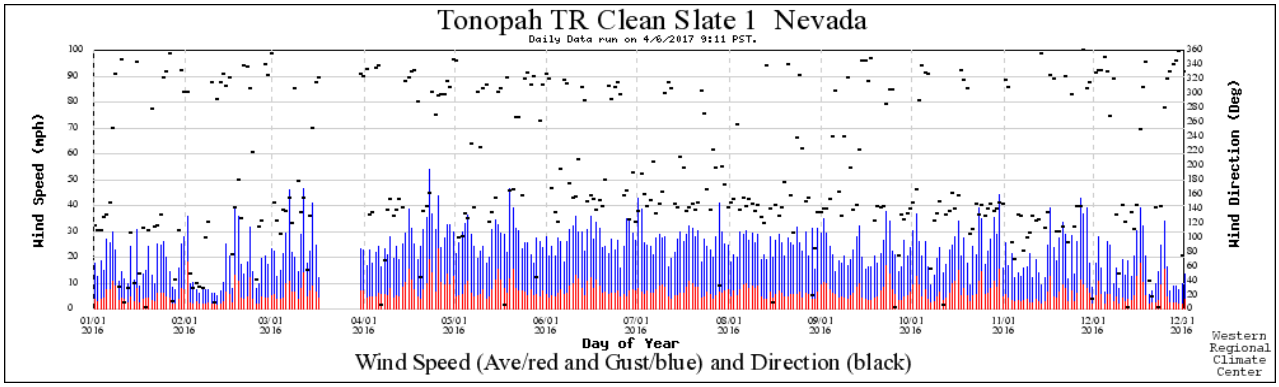

Figure C-16. Graphical summary of wind speed (daily average-red, daily peak gust- blue) and direction (black marks) data collected by the Clean Slate I station from January 1, 2016, until December 31, 2016. The data gap from March 17 to 29, 2016 was because of a communication problem.

Clean Slate I Station 402 CY2016

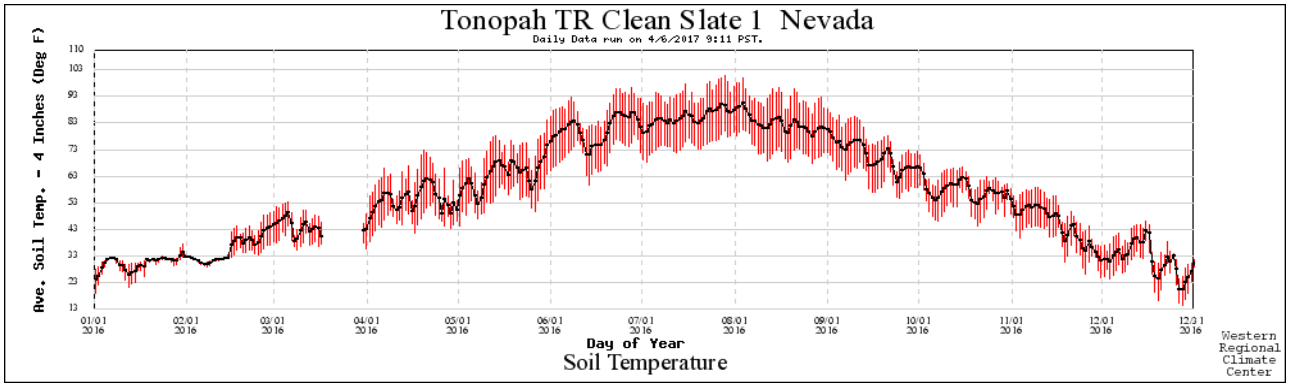

Figure C-17. Graphical summary of soil temperature data, daily maximum, minimum (red bar) and average (black line), collected by the Clean Slate I station from January 1, 2016, until December 31, 2016. The data gap from March 17 to 29, 2016 was because of a communication problem.

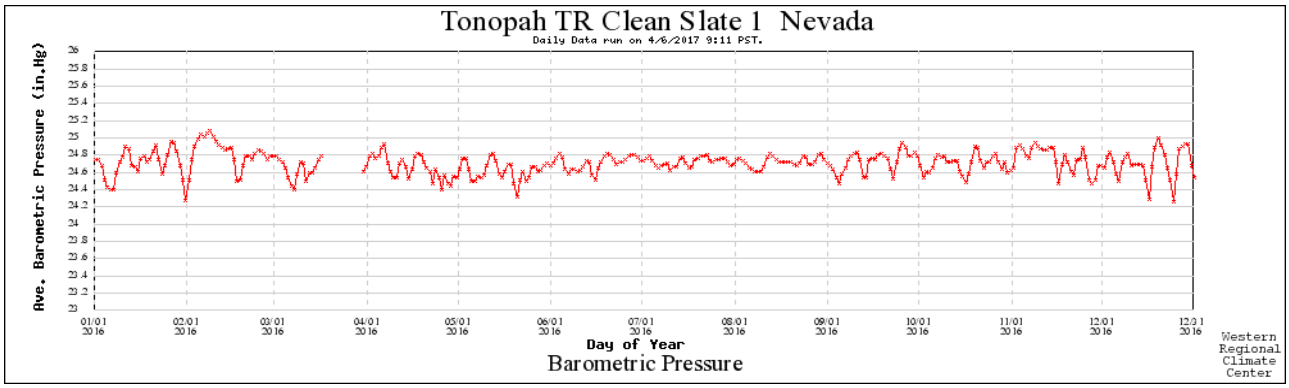

Figure C-18. Graphical summary of the daily average barometric pressure data collected by the Clean Slate I station from January 1, 2016, until December 31, 2016. The data gap from March 17 to 29, 2016 was because of a communication problem.

Clean Slate I Station 402 CY2016

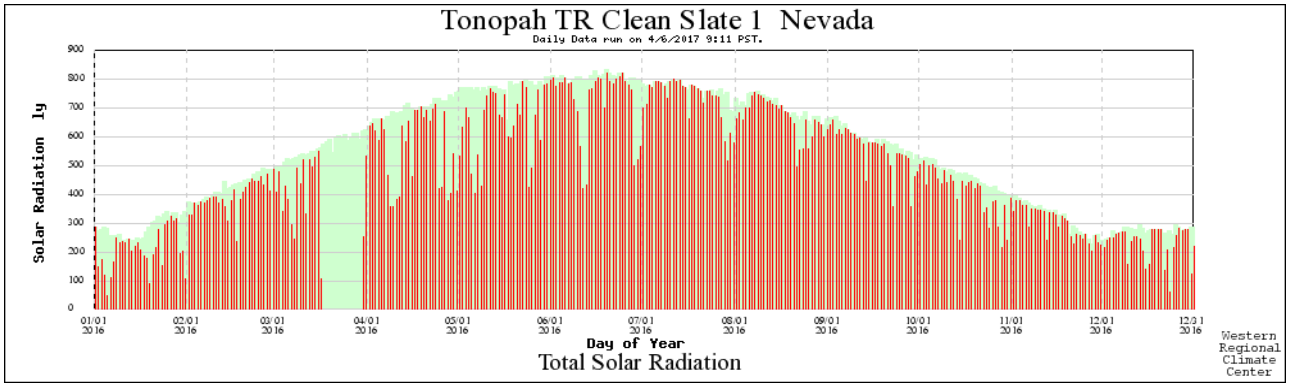

Figure C-19. Graphical summary of daily total solar radiation (red bar) data collected by the Clean Slate I station from January 1, 2016, until December 31, 2016. Underlying light green shaded area represents the station period-of-record maximum daily solar radiation. The data gap from March 17 to 29, 2016 was because of a communication problem.

STANDING DISTRIBUTION LIST

Robert Boehlecke
EM NV Program Manager
Nevada Field Office
National Nuclear Security Administration
U.S. Department of Energy
P.O. Box 98518
Las Vegas, NV 89193-8518
Robert.Boehlecke@nnsa.doe.gov

Acting, EM NV Deputy Program Manager, Operations
Nevada Field Office
National Nuclear Security Administration
U.S. Department of Energy
P.O. Box 98518
Las Vegas, NV 89193-8518

Kevin Cabble
Soils Activity Lead
Nevada Field Office
National Nuclear Security Administration
U.S. Department of Energy
P.O. Box 98518
Las Vegas, NV 89193-8518
Kevin.Cabble@nnsa.doe.gov

Tiffany Lantow
Long-Term Monitoring Activity Lead
Nevada Field Office
National Nuclear Security Administration
U.S. Department of Energy
P.O. Box 98518
Las Vegas, NV 89193-8518
Tiffany.Lantow@nnsa.doe.gov

Peter Sanders
Nevada Field Office
National Nuclear Security Administration
U.S. Department of Energy
P.O. Box 98518
Las Vegas, NV 89193-8518
Peter.Sanders@nnsa.doe.gov

Sarah Hammond, Contracting Officer
Office of Acquisition Management
NNSA Service Center
Pennsylvania and H Street, Bldg. 20388
P.O. Box 5400
Albuquerque, NM 87185-5400
Sarah.Hammond@nnsa.doe.gov

Jenny Chapman
DOE Program Manager
Division of Hydrologic Sciences
Desert Research Institute
755 E. Flamingo Road
Las Vegas, NV 89119-7363
Jenny.Chapman@dri.edu

Julianne Miller
DOE Soils Activity Manager
Division of Hydrologic Sciences
Desert Research Institute
755 E. Flamingo Road
Las Vegas, NV 89119-7363
Julie.Miller@dri.edu

Pat Matthews
Navarro, LLC
P.O. Box 98952
M/S NSF167
Las Vegas, NV 89193-8952
Patrick.Matthews@nv.doe.gov

Reed Poderis
National Security Technologies, LLC
P.O. Box 98521
M/S NLV082
Las Vegas, NV 89193-8521
poderirj@nv.doe.gov

*****Nevada State Library and Archives
State Publications
100 North Stewart Street
Carson City, NV 89701-4285

Archives Getchell Library
University of Nevada, Reno
1664 N. Virginia St.
Reno, NV 89557
tradniecki@unr.edu

DeLaMare Library 262
University of Nevada, Reno
1664 N. Virginia St.
Reno, NV 89557
tradniecki@unr.edu

Document Section, Library
University of Nevada, Las Vegas
4505 Maryland Parkway
Las Vegas, NV 89154
sue.wainscott@unlv.edu

†Library
Southern Nevada Science Center
Desert Research Institute
755 E. Flamingo Road
Las Vegas, NV 89119-7363

‡Nuclear Testing Archive
ATTN: Martha DeMarre
National Security Technologies, LLC
Mail Stop 400
PO Box 98521
Las Vegas, NV 89193-8521
demarrme@nv.doe.gov
(2 CDs)

ʃOffice of Scientific and Technical Information
U.S. Department of Energy
P.O. Box 62
Oak Ridge, TN 37831-9939

All on distribution list receive one electronic PDF copy, unless otherwise noted.

***** 12 paper copies
† 3 paper copies; CD with pdf (from which to print)
‡ compact disc only
ʃ electronic copy (pdf) only